IONIC LIQUID FUNCTIONALIZED β-CYCLODEXTRIN MODIFIED ELECTRODE AS ELECTROCHEMICAL SENSOR FOR 2,4-DICHLOROPHENOL

FAIRUZ LIYANA BINTI MOHD RASDI

FACULTY OF SCIENCE
UNIVERSITY OF MALAYA
KUALA LUMPUR

2020

IONIC LIQUID FUNCTIONALIZED β-CYCLODEXTRIN MODIFIED ELECTRODE AS ELECTROCHEMICAL SENSOR FOR 2,4-DICHLOROPHENOL

FAIRUZ LIYANA BINTI MOHD RASDI

THESIS SUBMITTED IN FULFILMENT OF THE REQUIREMENTS FOR THE DEGREE OF DOCTOR OF PHILOSOPHY

DEPARTMENT OF CHEMISTRY
FACULTY OF SCIENCE
UNIVERSITY OF MALAYA
KUALA LUMPUR

2020

UNIVERSITY OF MALAYA

ORIGINAL LITERARY WORK DECLARATION

Name of Candidate: **FAIRUZ LIYANA BINTI MOHD RASDI**

Matric No.: **SHC 140048**

Name of Degree: **DOCTOR OF PHILOSOPHY**

Title of Thesis ("this Work") :

"IONIC LIQUID FUNCTIONALIZED β-CYCLODEXTRIN MODIFIED ELECTRODE AS ELECTROCHEMICAL SENSOR FOR 2,4-DICHLOROPHENOL"

Field of Study: **ANALYTICAL CHEMISTRY**

I do solemnly and sincerely declare that:

(1) I am the sole author/writer of this Work,
(2) This Work is original,
(3) Any use of any work in which copyright exists was done by way of fair dealing and for permitted purposes and any excerpt or extract from, or reference to or reproduction of any copyright work has been disclosed expressly and sufficiently and the title of the Work and its authorship have been acknowledged in this Work,
(4) I do not have any actual knowledge nor do I ought reasonably to know that the making of this work constitutes an infringement of any copyright work,
(5) I hereby assign all and every rights in the copyright to this Work to the University of Malaya ("UM"), who henceforth shall be owner of the copyright in this Work and that any reproduction or use in any form or by any means whatsoever is prohibited without the written consent of UM having been first had and obtained,
(6) I am fully aware that if in the course of making this Work I have infringed any copyright whether intentionally or otherwise, I may be subject to legal action or any other action as may be determined by UM.

Candidature's Signature Date:

Subscribed and solemnly declared before,

Witness's Signature Date:

Name:

Designation:

IONIC LIQUID FUNCTIONALIZED β-CYCLODEXTRIN MODIFIED ELECTRODE AS ELECTROCHEMICAL SENSOR FOR 2,4-DICHLOROPHENOL

ABSTRACT

This thesis described the synthesis and characterization of ionic liquid monofunctionalized β-cyclodextrin (β-CD-1-BIMOTs) and ionic liquid difunctionalized β-cyclodextrin (β-CD-2-BIMOTs) for sensor applications. The physical characterizations of these compounds have been conducted using nuclear magnetic resonance (NMR), Fourier transform infra-red (FTIR), energy dispersive x-ray (EDX), x-ray diffraction (XRD) and Brunauer-Emmet-Teller (BET) analyses. These compounds were used as modifiers for carbon paste electrode (CPE). Cyclic voltammetry and chrono-amperometry methods were employed to examine the electrochemical responses of all prepared CPEs. All prepared electrodes show responses towards the target analyte of 2,4-dichlorophenol (2,4-DCP). Both β-CD-1-BIMOTs/CPE and β-CD-2-BIMOTs/CPE give higher current (*i*) responses compared to β-CD/CPE and native CPE. The optimum potential value for the oxidation of 2,4-DCP was decreased with the increase of IL substitution on β-CD which was from 0.75 V (β-CD-1-BIMOTs/CPE) to 0.68 V (β-CD-2-BIMOTs/CPE). Under the systematic optimized and validated conditions, the *i* response and the concentration of 2,4-DCP had a good linear relationship in the range of (4.3 – 100) $\times 10^{-6}$ mol L^{-1} and (13.8 – 100) $\times$ 10^{-6} mol L^{-1}; respectively for β-CD-1-BIMOTs/CPE and β-CD-2-BIMOTs/CPE. Both sensors were successfully applied for the determination of 2,4-DCP in leachates from landfill, mineral water and lake water with the recovery of 85.5% - 117.7%. From the interference study, β-CD-2-BIMOTs/CPE was unable to differentiate the response between 2,4-DCP and its analogues where the change of signals >5% in comparison to β-CD-1-BIMOTs/CPE. The possible interaction geometries of the β-CD-1-BIMOTs-2,4-DCP and β-CD-2-BIMOTs-2,4-DCP were

proposed to investigate the significant differences in the oxidation potential values and the selectivity properties between both sensors through spectroscopic techniques (NMR and ultraviolet-visible (UV-Vis)).

Keywords: β-cyclodextrin; ionic liquid; carbon paste electrode; electrochemical method; 2,4-dichlorophenol

ELEKTROD TERUBAHSUAI β-SIKLODEKSTRIN BERFUNGSIAN CECAIR BERIONIK SEBAGAI PENDERIA ELEKTROKIMIA UNTUK 2,4-DIKLOROFENOL

ABSTRAK

Tesis ini menerangkan tentang sintesis dan pencirian ke atas β-siklodekstrin berfungsianmono cecair berionik (β-CD-1-BIMOTs) dan β-siklodekstrin berfungsiandwi cecair berionik (β-CD-2-BIMOTs) untuk tujuan aplikasi penderiaan. Pencirian fizikal ke atas kedua-dua sebatian ini telah dijalankan dengan menggunakan kaedah resonan magnet nukleus (NMR), inframerah- transformasi Fourier (FTIR), pembelauan sinar-X (XRD), spektroskopi tenaga serakan (EDX) dan Brunauer-Emmett-Teller (BET). Kedua-dua sebatian ini telah digunakan sebagai pengubahsuai kepada elektrod pasta karbon (CPE). Kaedah kitaran voltammetrik dan krono-amperometrik telah digunakan untuk mengkaji tindakbalas elektrokimia kesemua CPE yang telah disediakan. Kesemua elektrod yang disediakan menunjukkan gerakbalas terhadap analit sasaran iaitu 2,4-diklorofenol (2,4-DCP). β-CD-1-BIMOTs/CPE dan β-CD-2-BIMOTs/CPE memberikan respons arus (*i*) yang lebih tinggi berbanding β-CD/CPE dan CPE yang asli. Nilai keupayaan optimum bagi pengoksidaan 2,4-DCP telah berkurang dengan penambahan bilangan cecair berionik ke atas β-CD iaitu dari 0.75 V (β-CD-1-BIMOTs/CPE) kepada 0.68 V (β-CD-2-BIMOTs/CPE). Di bawah keadaan yang telah dioptimumkan dan disahkan, respons *i* dan kepekatan 2,4-DCP mempunyai hubungan linear yang baik dalam julat (4.3 – 100) $\times 10^{-6}$ mol L^{-1} dan (13.8 – 100) $\times$ 10^{-6} mol L^{-1}; masing- masing untuk β-CD-1-BIMOTs/CPE dan β-CD-2-BIMOTs/CPE. Kedua-dua penderia ini telah berjaya diaplikasikan untuk menentukan kehadiran 2,4-DCP dalam larutan dari tapak pelupusan sampah, air mineral dan air tasik dengan peratusan pemulihan 85.5% - 117.7%. Melalui kesan gangguan, ternyata β-CD-2-BIMOTs/CPE tidak berupaya membezakan gerakbalas diantara 2,4-DCP dan analog-analognya dengan perubahan isyarat >5%

berbanding dengan β-CD-1-BIMOTs/CPE. Geometri interaksi β-CD-1-BIMOTs-2,4-DCP dan β-CD-2-BIMOTs-2,4-DCP yang berkemungkinan telah dicadangkan untuk mengkaji perbezaan nilai keupayaan optimum dan sifat kepilihan bahan tindakbalas kedua-dua penderia melalui teknik spektroskopi (NMR dan ultralembayung-nampak (UV-Vis)).

Kata kunci: β-siklodekstrin, cecair berionik, elektrod pasta karbon, kaedah elektrokimia, 2,4-diklorofenol

ACKNOWLEDGEMENT

First and foremost, praise be to ALLAH, the Almighty, the greatest of all, on whom we ultimately depend on, for sustenance and guidance. I would like to thank the Almighty Allah for giving me the opportunity, determination and strength to do and complete my research. I would like to show my deepest appreciation to both of my supervisors, Associate Professor Dr. Sharifah Binti Mohamad and Associate Professor Dr. Ninie Suhana Binti Abdul Manan for the valuable guidance, scholarly inputs and consistent encouragement I received throughout the research works. A special thanks to my mother Mdm. Zaiton binti Othman, my late father Mr. Mohd Rasdi bin Ismail and my siblings for their endless supports. This dissertation would not have been possible without the intellectual contribution from Prof Yatimah Alias, Dr. Nurul Yani, Dr. Muggundha, Mdm. Subhatra, Dr. Ahmad Razali, Dr. Siti Khalijah, Dr. Sherino Bibi, Dr. Muhammad Afzal and Dr. Hamid Rashidi Nodeh. Thanks to University of Malaya for the IPPP funding (PG050-2014B) and Ministry of Higher Education for the scholarship through Mybrain programme (MyPhD). I would like to extend my deepest appreciation to all the staffs and friends in the Department of Chemistry, Faculty of Science, for the kind supports and helps on the technical and the administrative aspect of the study.

TABLE OF CONTENTS

LIST OF FIGURES

LIST OF TABLES

LIST OF SYMBOLS AND ABBREVIATIONS

$\Delta\delta$	:	Chemical shift changes
A (nm^2)	:	Electrode-sample contact area
CPE	:	Carbon paste electrode
k_s	:	Standard rate constant
n	:	Number of electron transfer
α	:	Electron transfer coefficient
δ	:	Chemical shift in ppm
λ_{max}	:	Maximum absorption wavelength
β-CD-1-BIMOTs	:	6-monodeoxy-6-(3-benzylimidazolium)-β-cyclodextrin tosylate
β-CD-1-BIMOTs/CPE	:	6-monodeoxy-6-(3-benzylimidazolium)-β-cyclodextrin tosylate modified carbon paste electrode
β-CD-1-BIMOTs-2,4-DCP	:	Inclusion complex of 6-monodeoxy-6-(3-benzylimidazolium)-β-cyclodextrin tosylate - 2,4-dichlorophenol
β-CD-1-OTs	:	6-monodeoxy-6-tosyl-β-cyclodextrin
β-CD-2-BIMOTs	:	6,3-dideoxy-6,3-(3-benzylimidazolium)-β-cyclodextrin ditosylates
β-CD-2-BIMOTs/CPE	:	6,3-dideoxy-6,3-(3-benzylimidazolium)-β-cyclodextrin ditosylates modified carbon paste electrode
β-CD-2-BIMOTs-2,4-DCP	:	Inclusion complex of 6,3-dideoxy-6,3-(3-benzylimidazolium)-β-cyclodextrin ditosylates-2,4-dichlorophenol
β-CD-2-OTs	:	6,3-dideoxy-6,3-ditosyl-β-cyclodextrin
β-CD-IL	:	Ionic liquid functionalized β-cyclodextrin
β-CD-IL/CPE	:	Ionic liquid functionalized β-cyclodextrin modified carbon paste electrode
β-CD-OTs	:	Tosylated β-cyclodextrin

CHAPTER 1: INTRODUCTION

1.1 Introduction

Chlorophenols (CPs) are the most common encountered chloroaromatics compounds and it is commonly found in many industrial wastewaters (Olaniran & Igbinosa, 2011; Van Aken *et al.*, 2017; Wang *et al.*, 2015). CPs are also employed as preservatives and disinfectant due to its antimicrobial properties (Karci *et al.*, 2012). Direct or indirect release of wastewater containing CPs discharged in natural water reservoirs will lead to serious environmental and eco-toxicological problems (Biglari *et al.*, 2017; Zhang *et al.*, 2018). The released CPs tend to remain in water or in sediments due to its relatively high water solubility and its low air-water partition coefficients (Fytianos *et al.*, 2000).

The discharged CPs are a great global concerned due to its resistivity towards biodegradation with the known fact of their carcinogenic and mutagenic properties (Humayun *et al.*, 2019; Zada *et al.*, 2018). Moreover, the CPs intermediate tends to cause serious health problems; their formation of electrophilic metabolites might have tendency to bind and destroy the DNA or gene products (Igbinosa *et al.*, 2013; Michałowicz & Majsterek, 2010). 2,4-dichlorophenol (2,4-DCP) is one of the typical chlorophenol compounds which is listed as a priority pollutant by the US Environmental Protection Agency (EPA) (Honda & Kannan, 2018).

A regular monitoring is necessary prior to the removal of 2,4-DCP from the environmental water samples. A simple, fast, economical and efficient detection method which can be performed in real time is necessary to perform a long-term risk assessment regarding the release and the movement of CPs especially 2,4-DCP compound in the water system. For this purpose, a few sensitive methods such as gas chromatography (Chen *et al.*, 2019), high-performance liquid chromatography (Zhou *et al.*, 2019) and capillary electrophoresis methods (Fang *et al.*, 2014) had been applied. However, most of

the methods required a costly and complicated pre-treatment processes and the most highlighted issue was their incapability for real time monitoring. The electrochemical method was preferable owing to a fast response speed, ease of miniaturization, low cost, high sensitivity and capable for continuous real time detection (Liu *et al.*, 2019; Ramanathan *et al.*, 2019; Zhan *et al.*, 2019).

The electrochemical method that was associated with chemically modified electrode was proven to be more sensitive and selective for various analyte of interest detection especially the organic molecules (Butmee *et al.*, 2019; Safaei *et al.*, 2019; Sidwaba *et al.*, 2019). Over a couple of years ago, the fabrication of carbon paste electrode (CPE) were quite popular, it was widely accepted and used for electrochemical determination of various analytes (Sun *et al.*, 2015). The CPE provided a wide range of anodic and cathodic applications, low residual current, less noise and the ease of replacing the electrode material since it was simply the mixture of graphite with liquid binder (Saad *et al.*, 2019; Safaei *et al.*, 2019). Therefore, CPE becomes one of the convenient choices and score better over the other solid electrode materials.

Many researchers are viewing the electrode surface as a potential surface for immobilizing the important component onto them. For the host guest systems, the immobilization of the host onto a supporting material gives various opportunities for the host to be used in many of the potential application including the electrochemical applications. Hence, the CDs, crown ether, calixarenes, or porphyrins were introduced as the electrode artificial receptors (Vinodh *et al.*, 2012; Yu *et al.*, 2013). The fabrication and immobilization of the cyclodextrin host (CD) especially β-cyclodextrin (β-CD) onto CPE provide the surface with an agent of a specific recognition site for the accumulation of their specific desired analyte. Concurrently, it becomes an appropriate strategy to improve the selectivity and sensitivity of the electrodes towards specific guest analytes (Yu *et al.*, 2013).

Meanwhile, the use of the non-conducting binder i.e. mineral oils for the preparation of CPE had been investigated and reviewed since it had poor electrochemical capability of low conductivity property (Khani *et al.*, 2010). These components had been gradually replaced over the years; with the conducting binders such as room temperature ionic liquids (RTILs) (Li *et al.*, 2016). RTIL itself owned the property of low volatility, high chemical and thermal stability, offers high ionic conductivity, wider electrochemical windows towards the electrochemical measurement and it exhibited an excellent electrochemical behaviors (Duan *et al.*, 2019). The CPE that was mixed with the RTILs was known as carbon ionic liquid electrode (CILE); it was generally applied in electroanalysis and bio-electrochemistry (Beitollahi *et al.*, 2018; Farjami *et al.*, 2019). RTILs modification on CPE exhibited an outstanding increase in electron transfer rate for several organic and inorganic electroactive substances, inherent catalytic activity and preventing electrode from fouling (Sun *et al.*, 2015).

Until this recent years, a simultaneous modification on CPE by both of β-CD and RTILs had successfully been carried out by Yu and the co-workers (Yu *et al.*, 2013). The result had shown that both modifiers had improved the detection of the analyte of interest, i.e. bisphenol A. The molecular recognition hosted by β-CD formed a complex preferentially with the analyte for heterogeneous electron transfer while the RTILs was responsible for dissolving the substrate and facilitated the fast electron transportation at the electrode surface. This research had greatly promoted the development of the synthesized receptor-based CPE specifically the CILE to be used in on-site analysis.

In the meantime, the increase of interest on cyclodextrin research had provided a great opportunity to introduce various β-CD derivatives as artificial receptor on CPE as well as for other type of solid electrodes. Among the new feature of β-CD derivatives; a series of ionic liquid functionalized β-CD (β-CD-IL) were introduced in 2009 (Mahlambi *et al.*, 2010). According to the literature, β-CD-IL was described as a dual system where a

combination of both components (i.e. β-CD and IL) were capable of removing the organic and inorganic pollutants from water (Mahlambi *et al.*, 2010). Raoov *et al*. reported that the presence of IL moiety does directed the formation of inclusion complex with the desired analytes (Raoov *et al.*, 2014). Therefore, β-CD-IL is a possible candidate as CPE modifier for the selective and selective electrochemical detection of 2,4-DCP in water.

1.2 Background of study

To the best of our knowledge, there was no studies that had been undertaken to modify the CPE with β-CD-IL and specifically applied for the electrochemical detection of 2,4-DCP. However, in 2015, the first β-CD-IL was introduced as electrode modifier for glassy carbon electrode (GCE) (Sinniah *et al.*, 2015). The β-CD-IL namely mono-6-deoxy-6-(1-methylimidazolium)-β-cyclodextrin (β-CD-1-MIMOTs) had been magnetized and coated onto GCE surface for the electrochemical determination of bisphenol A. The position and number of the substitution of IL on β-CD would definitely give a different pattern to the formation of the inclusion complex with the 2,4-DCP. Herein, in this study, two β-CD-ILs of different number of IL substitution were prepared. The first β-CD-IL consisted of one position of benzylimidazolium substitution i.e. ionic liquid monofunctionalized β-CD (β-CD-1-BIMOTs). The other one consisted of two functionalization of benzylimidazolium at a different position on β-CD i.e. ionic liquid difunctionalized β-CD (β-CD-2-BIMOTs). Afterward, both β-CD-1-BIMOTs and β-CD-2-BIMOTs were applied as CPE modifiers for the electrochemical determination of 2,4-DCP.

1.3 Objectives of research

In achieving the research goal, there are three primary objectives of the research:

1. To synthesize and characterize ionic liquid functionalized β-cyclodextrin (β-CD-1-BIMOTs and β-CD-2-BIMOTs).

2. To develop and apply β-CD-1-BIMOTs and β-CD-2-BIMOTs as electrode modifiers for determination of 2,4-DCP in the real environmental samples.
3. To investigate the inclusion complex of β-CD-1-BIMOTs-2,4-DCP and β-CD-2-BIMOTs-2,4-DCP using spectroscopic techniques.

1.4 Scope of study

This research involved the synthesis of β-CD-1-BIMOTs and β-CD-2-BIMOTs from their precursor of monotosylated and ditosylated β-CD; respectively. The synthesized materials had undergone structural characterization using Fourier Transform Infrared (FTIR) spectroscopy, nuclear magnetic resonance (NMR) spectroscopy, energy dispersive x-ray (EDX) spectroscopy, x-ray diffraction (XRD) and Brunauer-Emmet-Teller (BET) techniques. Later, the β-CD-1-BIMOTs and β-CD-2-BIMOTs were fabricated onto CPE. These modified CPEs which β-CD-1-BIMOTs/CPE and β-CD-2-BIMOTs/CPE, were characterized using field emission scanning electron microscopy (FESEM).

The performance of β-CD-1-BIMOTs/CPE and β-CD-2-BIMOTs/CPE were evaluated with voltammetric analysis of ferricyanide-ferrocyanide redox couple. Next, the voltammetric screening for the oxidation of 2,4-DCP in phosphate buffer solution (pH 7.2) using β-CD-1-BIMOTs/CPE and β-CD-2-BIMOTs/CPE were investigated. Further method development of β-CD-1-BIMOTs/CPE and β-CD-2-BIMOTs/CPE were preceded with the optimization of all parameters. The optimized β-CD-1-BIMOTs/CPE and β-CD-2-BIMOTs/CPE were applied for the determination of 2,4-DCP in the environmental samples.

The final section of the research study was the spectroscopic investigation on the of β-CD-1-BIMOTs-2,4-DCP and β-CD-2-BIMOTs-2,4-DCP complexes. This subsequent analysis was conducted to support the finding obtained from the interference study which

involved several analogues of 2,4-DCP. Based on the result obtained from this section, the interaction geometry for the formation of β-CD-1-BIMOTs-2,4-DCP and β-CD-2-BIMOTs-2,4-DCP were proposed.

1.5 Outline of the thesis

The present thesis is organized into 5 chapters. Chapter 1 gives a brief introduction regarding the research background, research objectives and scope of the study. The next chapter, Chapter 2 provides a systematic review of related literature regarding to the research study. Chapter 3 gives the details methodology for the synthesis and characterization of the β-CD-ILs including, the fabrication, optimization, method validations and the application steps for both β-CD-1-BIMOTs/CPE and β-CD-2-BIMOTs/CPE. Besides, the procedure for the spectroscopic analysis of β-CD-1-BIMOTs-2,4-DCP and β-CD-2-BIMOTs-2,4-DCP are prepared and explained accordingly.

Chapter 4 discusses the results obtained from the structural characterizations of the synthesized materials, the optimization and method validation results as well as the application of the β-CD-1-BIMOTs/CPE and β-CD-2-BIMOTs/CPE for the electrochemical determination of 2,4-DCP in leachate from landfill, lake water and mineral water. The spectroscopic analysis outcomes are also explained in details and the possible interaction geometry for both β-CD-1-BIMOTs-2,4-DCP and β-CD-2-BIMOTs-2,4-DCP are discovered and elaborated in the same chapter. Finally, the overall conclusion and the future recommendation regarding the future direction of this research is provided in Chapter 5.

CHAPTER 2: LITERATURE REVIEW

2.1 Cyclodextrin

Cyclodextrins (CDs) are the widely studied examples of the host molecular receptor where this type of supramolecular system includes the organic, inorganic and biological molecules into their hydrophobic cavities and secure it via the non-covalent interactions (Floresta & Rescifina, 2019). CDs are cyclic oligosaccharides connected by α-1,4-linkages, which form a truncated cone with hydrophobic interior cavity (Liu *et al.*, 2018; Puglisi & Yagci, 2019). The torus shape cone has two rims with different sizes at both ends namely primary and secondary surfaces (Figure 2.1).

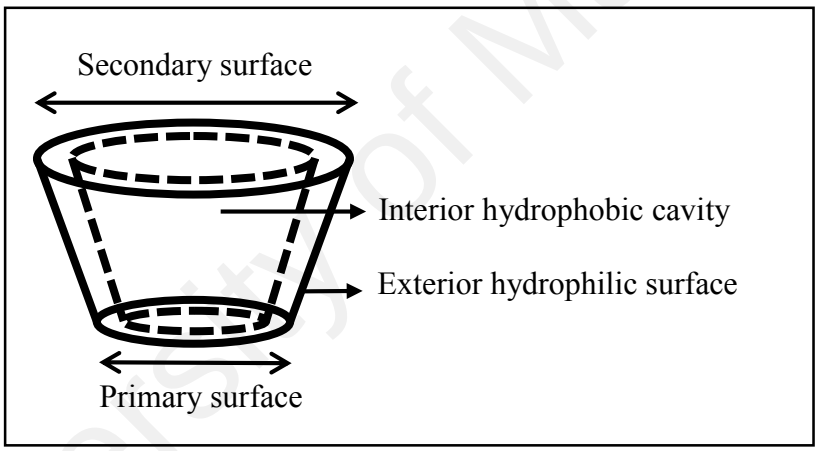

Figure 2.1: Schematic representations of the surfaces and regions of CD cylinder

Both rims contain the free hydroxyl group of glucose units where primary hydroxyl group is located at the primary surface whereas the secondary hydroxyl group is positioned at the secondary surface. There are three types of common CDs which are α-cyclodextrin (α-CD), β-cyclodextrin (β-CD) and γ-cyclodextrin (γ-CD) which contain three different glucose units of 6, 7,and 8; respectively (Figure 2.2). All three CDs have the same depth of length which is ~0.78 nm, however the cavity diameter of α-CD, β-CD and γ-CD are ~0.57, 0.78 and 0.95 nm; respectively (Srinivasan *et al.*, 2012).

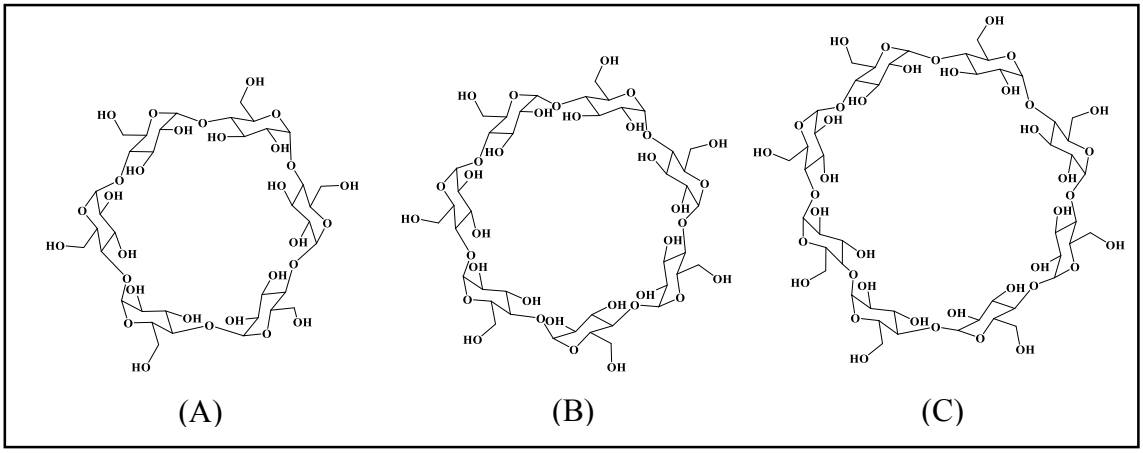

Figure 2.2: Chemical structure of (A) α-CD, (B) β-CD and (C) γ-CD with the illustration of their truncated cone

Each glucopyranose (Figure 2.3) contains the non-bonding electron pairs of the glycosidic oxygen bridges which is pointed towards the CDs interior cavity, producing a high electron density region and generating a cavity with lipophilic character due to its Lewis base characteristics (Parmar *et al.*, 2018). The hydrophilic nature of exterior surface of CDs owing to such characteristic of plenty of free hydroxyl groups at wider and narrow rims of CDs. The hydrophobic nature of the interior part of CDs and its hydrophilic exterior has encouraged CDs to act as a host for the formation of a complex with either polar or non-polar guests with many appropriately sized organic and inorganic ions and molecules (Abdolmaleki *et al.*, 2017; Banjare *et al.*, 2017).

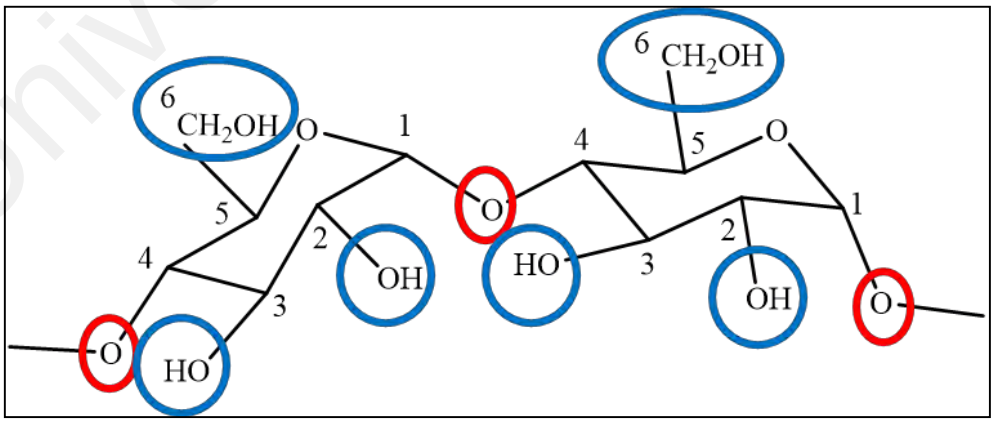

Figure 2.3: The α-1,4-glysocidic linkage between glucopyranose subunits of CD. The red circle represent the interior part of CDs while the blue circle represent the exterior cavity of CD. The number refers to the carbon position at each glucopyranose subunits

Several driving forces are proposed upon the formation of host-guest inclusion complex. This includes the van der Waals forces, hydrophobic interaction between the hydrophobic moieties of the guest with the hydrophobic cavity of CD, the hydrogen bonding between the free hydroxyl at the cavity exterior with the polar parts of the guest, the CD ring strain release on complexation, electrostatic and dipole-dipole interactions (Gidwani & Vyas, 2015; Mura, 2014). However, the hydrophobic interaction is frequently considered as the main driving force for complexation of CD with non-polar guest molecules. The host and its guest must fit a complimentary stoichiometric ratio upon complexation process where the conventional stoichiometry ratios are 1:1, 1:2 or other complicated complexes are also available (Fujita *et al.*, 2017; Parmar *et al.*, 2018).

2.1.1 Functionalization of CD

The modification of CD offers a wide range of opportunities to a broader application. Satisfyingly, CDs can be modified via various methods to attain the targeting specificity towards its guests. Through alterations, this supramolecule can increase the attraction not only for the neutral molecules but also for the molecule with charges depending on the structure of the substituent that has been attached to CD (Dai *et al.*, 2012). The functionalization of CD depends on the purpose of the CD derivative itself. Various type of a new version of CDs were prepared, validated and applied as a versatile receptors not only for molecular recognition purpose but also as the building block for functional groups and in drug delivery systems (Fujita *et al.*, 2017; Parmar *et al.*, 2018).

There are three positions of free hydroxyl group at the exterior site of CD that can be modified which are at C-6, C-2 and C-3 positions (Figure 2.4). The hydroxyl group at the C-2 and C-3 positions are located at the secondary surface of CD while hydroxyl group at C-6 belongs to the primary surface of CD. The substitution at any of the three locations

of hydroxyl group can break the limitation of utility with respect to the size, shape and functional groups of the guest (Khan *et al.*, 1998).

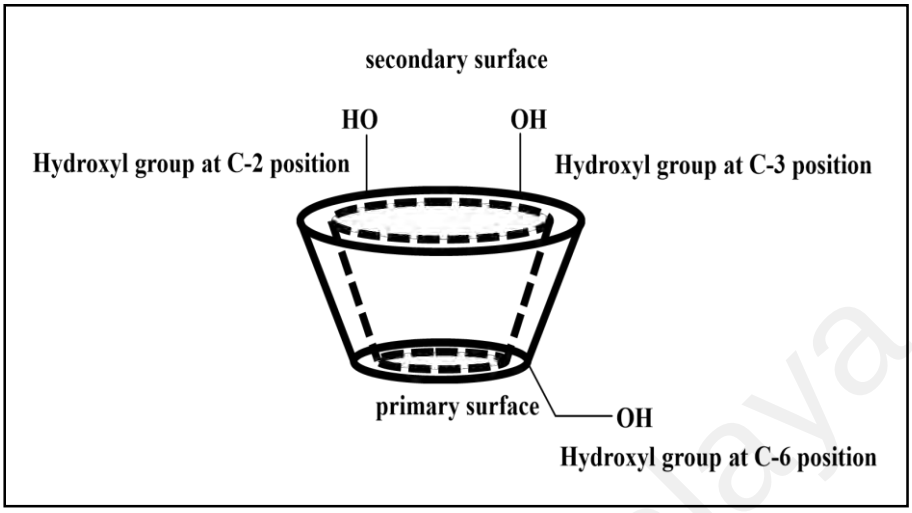

Figure 2.4: The possible sites of hydroxyl groups of CD for chemical modifications

The reactivity difference between the primary and the secondary hydroxyl groups requires a strategic functionalization on these three types of hydroxyls. The C-6 hydroxyl (OH) group is the most reactive and available functional moiety compared to the C-2 and the C-3 (OH) groups. The basic OH at C-6 which is attach to an alkyl group of ($HO\text{-}CH_2\text{-}CHR_2$) is connected to dihedral angle which allows multiple possibilities for hydrogen binding as well as highly reactive in nucleophilic substitution (Santillán-Mercado *et al.*, 2017). The OH of C-2 is considered to be acidic and less reactive than C-6 (OH). The least reactive will be C-3 (OH) which is possibly due to the steric hindrance reason. The order of hydroxyl reactivity from the highest to the least is as follows: C-6 (OH) > C-2 (OH) > C-3 (OH). Practically, a direct approach for modification of hydroxyl of CD must follow this order of reactivity. However, the indirect modification is possible for secondary OH (at C-2 and C-3) whenever the C-6 (OH) is chemically protected (Szejtli, 2013).

The direct approach for monofunctionalization of β-CD will firstly occur at the C-6 position. The first important step to attach the desired functional groups on C-6 or any

other position (C-2 and C-3) requires sulfonation on the selected CD hydroxyl site. The tosylated β-CD derivatives are often used as a precursor especially to access a series of new ionic liquid functionalized β-cyclodextrin (β-CD-IL) compounds (Mahlambi *et al.*, 2011). Generally, the most frequent β-CD precursor used to obtain the new series of β-CD derivatives is 6-O-toluenesulfonyl-β-cyclodextrin (tosylated β-CD). As a result of tosylation process, the following functional groups are successfully derivatized on β-CD: 6-deoxyazido, amino, alkylamino, hydroxyamino, thio, thioalkyl, halo, and formyl groups (Badruddoza *et al.*, 2010; Gonil *et al.*, 2011; Jouffroy *et al.*, 2013; Xiao *et al.*, 2012). There are other precursors used for the same purpose. However, a few by-products are produced upon functionalization which require extensive purification procedures (Tripodo *et al.*, 2013).

The tosylates group are good substrates for CD substitution reaction due to its good leaving group property. The hydroxyl group of CD (e.g. C-6 (OH)) is replaced by tosyl group simply by undergoing S_N2 nucleophilic substitution reaction. The nucleophile of C-6 (OH) attacked the electrophilic site of tosyl chloride at the same time pushing out the leaving group in a concerted fashion. The S_N2 nucleophilic substitution reaction mechanism for C-6 (OH) and tosylates is depicted in Figure 2.5.

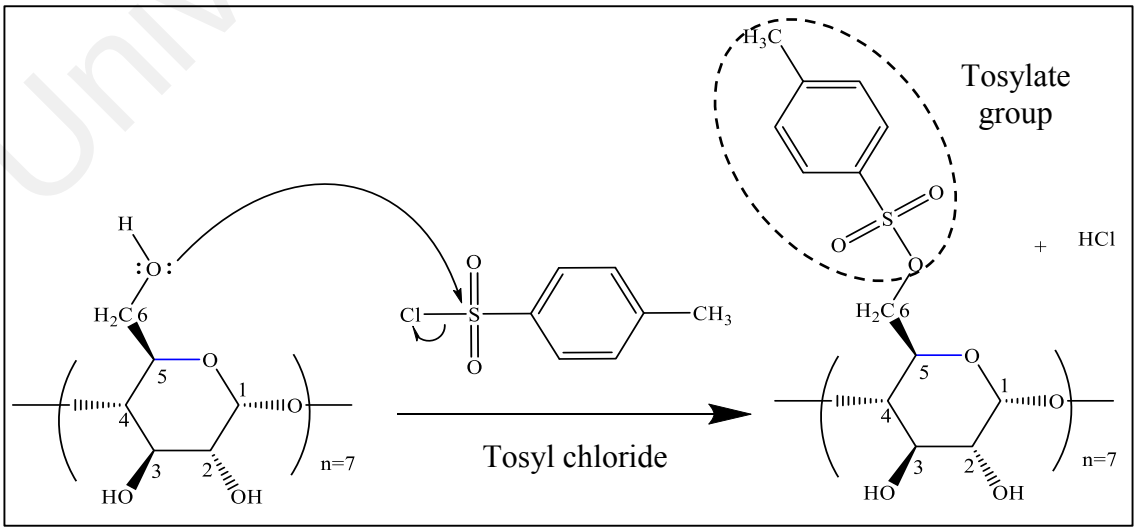

Figure 2.5: Schematic reaction mechanism for monotosylation process on β-CD (C-6-OH position)

The tosylation process at secondary hydroxyl group is also possible through both direct and indirect tosylation at C-2 (OH) and C-3 (OH) of β-CD. However, the regioselectively functionalization at the secondary hydroxyl is often a complex procedure which come with a low yield process (Brady *et al.*, 2000; Coleman *et al.*, 1991). The selective tosylation process urges to follow the rule of their reactivity unless the protecting group is used to protect the other hydroxyl of β-CD (Coleman *et al.*, 1991). Afterwards, Gonil *et al.* reported that the synthesis of tosylated β-CD at both C-6 (OH) and the secondary C-3 (OH) were possible (Gonil *et al.*, 2011) where a stepwise reaction of tosylation process was introduced through the experimental reports. The effect of tosyl chloride ratio to the β-CD, the basicity of the reaction medium as well as stirring effect were the important key factors upon the successfulness of the method. The percentage of the NaOH (as reaction medium) used determines the yield percentage especially referring to the effectiveness of the tosylation process at the secondary hydroxyl group.

2.1.2 Various applications of CD-based supramolecule

The molecular encapsulation property of CDs is responsible for the inclusion complexes formation with the variety of molecules. The non-covalent complexation approach offers a variety of physicochemical advantages for its guest molecules where the encapsulation occurs without forming any new chemical bonds as well as without any possible structural changes. The molecular complex formed inside the hydrophobic cavity of CDs, so called the inclusion complex had increased the solubility of the hydrophobic guest in water medium (Fujita *et al.*, 2017). Therefore, this property is widely exploited for the application of CDs especially in pharmaceutical, agriculture, foods technology as well as in cosmetics fields (Crini *et al.*, 2018; Fenyvesi *et al.*, 2016; Mura, 2014).

In pharmaceutical industry, the extensive use of CDs for it encapsulating property were extensively reported and at least 40 of pharmaceutical products were taking

advantage for CD's specialty (Brandariz & Iglesias, 2013; Concheiro & Alvarez-Lorenzo, 2013; Zhang & Ma, 2013). The inclusion complex between the CD and drug help to mask the unwanted odor or unpleasant smell of the drug in solution form (Tiwari *et al.*, 2010). Especially for antifungal research area, the nanosponge-like CD (in nanoparticle sizes) was utilized and used as formulation ingredient to improve the solubility and stability of the antifungal active compounds (Crini, 2014). Basically, CDs were very popular in nanotechnology area due to the involvement of CDs in the drug delivery system; mainly to overcome and encounter the drug solubility-related problems (Dhameja *et al.*, 2018; Osmani *et al.*, 2018; Patel *et al.*, 2019).

Other than that, in the fragrance and flavor industry, CD offers a protective encapsulation to the fragile flavor-type molecules to prevent volatility, to control flavor/fragrance release, increase their solubility as well as their bioavailability (Crini, 2014; Peila *et al.*, 2012). For the food technology, the CD's encapsulation help to protect the anti-oxidant molecules and CD itself is called as the secondary anti-oxidant due to its role of preventing the food from enzymatic browning (Crini, 2014; López-Nicolás *et al.*, 2014). The complexation of CD with natural colorant practically improved the natural dyes solubility and stability for food coloring property (De Boer *et al.*, 2019; Yang *et al.*, 2018). As for the agricultural industry, the treatment of seed with CD helps to delay the germination of the seed by inhibiting the activity of enzyme which is responsible for the degradation of the seeds (Ariz *et al.*, 2012; Del Valle, 2004).

Besides, the CD based materials have been frequently used in the electrochemical field especially for electrode modification (Zhu *et al.*, 2016a). Due to the supramolecular recognition property, CDs are fabricated on carbon materials such as on graphene (Liu *et al.*, 2014; Wei *et al.*, 2014) and carbon nanotubes (CNTs) (Gao *et al.*, 2015; Khaled *et al.*, 2012; Yang *et al.*, 2011). The modification of CD onto several electrodes shows that CD affected the voltammetric current response of the analytes studied due to their

function and capability of selective pre-concentration of the analyte at the electrode surface as well as the formation of the inclusion complex (host-guest of CD and analyte) (Lenik, 2017).

2.2 Introduction to ionic liquid

Another interesting feature involved in this entire research is the ionic liquid (IL). ILs are salts that entirely made up of positive and negative charge ions, which possess a wide range of liquid temperature ranges. Basically, the IL's cation consist of organic cation while the anion can either be inorganic or organic anion (Michałowicz & Duda, 2007). Most of ILs remains as liquids at room temperature due to the loose structure of its ions (Renner, 2001). The crystallinity and lattice energy is reduced as a result of weak coordination between the anions and cations component of the ILs; hence reducing the melting point (Freire *et al.*, 2007). Besides, the asymmetric composition of IL components leads to small lattice enthalpies and large entropy changes that favor the liquid state (Keskin *et al.*, 2007; Krossing *et al.*, 2006).

Generally, ILs are composed of the unsymmetrically substituted nitrogen-containing cations for example imidazole, pyrrolidine, and pyridine; with organic or inorganic anions (Zarei & Shemirani, 2011; Zhao *et al.*, 2002). The IL components can be tailored to meet the specific requirement or to ensure the compatibility of the IL according to it applications. To summarize, there are three generations of ILs which are tetrachloroaluminates (first generation, 1984), air- and water-stable ILs by tetrafluoroborate ion and other anions (second generation, 1992) and the task specific ILs (TSILs) (the third generation, 2000) (Vekariya, 2017). The component of TSILs are designed to tune their physical properties i.e. melting point, viscosity, density, solubility or hydrophobicity of ILs according to their requirements.

2.2.1 The characteristics of ILs

The properties of ILs were includes the non-volatility, non-flammable, good solubility of various organic and catalyst complexes, increased thermal stability, wide liquid temperature range, low melting points, high electrochemical windows and high ionic conductivity (Guo *et al.*, 2010; Mahlambi *et al.*, 2011; Moriel *et al.*, 2010; Stoimenovski *et al.*, 2010; Wang *et al.*, 2003). The imidazolium-, pyridinium- and pyrrolidinium- based ILs owned the property of high polarity and they possesses high solubilizing power upon carbohydrate (El Seoud *et al.*, 2007). Meanwhile, the conductivity of ILs were predicted with the abundance of charge carrier presented resulting from its anion and cation compositions. However, the conductivity of room temperature ionic liquids (RTILs) are very reliant on its viscosity since there is correlations between ion mobility and viscosity (El Seoud *et al.*, 2007).

Other than that, the decrease of planarity of the IL cation on imidazolium salt compared to tetrahedral arrangement of alkyl halide resulting on a higher IL conductivity property on the respective IL (Macfarlane *et al.*, 1999). The other interesting characteristic of IL is its wide electrochemical window. The electrochemical window is the voltage range of the tested substances where it is neither oxidized nor reduced (Hayyan *et al.*, 2013). It is also a function for working electrodes as well as for the electrolytes. A study conducted by Hayyan *et al.* on twelve types of ILs with respect to different cations and anions components had shown that the tested ILs provided a different wide range of electrochemical windows (Hayyan *et al.*, 2013). The ionic components strongly affects the electrochemical stability of ILs due to the presence of ion-ion interaction as well as hydrogen bonding that control their physicochemical properties (Zhao *et al.*, 2008).

2.2.2 The utilization of ILs

The employment of ILs are reported based on their unique properties, for instance as the extraction solvents (micro-extraction medium, task specific extraction, microwave-assisted synthesis solvent), dissolution solvents and as the separation medium of some separation processes in liquid chromatography (LC), gas chromatography (GC) and capillary electrophoresis (CE) (Tan *et al.*, 2012; Zheng *et al.*, 2011). Other than that, it is widely applied in mass spectrometry (MS), electrochemistry, sensor and spectroscopy (Sun & Armstrong, 2010). The ILs have shown to be an effective matrices to assist desorption/ionization process (MALDI-MS) as well as for matric enhanced secondary ion mass spectroscopy (MESIMS) (Fang *et al.*, 2014). The diversity of the ILs structure provides an enormous application in MALDI-MS where the ILs are utilized for the determination of a number of analytes especially proteins and peptide, sterols, oligonucleotides, polymers, carbohydrates, oligosaccharides, glycoconjugates, intact bacteria and DNA oligomers (Fang *et al.*, 2014).

Meanwhile, the research on ILs has also been emergent in selected spectroscopic techniques (Floresta & Rescifina, 2019). From the UV-Visible spectroscopy techniques, it was shown that certain ILs contained the solvated electron that showed two absorption peaks which was around 1000 to 1400 nm regions and the UV region (Sun *et al.*, 2009). Besides, the conformation of isomerism of ILs had been investigated using Raman spectroscopy. As an example, the study on the halide base ILs of [C4mim]Cl, [C4mim]Br, and [C4mim]I by Raman spectroscopy had shown that the smaller anions gave better stabilization on the trans-gauche conformational isomerism with respect to the N1–C7–C8–C9 dihedral angle of its butyl chain (Zhang *et al.*, 2010). Furthermore, the research studies of ILs had also been applied in dielectric relaxation spectroscopy, Rutherford backscattering spectroscopy, mass spectrometry, nuclear magnetic resonance, electron

paramagnetic resonance, impedance and electrochemical impedance and energy dispersive spectroscopic techniques (Floresta & Rescifina, 2019).

Besides, the scientific and technological importance of ILs today spans a wide range of applications including in electrochemical analysis and it is still growing. In electrochemistry, the employment of ILs were reported in electrodeposition, electrosynthesis, electrocatalysis, electrochemical capacitor, electrocatalysis (Endres *et al.*, 2017; Majidi *et al.*, 2019; Santos *et al.*, 2019; Zhang *et al.*, 2019). There are a few types of fabrication of IL-based sensing layers such as the direct fabrication of IL onto carbon to become carbon ionic liquid electrode (CILE) (Farjami *et al.*, 2019), casting and rubbing (Seymour *et al.*, 2018), physical adsorption (Zhang *et al.*, 2010), electrodeposition (Waldiya *et al.*, 2019), layer by layer methods (Wu *et al.*, 2009), the sol-gel encapsulation technique (Öter *et al.*, 2018) and sandwich-type immunoassays (Fu *et al.*, 2010).

Several electrochemical methods were related to the use of the ILs which was the ion selective electrodes (ISE) (Miao *et al.*, 2018), voltammetric sensors (Beytur *et al.*, 2018), gas sensors (Wan *et al.*, 2018) and biosensors (López & López-Ruiz, 2018). Based on the electrochemical method mentioned, the following studies were described regarding the use of the ILs. Wardak, and his co-worker reported that the use of 1-alkyl-3-methylimidazolium chloride as a replacement for conventional lipophilic additive in a solid contact Cu^{2+}-ISE (Wardak & Lenik, 2013). The constructed ISE successfully decreased the membrane resistance, reduced the response of time and improved the selectivity of the electrode. Farjamie *et al.* studied the voltammetric response of the doxepin using the graphite and the IL of 1-octylpyridinium hexaflourophosphate (OPFP) (Farjami *et al.*, 2019). From their observations, the presence of IL incited the electrocatalytic activity of the electrode towards the targeted analyte.

Next, a sensitive and fast detection of toxic ammonia (NH_3) and hydrogen chloride (HCl) gases had been demonstrated using the IL-based microchannels sensors (Ge *et al.*, 2019). The prepared sensor showed a promising prospective for the detection of a range of highly toxic gases with enhanced sensitivity and response times for real-time environmental monitoring. For biosensing research area, there were cases where the IL (1-vinyl-3-ethyl-imidazolium bromide ($ViEtIm^+Br^-$)) was utilized as an electrode modifier to immobilize the tyrosinase enzyme upon the detection of catechol and it was successfully applied in wastewater samples (Sánchez-Paniagua López & López-Ruiz, 2018).

In other cases, a few literatures had described the use of IL as one of the electrode component for simultaneous detection of the targeted analytes for example benserazide and levodopa (Miraki *et al.*, 2019), tert-butylhydroxyanisole in the presence of kojic acid (Shamsadin-Azad *et al.*, 2019), captopril and hydrochlorothiazide (Absalan *et al.*, 2018) and metals (zinc, cadmium and lead) (Chaiyo *et al.*, 2016). The IL was responsible for resolving the overlapping voltammetric response between the analyte as well as inciting the electrical activity of the electrode surface (Alavi-Tabari *et al.*, 2018).

2.3 Electrochemical sensor

The high demand in clinical analysis, environmental and industrial monitoring had further expanded the studies in multidisplinary field of sensors such as the electrochemical sensor and biosensor in line with rapid development in engineering, and science sectors (Chanysheva, 2016). The electrochemical devices for in-situ measurement were vibrantly developed nowadays since it had major contribution for monitoring of priority pollutants (Capodaglio *et al.*, 2016; Zhu *et al.*, 2017). An electrochemical device is described as the analytical device that is capable of converting the chemical information of a system to the electrical transducer through the chemical layer interface (Antuña-

Jiménez *et al.*, 2012). The construction of the in-situ electrochemical device must give an extra weight to the issue regarding to their long term stability, sensitivity and reversibility towards the analyte since these factors affecting the response of interest (Hanrahan *et al.*, 2004).

Electrochemical sensor offered portable, low-power requirements, simplicity, speed and low costs operation with an appropriate detection limits and it was often associated with sampling, liquid handlings, separation of the chemical compounds and many more including various biomedical applications (Bakker & Qin, 2006; Bandodkar *et al.*, 2015; Maduraiveeran *et al.*, 2018). From the analytical perspective, the electrochemical method appeared to be an alternative strategy of detection especially for the electroactive compounds where other techniques required neat and sometimes a long hour of pretreatment procedures. The electrochemical technique did not only provide a relatively good metrological parameters of sensitivity, selectivity, measurement range, linearity and response time but it merely require quick pretreatment and simple operation procedures (Szulczyński & Gębicki, 2017).

According to Stradiotto, *et al.*, there were three main range of modes of electrochemical detection which were potentiometric, voltammetric and conductometric (Stradiotto *et al.*, 2003). For voltammetric technique, the detected analyte was readily identified through the voltammetric peak potential however the detection potential was often overlapped with the concomitant substances. The best solution to overcome this problem was through the introduction of the chemically modified electrode for a better performance of voltammetric techniques at their few electrode material such as the carbon paste electrode (CPE), glassy carbon electrode (GCE), pencil graphite electrode (PGE), gold and platinum electrode and many more (Chillawar *et al.*, 2015).

2.3.1 Carbon paste electrode

The new modern electrode system which is the three electrodes system simply consist of a setup of working, auxiliary and reference electrodes (Figure 2.6). The working electrode surface is where the detection of targeted substances takes place. At the working electrode-electrolyte interface, the desired potential applied will cause the oxidation or reduction reaction of analyte to occur. Carbon type material such as graphite, fullerene, carbon nanotubes (CNT), graphene, diamond-like carbon (DLC) and diamond were chosen as electrode materials due to their electrochemical properties (high conductivity, wide potential windows) as well as their chemical inertness properties (Corb *et al.*, 2007; Kato & Niwa, 2013). Other than that, Kato & Niwa emphasized that the preference of the carbon as electrode material composition was due to its properties of structural polymorphism, chemical stability, well known surface rich chemistry with a strong internal carbon-carbon bonds (Kato & Niwa, 2013). Among all types of carbon materials that have been mentioned above, the use of graphite as electrode material had been reported frequently since 50 years ago (Švancara et al., 2009).

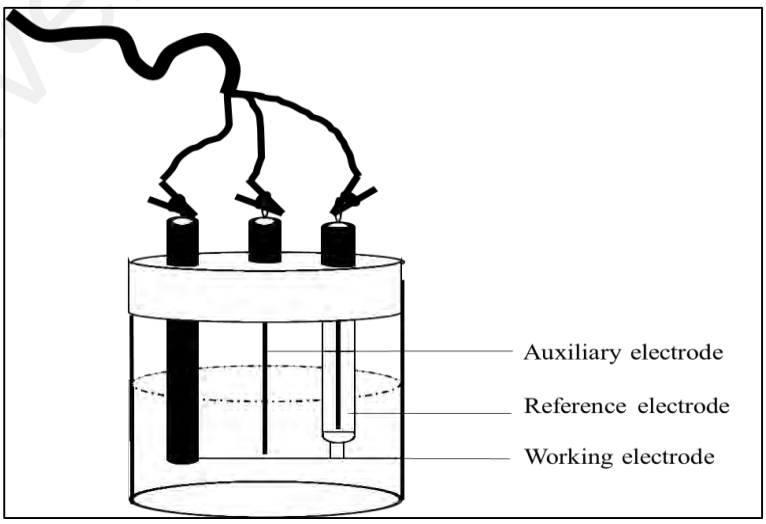

Figure 2.6: An illustration of the three electrode system cell

Carbon paste electrode (CPE) is a type of carbon electrode material that has been used as working electrode. It is the mixture of graphite and insulating liquid binder of their certain ratio resulting in a paste-like consistency material. The history of CPE began in 1950s where Ralph Norman Adams from the University of Kansas invented the CPE by mixing the electrical conducting graphite with pasting liquid for the purpose of voltammetric analysis (Kalcher, 1990; Vytřas *et al.*, 2009). Vytřas, *et al.* explained that the carbon paste like consistency was soft and non-compact material and the construction of CPE required a special body (i.e. short Teflon rod, glass tube, polyethylene syringe) and conducting wires (Vytřas *et al.*, 2009). The renewal of the electrode surface was done by pressing the piston on the compact carbon paste to create a new clean CPE surface. The illustration for the construction of CPE was given in Figure 2.7.

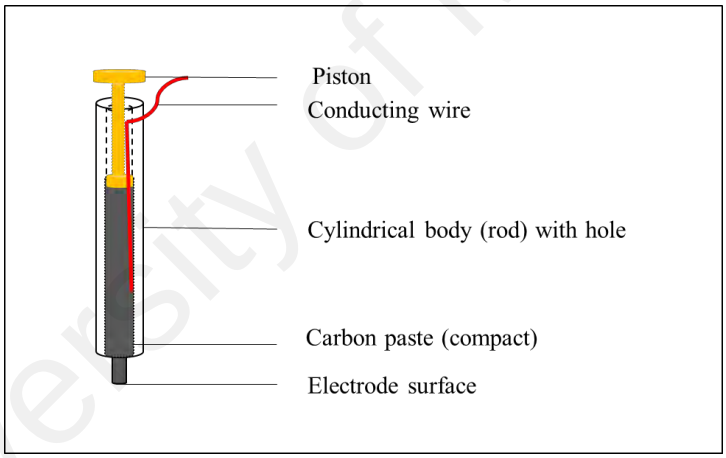

Figure 2.7: The construction of carbon paste electrode

2.3.2 Introduction to carbon paste electrode modifications

The application of CPE and other types of carbon electrodes were limited and restricted due to the electrode surface fouling process that was caused by several species (Chillawar *et al.*, 2015). As a result, the electrode surface became less sensitive and selective towards the analyte. The alternative way of improving the performance characteristic of CPE was through modification and tuning of the electrode material in accordance with the requirements of the analysis. The history of the modification began when the pioneer, Kuwana & French had successfully electrolyzed several insoluble

organic compounds (in aqueous solution) by mixing them with the CPE to circumvent their solubility problems (Kuwana & French, 1964). The electrolysis of the intimate mixture of CPE-insoluble organic compounds had successfully ionized the respective compound in other words became soluble in the electrolyte solution.

Later on, Cheek and Nelson prepared a new type of CPE; where the surface of the CPE chemically modified with diethylenetriamine via amidization process and the analyte of interest was silver (Cheek & Nelson, 1978). Afterwards, Ravichandran and Baldwin had introduced a simple preparation of modified CPE by direct mixing of modifier and CPE consequently spawn the research publication on modified CPE (Kalcher, 1990). According to Kalcher (1990), the reason for electrode modification was primarily to increase the effectiveness and compatibility of the surface electrode towards the targeted analytes.

The alteration of native electrode material had created a catalytic environment for specific detection of the target analytes such as by the amendment of mediator compounds (reaction catalysis). Other than that, the impregnation of the surface electrode with chemically active enzyme provided an active enzyme-substrates sites which create a specific environment for oxidation or reduction of the desired substrates. The fabrication of the electrode altered the native physicochemical and help to overcome the overlapping signals. Kalcher asserted that the modifier should not be directly involved in the electrochemical reaction (rather than act as mediator) within the window of the electrochemical reaction to overcome the 'high background currents' since the amounts of modifier used was rather high.

The selectivity and sensitivity of modifier towards the targeted analyte had been transferred to the modified electrode as the consequences for the alteration process (Afkhami *et al.*, 2014). The process had provided the electrode surface with special active

sites that had been 'tailored' for a significantly enhanced signal of the dedicated analyte. This will ultimately circumvent the false quantification which is caused by the contribution of the interfering compounds response that cannot be distinguished by the native electrode surface. Since CPE is soft and not compact, it can simply be fabricated with an ease of surface renewability. Referring to Bagheri, *et al.* study; like other carbon materials, CPE is chemically inert, possess low ohmic resistance, stable electrochemical response which is compatible with various types of modifier and it is economic construction techniques (Bagheri *et al.*, 2015).

The types of CPE modifier used depends on the targeted analytes itself. Recent studies had shown that there were various combinations that had been made so that the material could be a good modifier to the CPE. Numerous CPE modifiers showed their catalytic activities towards the respective desired analytes. For example, platinum-carbon nanotubes modified CPE with IL as the binder (Pt/CNTs/ILCPE) had shown a good catalytic activity for the oxidation of Sudan (I) (type of azo-dyes) (Elyasi *et al.*, 2013). The same technique; the fabrication of CPE by ethnylferrocene- nickel (II) oxide/ multiwall carbon nano tubes (NiO/MWCNT) was applied for simultaneous electrocatalytic detection of glutathione and acetaminophen (Shahmiri *et al.*, 2013). Besides, the metal organic framework that gives a large surface area to CPE had also provided electrocatalytic function for lead's detection (Wang *et al.*, 2013). There were more publications that applied the same catalytic function such as for the determination of nitrite (Afkhami *et al.*, 2014), vitamin B9 (Jamali *et al.*, 2014), vitamin C and NADH (simultaneous) (Arabali *et al.*, 2016a), hydrazine and phenol (simultaneous) (Beitollahi *et al.*, 2016) as well as hydrogen peroxide (Benvidi *et al.*, 2017).

The peak potential value of the targeted analyte was also reduced with the modification of CPE. The use of CdO/IL/CPE reduced the oxidation peak potential value of bisphenol A by 50 mV (Arabali *et al.*, 2016b). Other than that, nickel oxide

nanoparticles modified CPE showed similar abilities for determination of L-DOPA; a decrease of peak current potential with an enhanced signal by three-fold (Fouladgar *et al.*, 2015). The improvement of CPE materials was crucial for same cases since it was proven to reduce the overpotential problem that rise with unmodified CPE (Afsharmanesh *et al.*, 2013; Cheraghi *et al.*, 2016; Karimi-Maleh *et al.*, 2014; Pahlavan *et al.*, 2014).

For a simultaneous detection of more than one target analyte, the presence of modifier had resolved the overlapping of the analytes signals resulting in a well separated signal for each target analytes (Cheraghi *et al.*, 2016; Sanati *et al.*, 2014). Meanwhile, modification of CPE by certain compounds had created a new sensor material (i.e. CuO/CPE and NiO/SBA15/MWCNT/CPE) for the electrooxidation of glucose without the aid of enzyme which was very economic and became a new prospect in sensor applications (Amani-Beni & Nezamzadeh-Ejhieh, 2017; Baghayeri *et al.*, 2017). Last but not least, the use of a modifier that provide a uniform and high active sites on the CPE surface is a trend nowadays especially the material that had the molecular recognition capability for example β-CD (Fritea *et al.*, 2015; Upadhyay *et al.*, 2017). The β-CD modified CPE was shown to reduce overpotential of the electrode signals, lower detection limits and highly sensitive sensor (Fritea *et al.*, 2015; Yu *et al.*, 2013).

2.3.3 The carbon paste electrode modifier: Ionic liquid functionalized β-cyclodextrin as the potential candidate

Basically, the manipulation of CD as electrode modifier was due to its ability to perform inclusion complex with various types of compounds. During this few years, numerous work were published regarding the modification of electrode (including CPE) using β-CD (Pekec *et al.*, 2012; Rao *et al.*, 2010; Reddaiah *et al.*, 2012). A few studies had reported that the role of β-CD as receptors which had high affinity towards the analyte resulting in an enhanced sensitivity for the targeted analytes (Rao *et al.*, 2010; Yu *et al.*,

2010). Another advantage was the preconcentration effect by β-CD had improved the stability of the electrooxidation of the analyte due to the formation of the host-guest inclusion complex and the electrocatalytic effect of β-CD that contributed to the enhancement of oxidation peak of the analyte (Abbaspour & Noori, 2011; Pekec *et al.*, 2012; Reddaiah *et al.*, 2012).

However, the problem arise when a strong complexation occurred between β-CD and the guest analyte where this process hindered the charge transfer process to the electrode (Zhang *et al.*, 2013a). The strong bound complex had caused the increase of the peak potential value (the value shifted to more positive value) with a retained reversible peaks however the presence of strongly bound analyte (due to complexation) was higher than that of the oxidized form of the detected analyte (Xu *et al.*, 2011). This process will contribute to the occurring of a false quantification of analyte response. Various approach has been made to circumvent the liability of β-CD and this includes the introduction of carbon ionic liquid electrode (Yu *et al.*, 2013) (Yu *et al.*, 2013), the functionalization of β-CD onto mesoporous silica (Xu *et al.*, 2011) as well as the use of ionic liquid functionalized β-CD as the electrode modifier (Sinniah *et al.*, 2015).

In 2013, Yu, *et al.* developed a new modified CPE sensor for the determination of bisphenol A (BPA) (Yu *et al.*, 2013). The non-conductive paraffin oil was replaced by the IL (1-butyl-3-methylimidazolium tetrafluoroborate) and this carbon ionic liquid electrode was modified by β-CD as the recognition site for BPA. From their observations, both β-CD and IL were responsible for the enhancement of the detection of BPA at β-CD/IL/CPE without any inhibition problem recorded. The accumulation the BPA at the interface of medium-electrode surface was due to the stable host-guest inclusion complex of β-CD-BPA while the IL promoted the conductivity of the electrode with it inherent property as ionic binder. Hence, it was proven that both materials had improved the response signal of the electro-oxidation of BPA.

In late 2015, Sinniah *et al.* had introduced a new kind of modifier for glassy carbon electrode (GCE) which was the combination of magnetic nano particles and IL functionalized β-CD (β-CD-IL) for determination of BPA (Sinniah *et al.*, 2015). From their investigation, the magnetic nanoparticles (MNPs) had contributed to a relatively faster electron transfer due to its excellent electrical conductivity. The β-CD-IL had provided ionic conductivity (due to IL) as well as surface accumulation of the BPA (surface recognition at β-CD). The combination of both MNPs and β-CD-IL had succeeded in increasing the peak current response by almost 14-times fold compared to that of native GCE. Nevertheless, the peak current enhancement by MNPs modified GCE is not as high as MNPs/ β-CD-IL/ GCE proving that the ability of β-CD-IL itself as electrode modifier should be highlighted and well manipulated for fabrication purpose.

Generally, the chemical modified β-CDs were prepared to achieve a specific chemical and physical properties for example to increase the solubility of β-CD or to control their binding behavior (Popr *et al.*, 2014). Since the binding behavior was affected by the substituent group that is attached to β-CD, it was a great opportunity to improve and control the binding property of β-CD with their specific targeted analyte by means of β-CD derivatization. Based on this fact and by referring to the study conducted by Sinniah, S. *et al.*, we highly expected that the selectivity and sensitivity of the targeted analyte could be controlled by the IL that was installed on β-CD.

Thus, the integration of β-CD-IL as an alternative modifier for the economic and in expensive type of carbon material (i.e. CPE) was a favorable choice. The functionalization of β-CD with the material that possess high ionic conductivity perhaps will reduce the inhibition factor triggered by β-CD (strong bound analyte on β-CD cavity). Other than that, the immobilization of IL on β-CD could reduce the amount of IL used (instead of using IL as CPE binder) since there were certain IL that was very costly and expensive. The covalent attachment of the IL on β-CD prevented the leaking of IL that

can affect the reproducibility of the electrochemical measurement. Since IL can be tailored depending on its application, the IL functionalized β-CD can be designed based on the application of β-CD. Hence, the application of β-CD-IL/CPE can be expanded for various electroactive compounds especially the organic pollutants such as phenolic compounds and so on.

Recent work by Raoov, *et al.* had shown that the β-CD-IL polymer namely mono-6-deoxy-6-(3-benzylimidazolium)-β-cyclodextrin-TDI (β-CD-1-BIMOTs) exhibited higher sorption capacity towards the pollutant of 2,4-dichlorophenol (2,4-DCP) (Raoov *et al.*, 2013). The development of the electrochemical sensor for the in-situ measurement of 2,4-DCP is necessary to perform a long-term risk assessment regarding the release and the movement of this pollutant. For this purpose, the integration of β-CD-IL as an alternative modifier of the economic and in expensive type of carbon material which is CPE is a favorable choice. The β-CD-IL can be fabricated onto graphite and paraffin oil by mixing all of the materials together to form β-CD-IL modified CPE (β-CD-IL/ CPE).

2.4 The compound of interest: 2,4-dichlorophenol

Chlorophenols (CPs) are the most common encountered chloroaromatics compounds and commonly found in many industrial wastewaters (Garba *et al.*, 2019; Lim *et al.*, 2019). These pollutants have detrimental biological effect such as carcinogenicity, mutagenicity and chronic toxicity (Ceylan *et al.*, 2019). CPs tend to remain in water or in sediments due to its relatively high water solubility and its low air-water partition coefficients (El-Shal *et al.*, 2013). 2,4-dichlorophenol (2,4-DCP) (Figure 2.8) is the precursor for the production of 2,4-dichlorophenoxyacetate (2, 4-D) herbicides and it is the most abundant CPs in the aquatic environment (House *et al.*, 1997). It was reported that 2, 4-DCP had a good resistant towards biodegradation and also had the ability to be

accumulated in living organisms (Bors *et al.*, 2011; Trojanowicz *et al.*, 2002; Van Aken *et al.*, 2017).

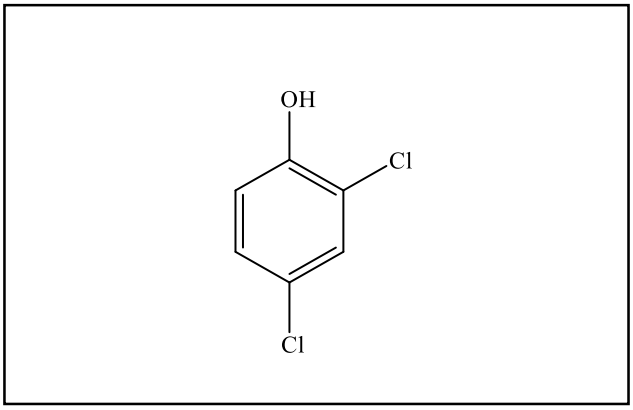

Figure 2.8: The structure of 2,4-dichlorophenol

An investigation on thousand people who was exposed to pesticides had shown that their urine contained 2,4-DCP with the highest percentage of 64% followed by 2,4,5-trichlorophenol (2,4,5-TCP) (20%) and 12% for 2,4-D (Bukowska, 2003). Ma *et al.*, (2012) reported that based on the in-vivo and in-vitro studies, 2,4-DCP can modulate the endocrine system (Ma *et al.*, 2012) including the expression of androgen (Li *et al.*, 2010a) and estrogen receptors (Zhang *et al.*, 2008). The inhalation of 2,4-DCP was reported to cause respiratory hazard such as cough, chronic bronchitis, altered pulmonary function as well as pulmonary lesions (Li *et al.*, 2010b). A regular monitoring is necessary prior to removal of 2,4-DCP from the environment.

2.4.1 The exposure of the environment to 2,4-DCP

The gradual release of 2,4-DCP into the water bodies, aquifer or any water sources through industrial, agricultural and domestics activities had consequently produced the eco-toxicological problems for all living organisms (Olaniran & Igbinosa, 2011). They had also ended-up in waste waters, sludge as well as in ground waters. The other contribution of 2,4-DCP was hazardous waste and municipal landfilling, accidental spilling, pharmaceutical production as well as from herbicides and pesticides (Yahaya *et al.*, 2019). The water chlorination by-products namely 2,4-DCP along with 2-CP, 4-CP

and 2,4,6-TCP were the major and significant toxic pollutant which was listed as the priority pollutant list of the US Environmental Protection Agency (Olaniran & Igbinosa, 2011; Sulaiman *et al.*, 2019; Yuan *et al.*, 2018).

The distribution of 2,4-DCP in the environment had been described by Olaniran & Igbinosa (Olaniran & Igbinosa, 2011). The water system was being polluted by 2,4-DCP majorly through the discharged of industrial effluent as well as by the landfill's leachate containing 2,4-DCP (Zhang & Bennett, 2005). The volatilization of 2,4-DCP contaminated the atmospheric composition; the emission of 2,4-DCP, 2-CP and 2,4,6-TCP (in the percentage of 5%) mainly comes through the manufacturing of chlorophenols (Atsdr, 2007). The lipophilic chlorophenols is quite persistent towards degradation; some of it will end up being bio-accumulated into the aquatic organism through the cell membranes (Pedroza *et al.*, 2007). According to Gaofeng, *et al.*, the degradation of 2,4-DCP was slow however it can be degraded under anaerobic condition where the best bacterium reported for the process was *Desulfomonile tiedje* (Gaofeng *et al.*, 2004).

2.4.2 Determination of 2,4-DCP

There were several developed and validated methods such as gas chromatography tandem with mass spectroscopy (GC-MS), gas chromatography coupled with electron-capture detection (GC-ECD), high-performance liquid chromatography with ultraviolet detection (HPLC–UV), liquid chromatography coupled with mass spectrometry (LC–MS) or tandem mass spectrometry (LC–MS/MS), UV-spectrophotometry and electrooxidation of 2,4-DCP by rotating glassy carbon disk electrode had been reported for the determination of 2,4-DCP in water samples (Feng *et al.*, 2011; Zheng *et al.*, 2011). However, some of the methods required tedious operation. In the meantime, the electrochemical sensors could offer a real-time response with high selectivity and selectivity for detection of 2,4-DCP. The 2,4-DCP and other CPs possessed the electro-

active nature and they can be oxidized at moderate potential range at glassy carbon electrode and other type of electrode materials such as gold, platinum and boron doped diamond (Huang *et al.*, 2018; Ureta-Zanartu *et al.*, 2002).

2.4.3 Determination of 2,4-DCP by electrochemical sensor methods

There were several reports on the use of modified sensor for electroanalysis of 2, 4-DCP. In 2007, multiwall carbon nanotubes (MWCNTs) carbon nanotubes self-decorated by horseradish peroxidase (HRP) had been utilized as a modifier for biosensing application of 2,4-DCP (Huang *et al.*, 2007). The HRP-MWCNTs-GCE had shown a good catalytic activity towards 2,4-DCP due to the HRP itself that act as electron donor for its (enzyme) regeneration while MWCNTs was responsible for the improvement of the current response to obtain a lower detection limits value. Under optimal conditions, the detection limit was calculated to be 0.38×10^{-6} M with the linear range of 1.0×10^{-6} - 1.0×10^{-4} M. The stability of this modified GCE was retained at least for two weeks. This biosensor was recommended for the determination of 2,4-DCP in waste water.

The tyrosinase immobilized on multiwall carbon nanotubes (MWCNTs) and polydiallyldimethylammonium chloride (PDDA) had been used as glassy carbon electrode modifier for detection of 2,4-DCP (Kong *et al.*, 2009). A sensitive response was obtained at the surface of the biosensor where it exhibited a fast amperometric response (within 7 s). This biosensor had good storage stability which was very suitable for long term monitoring of 2,4-DCP. The linear range of the detection was from 2×10^{-6} M to 100×10^{-6} M; where the limit of detection was calculated to be 0.66×10^{-6} M. This sensor was successfully applied for the detection of 2,4-DCP in the environmental water samples.

Enzyme biosensor based on *Trametes versicolor lacase* (Lac) (i.e. PVA/FVA/F108/Au NPs/ Lac) was developed for simultaneous detection of 4-

chlorophenol (4-CP), 2,4-dichlorophenol (2,4-DCP) and 2,4,6-trichlorophenol (2,4,6-TCP) (Liu *et al.*, 2011). Gold nanoparticles (Au-NPs), polyvinyl alcohol (PVA), Lac was mixed by using electrospinning method to form laccase nanofibers. F108 (PEO-PPO-PEO) was used as enzyme stabilizing additives. The constructed biosensor had shown a very high sensitivity towards 2,4-DCP compared to 4-CP and 2,4,6-TCP due to the suitability of the electrochemical interface of PVA/FVA/F108/Au NPs/ Lac. The lowest detection limit belongs to 2,4-DCP which is 0.04×10^{-6} M (S/N=3) and the highest detection limit value was found to be 12.10×10^{-6} M (4-CP). The stability of Lac retained by 65.8% after 30-days of storage periods. This sensor was suitable for monitoring of 2,4-DCP since it exhibited good reproducibility and repeatabilities. Besides, this electrospun nanofibers was an appropriate method for the immobilization of enzymes.

Sun *et al.* had reported the determination of 2, 4-DCP by myoglobin immobilized agarose hydrogel glassy carbon electrode biosensor (Sun *et al.*, 2012). Under the anaerobic phosphate buffer solution (PBS), the modified GCE biosensor shows their electrocatalytic properties towards 2,4-DCP. Based on UV spectra, they observed that 2, 4-DCP interacted with the amino acid residues of the myoglobin and from the reversibility of the electron transfer reaction was significantly improved. The limit of detection of 2, 4-DCP was calculated to be 2.06×10^{-6} M with the linear detection range of 12.5- 208 $\times 10^{-6}$ M. This study helps to give better understanding on the mechanisms involved in the hemoproteins with chlorophenols at the same times as the guidelines to assess the toxicity of 2,4-DCP.

The molecular imprinted technique was also utilized in the determination of 2,4-DCP where a newly design molecularly imprinted polymer of a combination of methacrylic acid (MAA) and chlorohemim was synthesized (Zhang *et al.*, 2013c). The immobilization of chlorohemim-MIP was successfully coated on GCE with the aid of 1% of chitosan in 0.8% acetic acid and 0.5% of Nafion® in acetonitrile (total volume of 6 µL). The carbonyl

group from the MAA and chlorohemim formed a relatively strong hydrogen bonds with the chlorine/oxygen atom of 2,4-DCP molecule. The reaction at the decorated/modified GCE surface had catalytic property towards the 2,4-DCP since chlorohemim introduced an active site on MIP to anchor the 2,4-DCP molecules. The linear detection range for the determination of 2,4-DCP was from 5×10^{-6} M to 100×10^{-6} M with the detection limit of 1.6×10^{-6} M. This imprinted polymer sensor proposed is suitable for quantification of 2,4-DCP in water samples since it exhibited a good stability and acceptable repeatability.

In 2016, another 2,4-DCP sensor was developed based on nanocomposite of carbon dots (CDs), hexadecyltrimethyl ammonium bromide (CTAB) and chitosan (CS) (Yu *et al.*, 2016). This new electrochemical sensor exhibited an excellent and improvised electrocatalytic activity towards anodic reaction of 2,4-DCP. The electron transfer rate was improved and the oxidation peak of 2,4-DCP was enhanced dramatically due to the synergic property of CDs-CTAB nanocomposite. Meanwhile, the presence of CS that was casted on the CDs-CTAB/GCE electrode surface was to circumvent the loss of CDs-CTAB resulted by the dissolution of the nanocomposite into phosphate buffer solution (PBS). The linear working range for the determination of 2,4-DCP was from 0.04×10^{-6} M to 8.0×10^{-6} M with the detection limit of 0.01×10^{-6} M. The optimized and validated method was successfully applied for the detection of 2,4-DCP in the waste water with a satisfactory recovery.

Liang *et al.* had introduced the molecular imprinted polymer (MIP) site specifically for the electrochemical detection of 2,4-DCP (Liang *et al.*, 2017). For that purpose, the MIP/graphene oxide (GO) was fabricated onto GCE (MIP/GO/GCE). The high binding affinity and the π-π interactions contributed from the GCE modifiers had incited the sensitivity of the electrode towards 2,4-DCP with the linear range was from 0.004×10^{-6} M to 10.0×10^{-6} M (limit of detection: 0.005×10^{-7} M). Later in 2019, there were three new type of sensors that were reported for the determination of 2,4-DCP which were

MIP/polydopamine-reduced GO/GCE (Liu *et al.*, 2019), ultrathin lamellar graphitic-C_3N_4 ionic liquid nanostructure (IL-CNNS)/GCE (Zhan *et al.*, 2019) and MIP/Carica papaya reduced graphene oxide (PRGO)/GCE (Ramanathan *et al.*, 2019).

Various electrochemical sensors had been constructed and evaluated for the determination of 2,4-DCP. However, the compatibility of the electrode surface material with the analyte of interest was crucial since the sources of 2,4-DCP contamination came with different backgrounds of interferences (in different types of medium). The main characteristic of electrochemical sensor strictly depended on its working electrode. Hence, the working electrode needs to be tailored and altered for the desired application. A strong input in electrochemical technology can be expected from improved sensing materials (especially working electrode material) so that the methods can be applied in the field measurements especially for monitoring purposes.

CHAPTER 3: RESEARCH METHODOLOGY

3.1 Chemicals, materials and reagents

β-CD was commercially available from Acros (Acros, Geel, Belgium, 99%). 1-benzylimidazole (1-BIM), 2,4-dichlorophenol (2,4-DCP), sodium dihydrogen phosphate and sodium monohydrogen phosphate was purchased from Sigma-Aldrich (Aldrich, Buches, SG, Switzerland). *p*-Toluene sulfonyl chloride, *p*-toluene sulfonic acid and all anhydrous of dichloromethane, n-hexane and n,n-dimethylformamide were purchased from Merck (Merck, New York, USA). Hydrochloric acid was purchased from Merck (Merck kGaA, Darmstadt, Germany). The graphite powder was supplied from HmBG Chemicals (Hamburg, Germany).

Other reagents and chemicals were of analytical grade and were used without further purification. All standard solutions were prepared with double distilled water (UPW; Milli-Q water purification system, Millipore, Billerica, MA, USA) or otherwise stated. 1000 mg L^{-1} of stock solution of 2,4-DCP was prepared in methanol and stored at 4 °C. Phosphate buffer solution (PBS, 0.1 M) of pH 7.2 was used as the supporting electrolyte. All working standards were freshly prepared by dilution with an appropriate amount of double distilled water (18.2 MΩ cm^{-1}) to obtain the desired concentrations.

3.2 Characterization of the samples

A Perkin-Elmer FTIR spectrometer (Spectrum 400, Perkin Elmer, Waltham, MA, USA) with a diamond ATR, the absorption mode with 4 scans at a resolution of ±4 cm^{-1} and a wavenumber range of 4000 to 450 cm^{-1} was used for all infrared (IR) spectral measurements. All NMR spectra were recorded on AVN 400 Hz (Bruker BioSpin Corp., Billerica, MA, USA) with the use of dimethyl sulfoxide (DMSO-D6) as solvent. The chemical shift was reported in parts per million (ppm) using the residual signal DMSO-D6 as an internal reference. Energy dispersive X-ray spectrometry (EDX) analysis was

performed using XMX1011, OXFORD Instruments. X-ray diffraction (XRD) patterns were recorded using an Empyrean X-ray diffractometer from 2θ = 15° to 75° using Cu Kα radiation (λ = 1.5418 Å) at a scan rate of 0.02 s^{-1}. Brunauer –Emmett-Teller (BET) surface area and porosity of the materials were determined from the nitrogen adsorption-desorption analysis at 77 K on the surface analyzer (Quantachrome, Boynton Beach, FL, USA).

The surface morphology of the modified electrodes was analyzed using field emission scanning electron microscopy FEG Quanta 450 (FEI, Eindhoven, Netherlands). All electrochemical experiments were performed on a computer-controlled Autolab potentiostat (PGSTAT 101, Utrecht, Netherlands). For the three electrode systems, a platinum wire and Ag/AgCl/3 M KCl were used as the counter and the reference electrodes, respectively. The prepared materials were used as working electrodes. The electrodes were inserted into the cell through holes in its Teflon cover. Cyclic voltammetry experiments were performed at 0.10 V s^{-1}. The amperometric experiments were carried out by applying the desired potential. All electrochemical measurements were conducted at the room temperature.

Meanwhile, for the inclusion complex study, the proton nuclear magnetic resonance (^{1}H NMR) spectra were recorded on Lambda JEOL 400 MHz FT-NMR spectrometer (JEOL, USA) while the two-dimensional nuclear overhauser effect spectroscopy (2D NOESY) spectrum were recorded on Bruker Avance 600 MHz spectrometer (Bruker BioSpin Corp., Billerica, MA, USA) and DMSO-D6 was used as the solvent. Tetramethylsilane (TMS) was used as an internal reference standard. The chemical shifts were reported in part per million (ppm) value relative to TMS. The spectrophotometric measurements were made with a Shimadzu Ultraviolet-Visible spectroscopy UV-1800 (UV-Vis, Kyoto, Japan) recording spectrophotometer equipped with 1 cm quartz cells.

3.3 Synthesis route of ionic liquid mono and difunctionalized β-cyclodextrin

There are three steps required for the synthesis of ionic liquid monofunctionalized β-cyclodextrin (β-CD-1-BIMOTs). The first step is the synthesis of the starting material of *p*-toluenesulfonyl anhydride (Ts_2O), followed by the preparation of monotosylated β-cyclodextrin precursor (β-CD-1-OTs). The third step is the preparation of β-CD-1-BIMOTs. Meanwhile, the synthesis of ionic liquid difunctionalized β-cyclodextrin (β-CD-2-BIMOTs) is a two steps synthesis. First, the synthesis of ditosylated β-cyclodextrin precursor (β-CD-2-OTs) from the starting material of native β-CD and *p*-toluenesulfonyl chloride that is readily available. Finally, the second step is the preparation of ionic liquid difunctionalized β-cyclodextrin (β-CD-2-BIMOTs).

3.3.1 Preparation of *p*-toluene sulfonic anhydride (Ts_2O) for monotosylated β-cyclodextrin precursor

p-Toluene sulfonic anhydride (Ts_2O) was prepared according to the previous method (Zhong *et al.*, 1998). Briefly, *p*-toluene sulfonyl chloride (2.00 g, 10.4 mmol) was dissolved in 12.5 mL of dichloromethane. Under nitrogen atmosphere and vigorous stirring, *p*-toluene sulfonic acid (0.52 g, 2.63 mmol) was gradually added to the solution. After an overnight stirring, the mixture was filtered to remove the unreacted *p*-toluene sulfonic acid. The filtrate was treated with hexane (50 mL) to obtain precipitate. The precipitate was dried overnight under reduced pressure to afford white crystal product. The scheme for the preparation of Ts_2O was shown in Figure 3. 1.

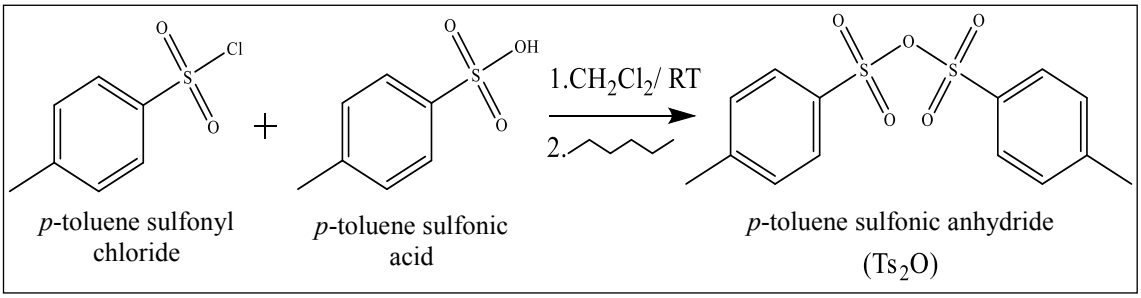

Figure 3.1: Synthesis pathway of *p*-toluene sulfonic anhydride

3.3.2 Synthesis of 6-monodeoxy-6-tosyl-β-cyclodextrin precursor (β-CD-1-OTs)

The precursor was prepared according to Zhong and co-workers (Zhong *et al.*, 1998) as reported by Raoov *et al.*, 2013 (Raoov *et al.*, 2013). A solution of β-CD (11.5 g, 10 mmol) and *p*-toluenesulfonic anhydride (Ts_2O) in 250 mL of water was stirred at room temperature under an inert atmosphere for 2 hours. A solution of NaOH (5.0 g in 50 mL of H_2O) was added after 2 hours. After 10 minutes, the unreacted Ts_2O was removed by filtration through silica gel. The pH of the filtrate was adjusted to ~8 by the addition of ammonium chloride. The supernatant solution was removed via filtration and the resulting white solid was dried under reduced pressure after overnight refrigeration affording β-CD-1-OTs (1 g, 80% yield).

IR, cm^{-1} 3279 (OH), 2927 (C-H), 1642 (C=C), 1362 (Assym. SO_2), 1167 (SO_2 Sym).

^{1}H NMR/ppm, **DMSO-D6**: H8 (7.75, d), H9 (7.43, d), OH-2-OH-3 (5.62-5.86, m), H1 (4.84, s), H1* (4.76, s), OH-6 (4.15-4.55, m), H5, H3, H6 (3.38-3.75, m), H4, H2 (3.18-3.34, m), H11 (2.43, s).

3.3.3 Synthesis of 6,3-dideoxy-6,3-ditosyl-β-cyclodextrin precursor (β-CD-2-OTs)

The 6,3-dideoxy-6,3-ditosyl-β-cyclodextrin was synthesized according to Gonil *et al.*, 2010 with a little modification (Gonil *et al.*, 2011). β-CD (25 g, 22 mol) was dissolved in 350 mL of NaOH (10% w/v). After the overnight storage at 4 °C, *p*-toluenesulfonyl chloride (10 g, 52 mmol) was added and the solution was stirred at 0-5 °C in an ice water bath. After 2 hours of vigorous stirring at 0-5°C, another portion of *p*-toluenesulfonyl

chloride (15 g, 78.5 mmol) was added and stirred continuously at the same temperature for 3 hours. Later, the unreacted *p*-toluenesulfonyl chloride was separated via filtration through Celite on a sintered glass funnel. The filtrate was brought to pH 1~2 by drop wise addition of hydrochloric acid in an ice water bath. Overnight refrigeration of the resultant precipitate followed by drying and recrystallization with hot water led to the isolation of β-CD-2-OTs as a white powdery solid (6.36 g, 20.02% yield).

IR, cm^{-1} 3304 (OH), 2921 (C-H), 1636 (C=C), 1358 (Assym. SO_2), 1167 (SO_2 Sym).

^{1}H NMR/ppm, **DMSO-D6**: H8 (7.74, d), H9 (7.43, d), OH-2-OH-3 (5.63-5.88, m), H1 (4.83, s) H1* (4.76, s) OH-6 (4.47-4.62, m), H5, H3, H6 (3.51-3.73, m), H4, H2 (3.15-3.45), H11 (2.42, s).

3.3.4 Synthesis of 6-monodeoxy-6-(3-benzylimidazolium)-β-cyclodextrin tosylate (β-CD-1-BIMOTs)

Dry β-CD-1-OTs (1.00 g, 78 mmol) and benzylimidazole (BIM) (10 molar equiv.) was dissolved in anhydrous DMF (40 mL). The solution was stirred at 90°C under nitrogen for 48 hours. Acetone was added after the solution was cooled down to the room temperature and stirred for 30 minutes. The precipitate formed was filtered and washed once with acetone and dried under vacuum affording white powdery solid β-CD-1-BIMOTs. A brief pathway was shown in Figure 3.2.

IR, cm^{-1} **IR**, cm^{-1} 3290 (OH), 2927 (C-H), 1655 (C=C), 1152 (C-N).

^{1}H NMR/ppm, **DMSO-D6**: Hf (9.19, s), Hd (8.21, s), He (7.74, s), Hb (7.78, t), Hc (7.74, s), Ha (7.47, s), H8 (7.40, d), H9 (7.15, d), OH2-OH3 (5.60-5.85, m), Hg (4.93, s), H1 (4.83, s), OH6 (4.48, m), H6* (3.91, s), H6, H3, H5 (3.5- 3.7, m), H4, H2 (3.2-3.33, m), H11 (2.28,s).

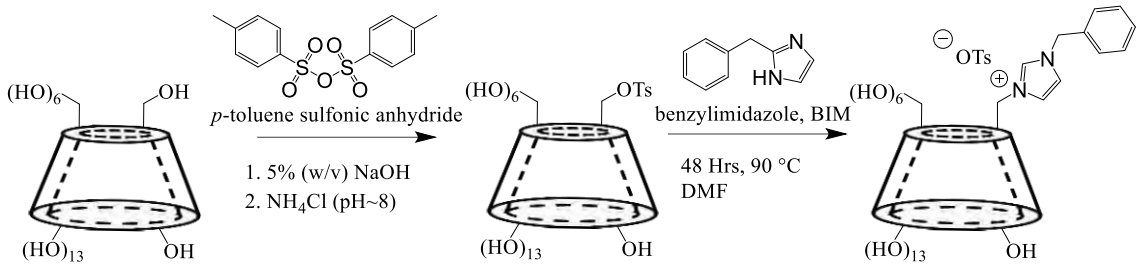

Figure 3.2: Synthesis pathway for β-CD-1-BIMOTs

3.3.5 Synthesis of 6, 3-dideoxy-6, 3-(3-benzylimidazolium)-β-cyclodextrin ditosylates (β-CD-2-BIMOTs)

Fresh dried β-CD-2-OTs (1.00 g, 68 mmol) and BIM (20 molar equiv.) was dissolved and stirred in anhydrous DMF (60 mL). The stirring was continued at 90°C under nitrogen for 72 hours. Consequently, the following procedure was the same as reported in Section 3.3.3 to afford white powdery solid β-CD-2-BIMOTs. A brief pathway was shown in Figure 3.3.

IR, cm^{-1} 3307 (OH), 2931 (C-H), 1659 (C=C), 1154 (C-N).

^{1}H NMR/ppm, **DMSO-D6**: Hf (9.19, s), Hd (8.21, s), He (7.95, s), Hb (7.78, t), Hc (7.49, s), Ha (7.47, s), H8 (7.40, d), H9 (7.15, d), OH2-OH3 (5.60-5.85, m), Hg (4.93, s), H1 (4.83, s), OH6 (4.48, m), H6* (3.91, s), H6, H3, H5 (3.5- 3.7, m), H4,H2 (3.2-3.33, m), H11 (2.28, s).

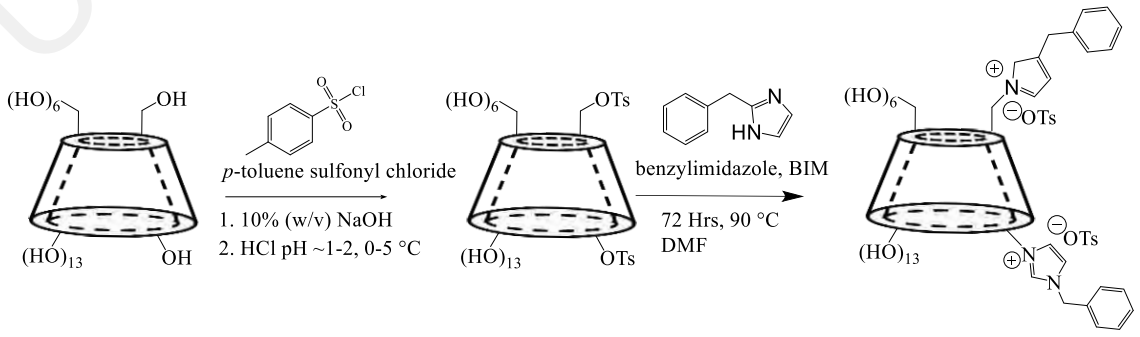

Figure 3.3: Synthesis pathway for β-CD-2-BIMOTs

3.4 The preparation of the unmodified and modified carbon paste electrode materials for the electrochemical measurements

The procedure for the preparation of CPE was illustrated as in Figure 3.4 and the same procedure was applied for all modified CPEs. The unmodified CPE was prepared by the following procedure; the graphite powder and paraffin oil were mixed in the ratio of 3:1 (w/w) in an agate mortar. The mixture was firmly packed into a syringe (3.0 mm id syringe tip, measured electrode area, A=0.0707 cm^2), with copper wire as the electrical contact. The β-CD-1-BIMOTs/CPE and β-CD-2-BIMOTs/CPE were prepared according to the optimized ratio by mixing 0.225 g of graphite powder, 0.075 g of the synthesized material (β-CD-1-BIMOTs or β-CD-2-BIMOTs) and 0.135 ml of the liquid paraffin. For comparison, β-CD/CPE was also prepared. Then, the mixture was mixed well and filled firmly into the syringe. Prior to use, the unmodified/modified electrode was dried at 60°C for 1 hour and the electrode surface was polished with a piece of weighing paper and rinsed with UPW.

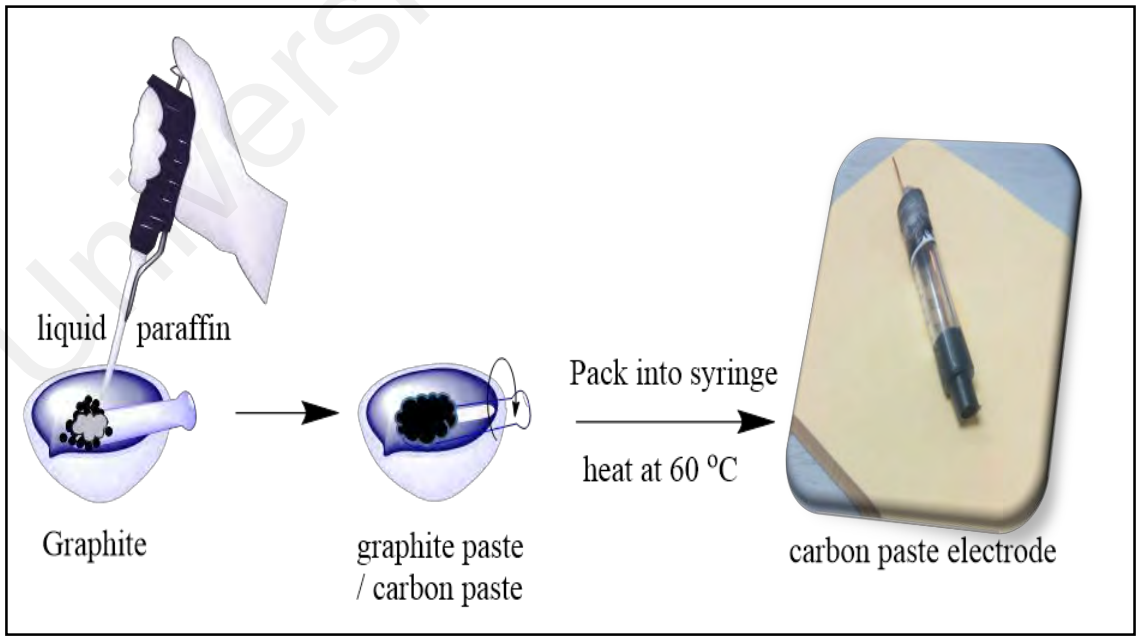

Figure 3.4: The illustration for the preparation of CPE

3.4.1 Optimization of the ratio of the modified electrode materials

First, the ratio of the graphite, modifier (β-CD-1-BIMOTs/β-CD-2-BIMOTs) and paraffin oil were varied and their current responses, *i* were measured using cyclic voltammetry technique (n=3 replicates). Then, the electrode material with the highest *i* value was applied throughout the electrochemical measurements.

3.4.2 Ferrocyanide-ferricyanide redox couple for accessing the electrochemical activity of the modified CPE and their diffusion coefficient values

The prepared electrode was immersed in the solution containing 50×10^{-6} mol L^{-1} of potassium ferricyanide ($K_3[Fe(CN)_6]$) in 0.1 mol L^{-1} of potassium chloride electrolyte solution. The cyclic voltammetry for all electrodes were recorded and their voltammogram were overlaid. The scan rates studies for redox reaction of $[Fe(CN)_6]^{3-}$-$[Fe(CN)_6]^{4-}$ couple were performed for all prepared electrodes and based on the scan rate data, their diffusion coefficients (D) were calculated and compared.

3.4.3 The cyclic voltammetry screening on the behavior of 2,4-DCP at all prepared electrodes

Briefly, the bare CPE was immersed into 0.1 mol L^{-1} phosphate buffer solution (PBS) (pH 7.2) containing 50×10^{-6} mol L^{-1} of 2,4-DCP. The cyclic voltammetry analysis was performed in the potential range of -0.4 to 1.0 V at 0.10 Vs^{-1}. All other prepared electrodes were carefully washed with UPW for further use. For comparison, the behavior of 2,4-DCP at β-CD/CPE was also observed. The cyclic voltammetry for all electrodes were recorded and their voltammogram were overlaid.

3.4.4 The optimization of parameters that affecting the sensor performance

The cyclic voltammetric technique was frequently used in electrochemical measurement. The study of pH was also conducted using cyclic voltammetry technique

and the optimum pH was selected based on their highest current response. However, the background current was reported to be a barrier to acquire a low detection limit in the electrochemical analysis (Abdul Aziz & Kawde, 2013). Chrono-amperometry yielded a higher sensitivity with a better suppression of undesirable background current and the study of optimum potential was conducted through these techniques. Consequently, all electrochemical measurements were conducted using the chrono amperometry techniques based on the optimum pH and the best potential obtained through the analyses.

3.4.5 Method validation

The evaluation of this electrochemical methods will include the selectivity, precision (repeatability, reproducibility), limit of detection, limit of quantification, working range and linearity as well as recovery studies.

3.4.5.1 Precision

The precision of the measurement is the closeness of agreement between independent test results obtained from homogenous test material under specified conditions of use. The precision of this method was evaluated by seven (n=7) measurement of the samples containing the analyte of interest which is expressed as coefficient of variations or known as relative standard deviation (RSD). The repeatability (intraday-precision) and the reproducibility (interday-precision) were measured based on the RSD formula in Eq. 3.1, where SD is standard deviation (Eq. 3.2), x is the result of every measurement and $\bar{x}$ is the mean of the measurements. The precision of the measurement was achieved with the RSD if the intraday- and interday- precision were below 5%.

$$\text{Relative standard deviation (RSD)} = \frac{\text{SD}}{\bar{x}} \times 100\% \qquad (\textbf{Eq. 3. 1})$$

$$\text{Standard deviation (SD)} = \sqrt{\frac{\Sigma\,(x - \bar{x})^2}{n - 1}} \qquad (\mathbf{Eq.\,3.2})$$

3.4.5.2 The stability of the electrode measurements and lifetime of the electrode

The stability of the electrode measurement was also calculated based on the intraday- and interday- precision. At the same time, the lifetime or the long-term stability of the electrode was evaluated based on the stability of the amperometric response of 2,4-DCP for ten consequence days. The RSD value for the measurement must also be less than 5%. Within the consequence days, the *i* value must be retained close to the original value measured.

3.4.5.3 Linear range, limit of detection, limit of quantification and sensitivity of the electrodes

The linear range lies within the working range where at the lower end of the concentration range, the limiting factor is the value of the limit of detection (LOD) and the limit of quantification (LOQ). The working range was obtained by preparing a certain standard concentration of the analyte of interest within the desired range. This so called calibration curve was acquired by plotting the peak current value at y-axis against the concentration of desired analyte at x-axis. From the calibration plot, the linearity was evaluated based on the value of correlation coefficient (R^2).

Limit of detection (LOD) and limit of quantification (LOQ) were expressed in the form of analyte concentration based on the standard deviation of the blank solution response and the calibration slope. The lowest quantity of substances that can be distinguished from the absence of that substance (blank value) was referred to LOD while the LOQ was the lowest concentration at which analyte that was measured and can be determined with an acceptable level of repeatability, precision and trueness. A total of 10

replicates (n = 10) of blank samples were analyzed and the mean values and its standard deviations were determined. The value of LOD and LOQ were estimated based on the following Eq. 3.3 and Eq. 3.4; respectively.

$$\mathrm{LOD} = \frac{3 \times \mathrm{SD}}{\mathrm{m}} \qquad (\mathbf{Eq.\,3.3})$$

$$\mathrm{LOQ} = \frac{10 \times \mathrm{SD}}{\mathrm{m}} \qquad (\mathbf{Eq.\,3.4})$$

Where,

SD: Standard deviation of blank solution

m: Slope of the regression line

From the regression line, the sensitivity of the modified electrodes can be calculated based on the Eq. (3.5) where m is the slope value and A is the electrode surface area (Eq. 3.6).

$$\text{Sensitivity} = \frac{\mathrm{m}}{\mathrm{A}} \qquad (\mathbf{Eq.\,3.5})$$

$$\mathrm{A} = \pi \mathrm{r}^2 \qquad (\mathbf{Eq.\,3.6})$$

3.4.5.4 Recovery study

The validation of this developed method was further tested with recovery studies to evaluate the accuracy of the method. This study was performed by spiking the samples with known concentration of analyte at three different analyte concentration within the

regression line. The percentage of recoveries (R (%)) of the targeted analyte was calculated by using the following Eq. (3.7).

$$\mathrm{R}\ (\%) = \frac{\mathrm{concentration}_{\text{spike sample}} - \mathrm{concentration}_{\text{unspike sample}}}{\mathrm{concentration}_{\text{spike added}}} \times 100$$

... (**Eq. 3.7**)

3.4.5.5 Interference from analogues compounds or foreign ions

In order to assess the possible analytical application of the proposed electrochemical sensor, the effects of some common anions and cations, phenol and other chlorophenols were examined in 0.1 mol L^{-1} phosphate buffer solution (PBS, pH 7.2) containing 100 × 10^{-6} mol L^{-1} 2,4-DCP. For this purpose, the ratio for the phenol and chlorophenol compounds to the 2,4-DCP was set to 1:1. Meanwhile, the concentration ratio of common anions and cations to 2,4-DCP was prepared in 100:1. Through this investigation study, the selectivity of the electrode material towards 2,4-DCP can be obtained, where the calculated RSD value of the measurement must be <5%.

3.4.6 Determination of 2,4-DCP in environmental real samples

Real samples (lake water, mineral water, leachate from landfill) were filtered and stored in the refrigerator immediately after collection. All samples were adjusted to pH 7.2 using PBS pH 7.2. The solution was transferred into the voltammetric cell to be analyzed without any further pre-treatment. Later, 25, 50 and 80 × 10^{-6} mol L^{-1} of 2,4-DCP were spiked into the real sample solution, the amperometry voltammograms were recorded and the recovery (%) of the 2,4-DCP in the real samples were calculated.

3.5 The complexation of 2,4-DCP with β-CD-1-BIMOTs and β-CD-2-BIMOTs

The formation and structure of inclusion complexes of 2,4-DCP with β-CD-1-BIMOTs and β-CD-2-BIMOTs were studied using the following techniques which were ^{1}H NMR, 2D NOESY NMR, UV-Vis spectroscopies.

3.5.1 The preparation of β-CD-1-BIMOTs-2,4-DCP and β-CD-2-BIMOTs-2,4-DCP inclusion complexes for ^{1}H NMR and the 2D NOESY NMR analysis

The preparation of the β-CD-1-BIMOTs-2,4-DCP and β-CD-2-BIMOTs-2,4-DCP powders were accomplished by kneading method according to the previous method (Cwiertnia *et al.*, 1999). 1 g of β-CD-1-BIMOTs was mixed with ethanol in a mortar and kneaded to form a paste. After that, an equimolar of 2, 4-DCP (0.1126 g, 6.91×10^{-4} mol) was added and the kneading process was continued for 1 hour and subsequently dried for constant mass affording white powdery precipitate. The same procedure was applied for β-CD-2-BIMOTs. The inclusion complex of 2,4-DCP with the β-CD-1-BIMOTs and β-CD-2-BIMOTs were observed through ^{1}H NMR and the 2D NOESY NMR analysis. From the analyses, the inclusion complex of β-CD-1-BIMOTs-2,4-DCP and β-CD-2-BIMOTs-2,4-DCP were identified and the geometrical interaction for the complex formations were proposed.

3.5.2 The preparation of β-CD-1-BIMOTs-2,4-DCP and β-CD-2-BIMOTs-2,4-DCP inclusion complexes for UV-Vis spectroscopy study

A 2.0 mL portion of 0.05 mmol L^{-1} 2,4-DCP aliquot and 3.2 mL of 0.0032 mol L^{-1} β-CD-1-BIMOTs were adjusted to pH 7.2 and transferred into 10 mL volumetric flask, diluted to the calibration mark with double distilled water. The absorption spectra of β-CD-1-BIMOTs-2,4-DCP complex was recorded against the blank that was prepared with the same reagent concentration. The absorption spectra of 2,4-DCP and β-CD-1-BIMOTs alone were also recorded. All of the spectra were recorded at 261 nm separately against

the blank reagent. For the formation of the constant curve, the concentration of 2,4-DCP was held constant at 0.05 mmol L^{-1} meanwhile the concentration of β-CD-1-BIMOTs was varied (0, 0.001, 0.002, 0.003, 0.004 and 0.005 mol L^{-1}). This procedure was in replicates by three or more. The inclusion complex of β-CD-1-BIMOTs with phenol, 2-chlorophenol, 3-chlorophenol and 4-chlorophenol were also prepared and examined. The same procedure was applied for β-CD-2-BIMOTs. From the data obtained, the formation constant were calculated using Benesi-Hildebrand equation (Eq. 3.8) (Wang *et al.*, 2007).

$$\frac{1}{A} = \frac{1}{\varepsilon[C]_0 K[CD]} + \frac{1}{\varepsilon[C]_0} \qquad (\mathbf{Eq.\,3.8})$$

Where,

A: Absorbance of the guest analyte solution at each β-CD derivative (β-CD-1-BIMOTs or β-CD-2-BIMOTs) concentration

$[C]_0$: The initial concentration of guest analyte

K: The apparent formation constant

[CD]: The concentration of β-CD-1-BIMOTs or β-CD-2-BIMOTs

ε: Molar absorptivity

CHAPTER 4: RESULTS AND DISCUSSION

4.1 Synthesis and the characterization of synthesized materials

The functionalization of β-CD was well described in Section 2.1.1 where there were three type of hydroxyl positions that were mainly possible for the substitution; i.e. C-6 (OH), C-3 (OH) and C-2 (OH). Previously, based on the report on the β-CD-IL prepared by Raoov, *et al.*, it shown that the IL had been installed on the C-6 (OH) position which was located on the primary rim of β-CD (Raoov *et al.*, 2013). Since the other two hydroxyl positions were located on the other rim of β-CD (secondary rim), the interaction of the analyte with the β-CD-ILs (the IL substituted at different position of hydroxyl group) was expected to be vary; even though the same IL was introduced. The explanation was illustrated as in Figure 4.1.

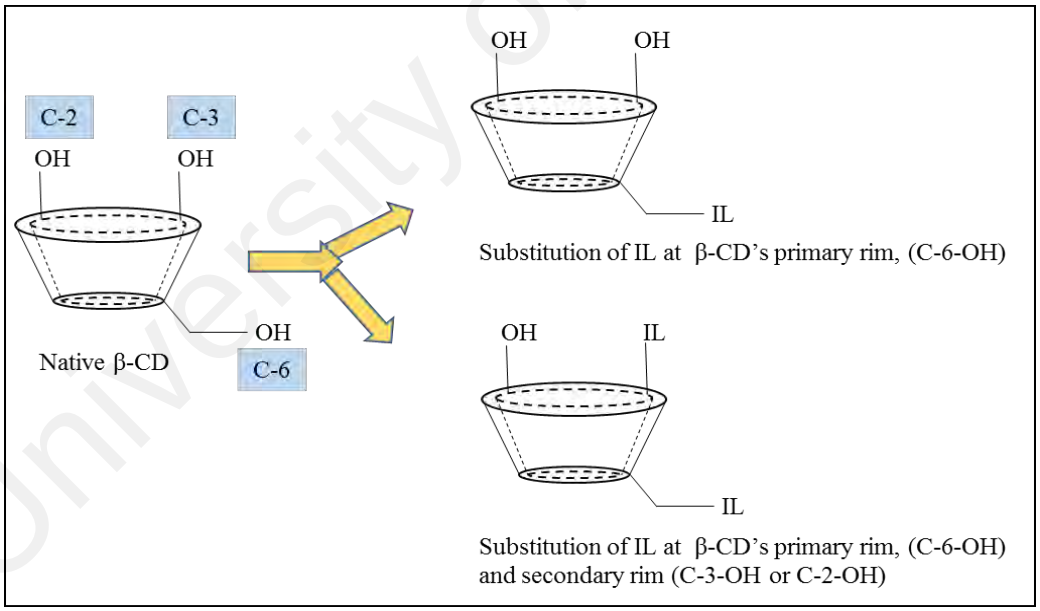

Figure 4.1: The positions of substituted IL on β-CD that possibly give different effect on the β-CD-IL-2,4-DCP inclusion complex

4.1.1 Nuclear magnetic resonance (NMR) analysis

4.1.1.1 β-CD-1-OTs and β-CD-2-OTs

Tosylate is an excellent leaving group for the nucleophilic substitution reaction on the tosylated-β-CD (Chen *et al.*, 2012; Jicsinszky *et al.*, 2016). The strong nucleophilic reagent of *p*-toluenesulfonyl anhydride gives a satisfactory yield of monotosylated β-CD (β-CD-1-OTs) (occurred at C-6 (OH)) (Zhong *et al.*, 1998). We managed to prepare this starting reagent with the percentage yield of 57% and the affordable reagent does not require any purification steps. Figure 4.2 showed that there are three signals in the ^{1}H NMR spectrum of *p*-toluenesulfonic anhydride. The singlet signal for the proton of methyl group attached to the benzene ring (H5) was located in the upfield region (δ = 2.243 ppm). The proton on the carbon (H3) were expected to be doublet (δ = 7.085-7.104 ppm). The adjacent proton (H2) which was nearer to the sulfur group appeared downfield as doublet at δ = 7.440-7.461 ppm.

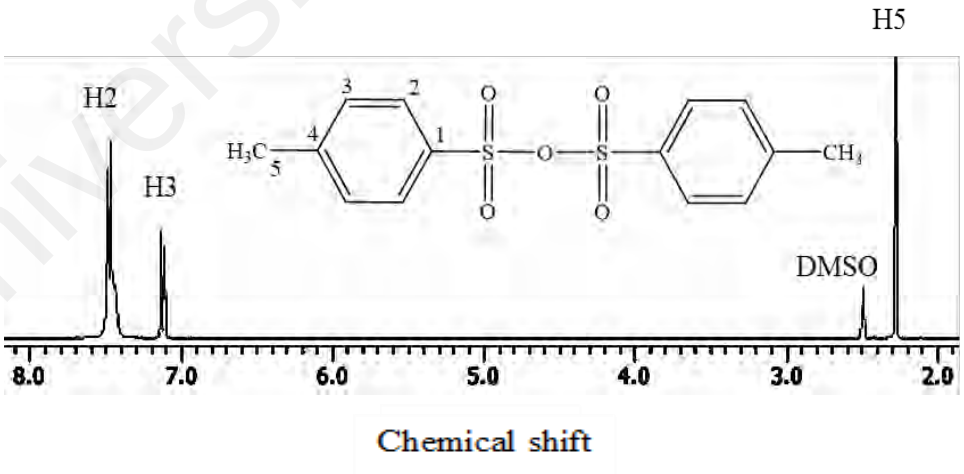

Figure 4.2: The ^{1}H NMR spectrum of *p*-toluenesulfonic anhydride

Subsequently, the 6-monodeoxy-6-tosyl-β-cyclodextrin precursor (monotosylated β-CD) was synthesized by the reaction of β-CD and *p*-toluenesulfonic anhydride in an alkaline aqueous medium (NaOH, 5% w/v). In this reaction, the proton at C-6-OH was removed and became O^-, which was substituted by the tosylate group affording a monotosylated β-CD (β-CD-1-OTs) intermediate. Figure 4.3 showed the spectrum of (a) β-CD, (b) β-CD-1-OTs and (c) β-CD-2-OTs in DMSO-D6 solvent where the resonance assignments were in a good agreement with the previous report (Raoov *et al.*, 2014). From Figure 4.3 (b), the monotosylation process on β-CD can be observed by the presence of a new resonance at δ= 7.43 ppm (H9) and δ= 7.75 ppm (H8) for β-CD-1-OTs which belong to the phenolic group protons of tosyl group. The other resonance was at δ= 2.43 ppm which stand for methyl proton of the tosylate group (H11).

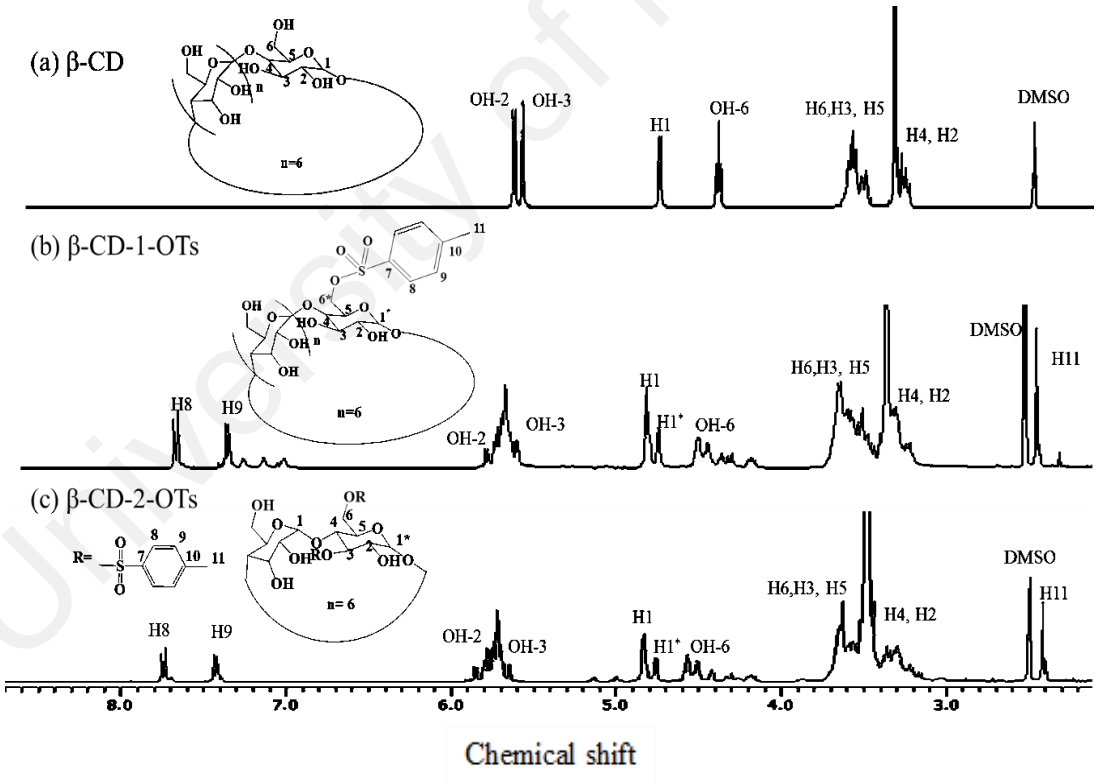

Figure 4.3: The ^{1}H NMR spectrum of (a) β-CD, (b) β-CD-1-OTs and (c) β-CD-2-OTs

The ditosylation process followed the method by Gonil *et al.* where *p*-toluenesulfonyl chloride (tosyl chloride) was used as a precursor (Gonil *et al.*, 2011). The concentration of NaOH used was increased up to 10% (w/v) in order to increase the percentage yield of

the ditosylated β-CD intermediate prepared as much as 22%. Figure 4.3 (c) showed the ^{1}H NMR spectra of β-CD-2-OTs in DMSO-D6. From β-CD-2-OTs spectrum, there were peaks of tosylate groups at δ = 7.74 and 7.43 ppm and methyl proton (H11) of tosylate group appeared at 2.42 ppm. A new peak (H1*) at δ=4.83 ppm that appeared in β-CD-2-OTs spectrum corresponded to substituted β-CD. The intensity of the C-6-OH peak at δ=4.1-4.6 ppm and C-3-OH δ=5.64 ppm were reduced upon the substitution at each positions. Meanwhile the intensity of C-2-OH peak at δ=5.72 ppm remained unchanged. This result confirmed the successful of ditosylation process on β-CD at C-6-OH and C-3-OH. The yield of β-CD-2-OTs was 20.02%.

Based on the ^{1}H NMR spectrum, the degree of tolylation (DT) of β-CD-1-OTs and β-CD-2-OTs were determined using Eq. (4.1).

$$\mathrm{DT}\ (\%) = \frac{(\mathrm{Ar}/_{4})}{\{[\mathrm{H1} - \mathrm{H6}]/7] \times 7\}} \times 100 \qquad (\mathbf{Eq.\ 4.1})$$

Where DT (%) is the degree of tolylation, Ar is the integral area of β-CD aromatic protons at δ7.8-7.4 ppm, and H1- H6 is the integral areas of the β-CD protons at δ5.9-3.2 ppm. Based on this equation, the degree of tolylation for β-CD-1-OTs was calculated to be 1.12 which is considered as 1 where it was proven that only one tosylation occurred on β-CD. Meanwhile, the DT for β-CD-2-OTs appeared to be 1.92 which is >1. This strengthen the occurrence of the ditosylation of β-CD backbones.

Nevertheless, the tosylation on C-3-OH did not meet the agreement with the reactivity of hydroxyl group of β-CD (C-6-OH> C-2-OH>C-3-OH). The C-3 secondary hydroxyl group of β-CD was actually less reactive than the C-2 secondary hydroxyl group due to the steric hindrance reason. However, in our case the second substitution was proven to occur at C-3 site instead of C-2. This was due to the property of C-3-OH that became more reactive under alkaline solution compared to the C-2-OH (Onozuka *et al.*, 1980).

Under an alkaline solution, the acidic tosyl chloride formed 1:1 complex inside the β-CD cavity. Under this condition, the sulfonyl group of the tosyl chloride is positioned nearer to both the secondary hydroxyl groups. However, the distance of sulfur was shorter towards C-3-OH compared to C-2-OH, making it easier to perform a specific monotosylation on the secondary OH via nucleophilic substitution at C-3-OH position after the first tosylation on C-6-OH (Onozuka *et al.*, 1980).

4.1.1.2 β-CD-1-BIMOTs and β-CD-2-BIMOTs

Figure 4.4 showed ^{1}H NMR spectra for (a) β-CD-1-BIMOTs and (b) β-CD-2-BIMOTs in DMSO-D6 solvent. From Figure 4.4 (a), the peak assignments for β-CD-1-BIMOTs were consistent with the result reported earlier by Raoov et al. (2014) (Raoov *et al.*, 2014). All benzylimidazole protons appeared downfield except for the proton located at the carbon in between benzene and imidazole group which was the Hg proton. The Hg proton appeared at δ= 4.93 ppm. The proton of imidazole ring (Hd, He, Hf) appeared at δ= 8.21 ppm, δ= 7.74 ppm and δ= 9.19 ppm; respectively. The Ha, Hb and Hc proton of the benzene ring appeared at δ=7.47 ppm, δ= 7.78 ppm and δ= 7.74 ppm; respectively. The new peak of H6* proton appeared after the functionalization occurred at C-6 at δ= 3.91 ppm. Based on the spectrum, the nucleophilic substitution process of benzylimidazole was clearly taken place on β-CD-1-OTs and affording this ionic liquid monofunctionalized β-CD compound. The yield of β-CD-1-BIMOTs was 81.63%.

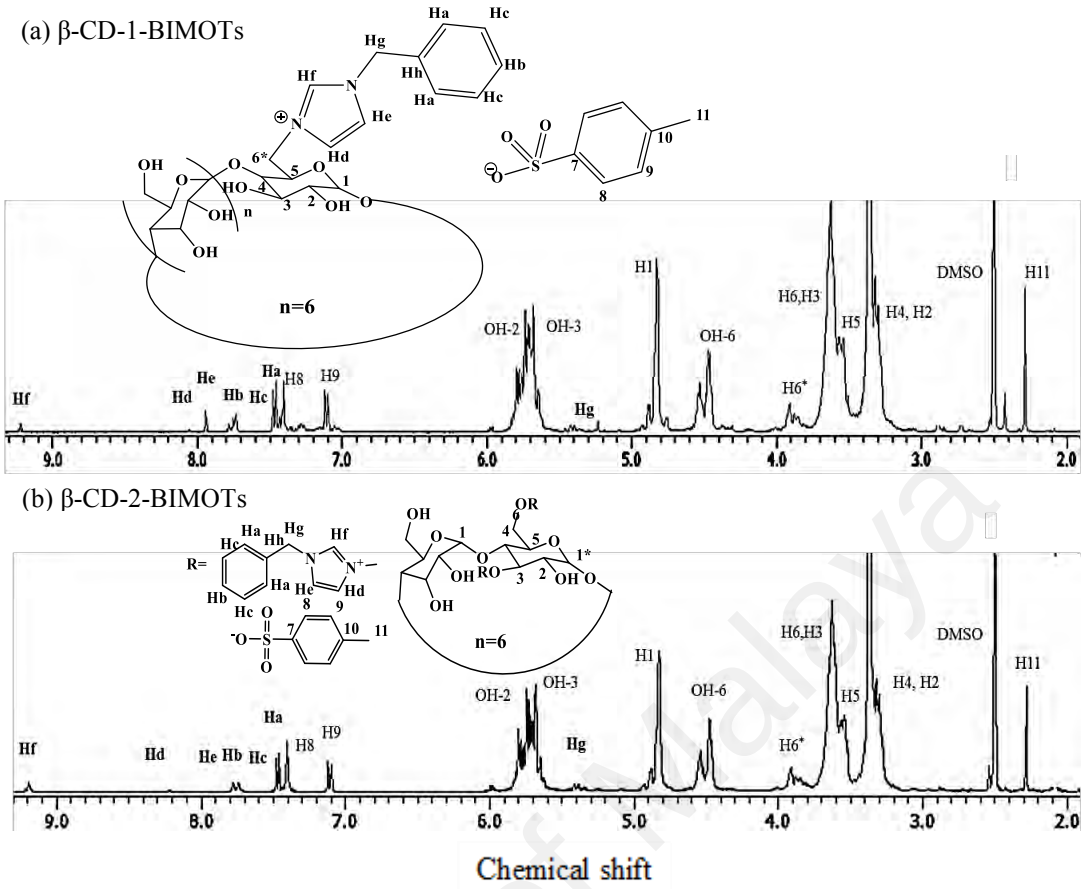

Figure 4.4: The ^{1}H NMR spectrum of (a) β-CD-1-BIMOTs and (b) β-CD-2-BIMOTs

The ^{1}H NMR spectrum (Figure 4.4 (b)) showed that β-CD-2-BIMOTs was successfully synthesized. There are protons of imidazole ring that appeared at the downfield region which is Hf (δ=9.17 ppm, s), Hd (δ=8.21 ppm, s) and He (δ=7.93 ppm, s). The aromatic protons of benzyl moiety (Ha, Hb, Hc) were observed at δ=7.47, δ=7.76 and δ=7.49 ppm; respectively. The methyl proton (Hg) that was attached to the carbon in between of imidazole and benzene ring appeared in the upfield region which was at δ=5.3-5.5 ppm. There was a new peak that appeared at δ=3.99 ppm, corresponding to the proton H6* of the functionalized β-CD. Based on the spectrum, it was confirmed that the ditosylation of β-CD-2-OTs was successful affording β-CD-2-BIMOTs with the percentage yield of 87.5%.

4.1.2 Fourier Transform Infrared (FTIR) analysis

The tosylation as well as the ionic liquid functionalization processes on β-CD were monitored with Fourier transform infra-red (FTIR) spectroscopy. Figure 4.5 showed the FTIR spectra for β-CD, the synthesized precursors and β-CD-ILs. The characteristic wavenumber of (a) β-CD were observed at all spectra where the OH, C-H and C=C stretching appeared approximately at 3291 cm^{-1}, 2924 cm^{-1} and 1636 cm^{-1}; respectively. The SO_2 asymmetric and symmetric peak appeared around 1362 cm^{-1} and 1167 cm^{-1} respectively for both (b) β-CD-1-OTs and (c) β-CD-2-OTs, proving that the tosylation successfully took part on β-CD. Further reaction for replacing the tosylate group with benzylimidazole group resulted in the extra C-N peak which appear approximately at 1152 cm^{-1} and 1154 cm^{-1} for both (d) β-CD-1-BIMOTs and (e) β-CD-2-BIMOTs respectively with the intensity for asymmetric and symmetric peak of SO_2 becoming less observable.

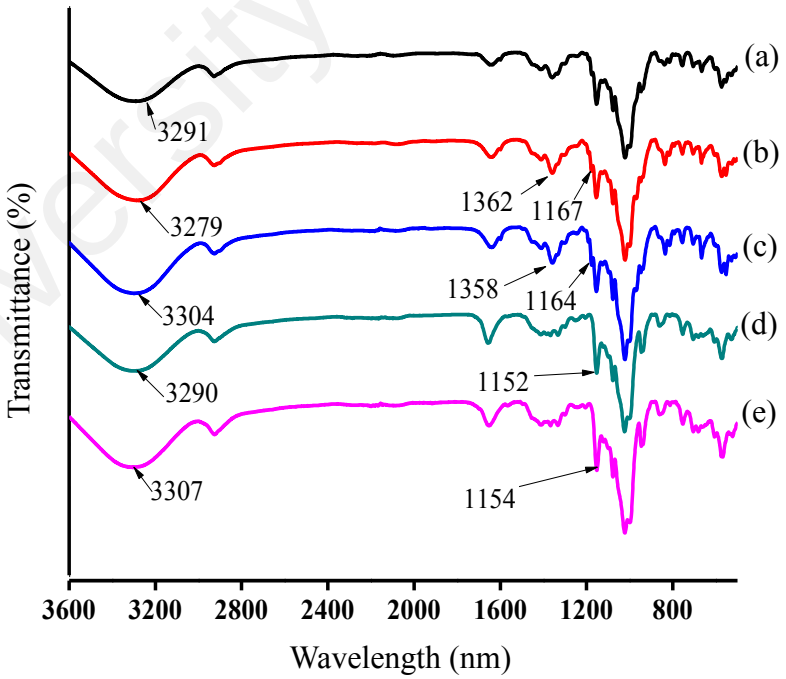

Figure 4.5: FTIR spectra of (a) β-CD, (b) β-CD-1-OTs (c) β-CD-2-OTs, (d) β-CD-1-BIMOTs and (e) β-CD-2-BIMOTs

4.1.3 Energy Dispersive X-rays (EDX) analysis

The elemental analysis was performed on β-CD-1-BIMOTs and β-CD-2-BIMOTs to ascertain the modification. The energy dispersive x-ray (EDX) analysis was conducted to determine the quantitative composition of both modified β-CDs. From Figure 4.6, the EDX analysis confirmed the presence of IL and β-CD in the β-CD-1-BIMOTs (Figure 4.6 (a)) and β-CD-2-BIMOTs (Figure 4.6 (b)) with the C, N, O and S signals. The N content contributed by the imidazolium group of the cationic part of the IL whereas the S content belonged to the tosylate anion of the IL component. From the results, the weight percentage of sulfur (S) content in β-CD-2-BIMOTs was higher (2.03%) than in β-CD-1-BIMOTs (0.96%). This result had proven that β-CD was successfully difunctionalized with IL.

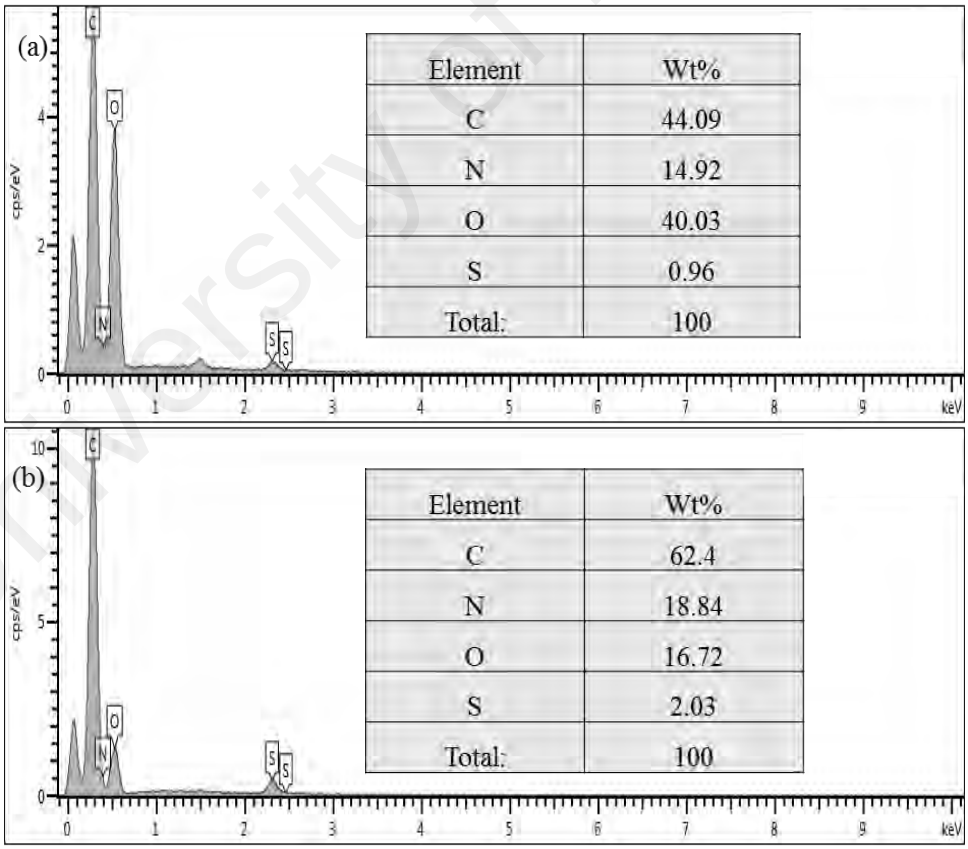

Element	Wt%
C	44.09
N	14.92
O	40.03
S	0.96
Total:	100

Element	Wt%
C	62.4
N	18.84
O	16.72
S	2.03
Total:	100

Figure 4.6: EDX spectra of (a) β-CD-1-BIMOTs and (b) β-CD-2-BIMOTs

4.1.4 X-Ray Diffraction (XRD) analysis

The XRD diffractogram of β-CD-1-BIMOTs and β-CD-2-BIMOTs were demonstrated in Figure 4.7. The XRD pattern of β-CD indicated high crystallinity in β-CD due to the characteristic sharp peak at 2θ = 9.12°, 10.81°, 12.63°, 13.76° and 18.23°. Based on Figure 4.7, the native β-CD crystal structure was classified as a typical cage-like structure. The substitution of the IL was found to alter the original crystal lattice of β-CD and its x-ray diffraction pattern. The XRD profiles for β-CD-1-BIMOTs and β-CD-2-BIMOTs had shown low crystallinity with numerous weaker intensity peak. The diffraction pattern of β-CD-2-BIMOTs was quite similar to that of β-CD-1-BIMOTs. However, it had shown a marked decrease in the intensity of the diffraction peaks compared to β-CD-1-BIMOTs. The changes in the diffraction peak intensity had proven that the new β-CD derivatives had successfully formed with some of β-CD characteristic peaks remained observable for both compounds.

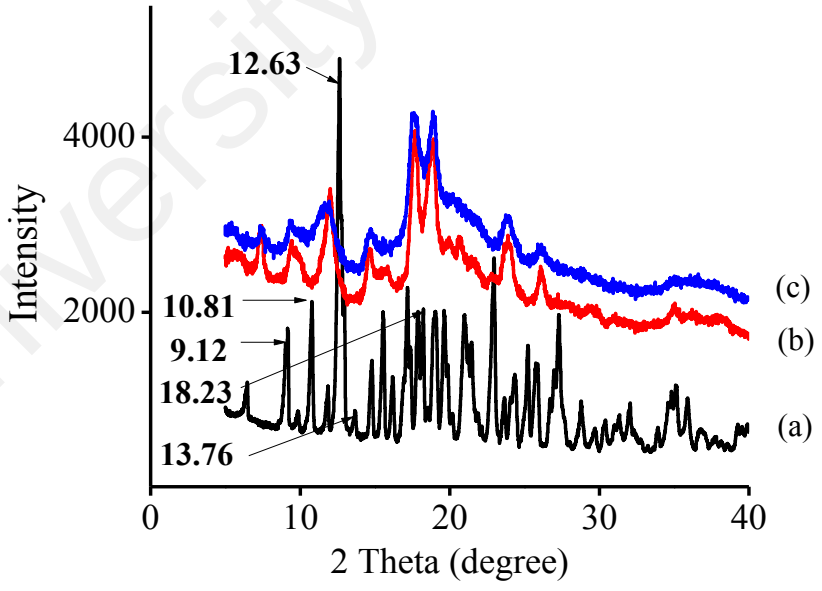

Figure 4.7: XRD analysis of (a) β-CD, (b) β-CD-1-BIMOTs and (c) β-CD-2-BIMOTs

4.1.5 Brunauer-Emmet-Teller (BET) analysis

Figure 4.8 showed the nitrogen adsorption–desorption of β-CD-1-BIMOTs and β-CD-2-BIMOTs. The nitrogen adsorption–desorption analysis was used to determine the Brunauer-Emmet-Teller (BET) surface area, total pore volume and pore size of the compounds. The surface area, pore size and total pore volume of β-CD-1-BIMOTs and β-CD-2-BIMOTs was calculated and summarized in Table 4.1. From the diagram (Figure 4.8), it had shown that β-CD-1-BIMOTs and β-CD-2-BIMOTs exhibited a resolved type IV isotherm with a steep desorption branch and the H3 type hysteresis loop according to the IUPAC (Sing, 1985). This indicated that the materials were having mesoporous structures. From the BJH pore size (Table 4.1), β-CD-1-BIMOTs was a mesoporous material with the pore size of 35.68 nm and pore volume of 3.86 $\times 10^{-9}$ m^3/g. The β-CD-2-BIMOTs mesoporous size was smaller than β-CD-1-BIMOTs which was 26.31 nm with its total pore volume of 6.14 $\times 10^{-9}$ m^3/g. The BET specific surface area of ionic liquid monofunctionalized β-CD (β-CD-1-BIMOTs) was 3.08 m^2/g. However, the specific surface area of IL difunctionalized β-CD (β-CD-2-BIMOTs) was calculated to be lower (1.88 m^2/g) than β-CD-1-BIMOTs.

According to the prevalence study, the modification of IL on the surface of β-CD cavity had covered the adsorption sites by the organic moiety (IL group and tosylate ion) and consequently reducing the adsorption of N_2 onto the binding sites (Alahmadi *et al.*, 2012; Raoov *et al.*, 2014). For our case, the β-CD-1-BIMOTs had one functionalized IL moiety that was capable of covering the primary surface of the β-CD cavity. The ionic liquid difunctionalized β-CD (β-CD-2-BIMOTs) had the IL moieties covering both sides of the cavity. From this phenomenon, we can deduce that the increase of IL substituents had 'masking' the adsorption of N_2 hence reducing the specific surface area of the material. The increase of IL moieties (β-CD-2-BIMOTs) will make the binding sites

unavailable for the adsorption and this explained why the specific surface area of β-CD-2-BIMOTs was lower than β-CD-1-BIMOTs.

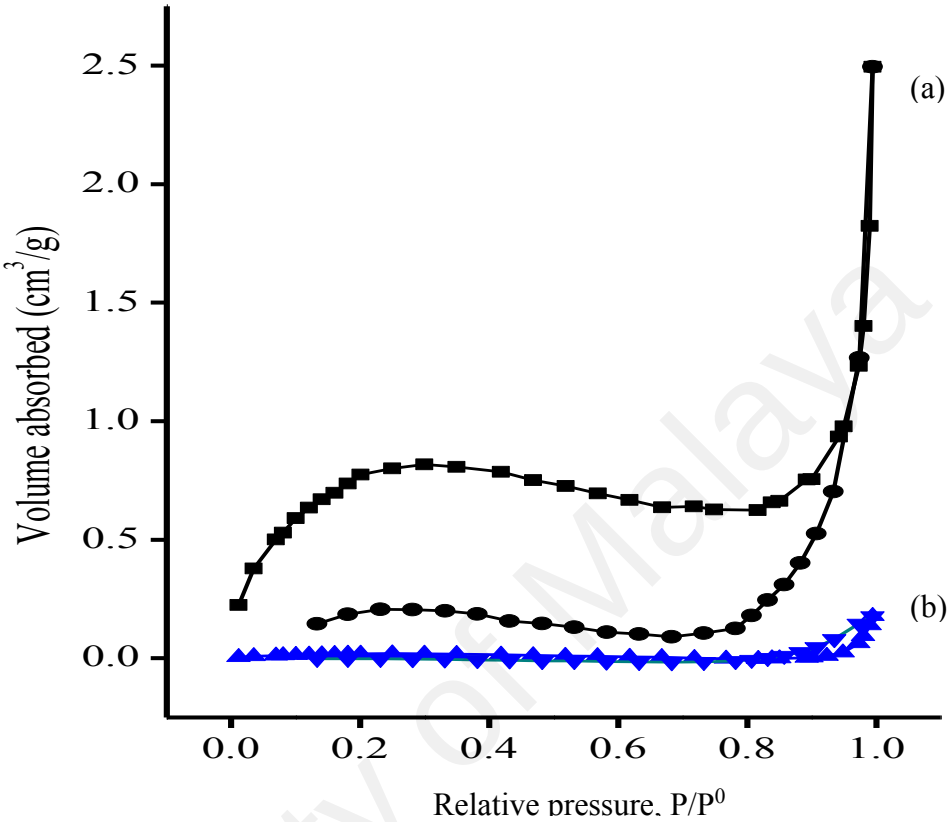

Figure 4.8: Nitrogen adsorption-desorption profiles (a) β-CD-1-BIMOTs and (b) β-CD-2-BIMOTs

Table 4.1: Structural parameters of the synthesized compounds

Compounds	Specific surface area (m^2/g)	Total pore volume $\times 10^{-9}$ (m^3/g)	Average pore size (nm)	Pore size distribution
β-CD-1-BIMOTs	3.08	3.86	35.68	>2 nm,<50nm (mesopore)
β-CD-2-BIMOTs	1.88	6.14	26.31	>2 nm,<50nm (mesopore)

4.2 The electrochemical study of 2,4-DCP at β-CD-ILs modified carbon paste electrodes

The chemical modification of hydroxyl group of the primary surface (C-6 position) and the secondary surface (C-2 and C-3 positions) gave different properties to β-CD hence it was a good opportunity to explore and investigate the capability of modified β-CD towards the target analyte using sensor application. Herein, we developed a sensor system by taking advantage on the interaction of 2,4-DCP with β-CD-ILs where the position and the number of IL substitution on β-CD was the major concern. Two characterization studies and electrochemical methods were applied and monitored to this new modified carbon paste electrodes in order to assure the successfulness of this study.

4.2.1 Characterization of the new carbon paste modified electrodes

4.2.1.1 Field Emission Scanning Electron Microscopy (FESEM)

The physical morphology of the electrode surface material had greatly influenced its detection ability towards the target analyte. The morphology of CPE, β-CD/CPE, β-CD-1-BIMOTs/CPE and β-CD-2-BIMOTs were shown in Figure 4.9. A typical morphological surface of CPE was observed as in Figure 4.9 (a), where it consisted of the isolated and unorganized flake graphite with clearly distinguished layer. In Figure 4.9 (b), a more dense and solid surface structure with slight blurry shape was observed on the surface of β-CD/CPE. Meanwhile, the fabrication of ionic liquid monofunctionalized β-CD on CPE (β-CD-1-BIMOTs/CPE) as displayed in Figure 4.9 (c) clearly changed the physical morphology of CPE into a uniform solid surface structure with the flake graphite merely invisible. From Figure 4.9 (d), it can be seen that there are a majorly uniform surface structure with insignificant layer of graphite flake upon addition of β-CD-2-BIMOTs as well.

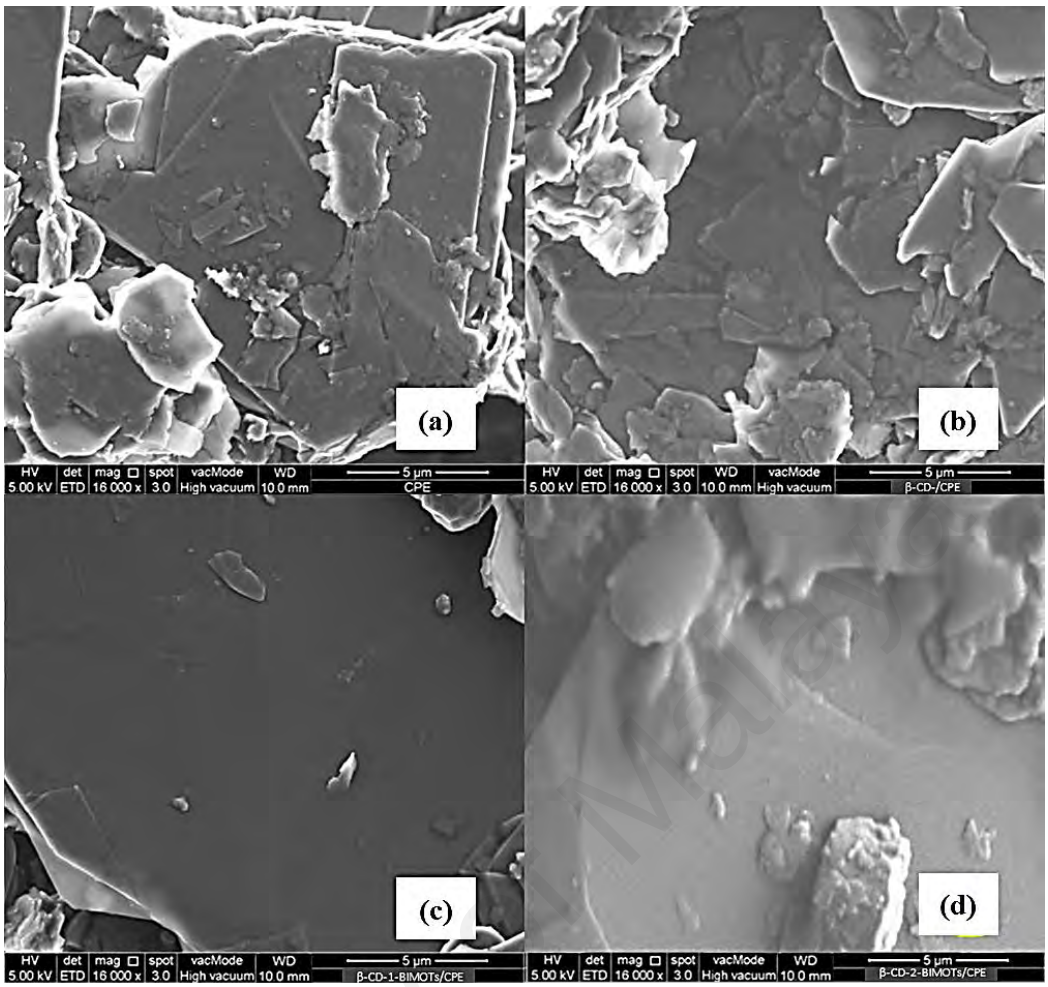

Figure 4.9: Surface morphology images of (a) CPE (b) β-CD/CPE (c) β-CD-1-BIMOTs/CPE and (d) β-CD-2-BIMOTs/CPE

There were plenty of reports that had described the use of IL as binder for electrode materials and it was proven that the IL acted as the ion carrier between carbon layers, which lead to improve conductive performance of the electrode (Liu *et al.*, 2005; Yu *et al.*, 2013). Only few reports had mentioned the use of solid form of IL as electrode modifiers. For example, Yaman *et al.* had described the use of IL as modifier for Bismuth/graphite electrode (Yaman *et al.*, 2018). According to the study, the electrodeposit ion of IL onto Bismuth/graphite had contributed to a uniform and cloudy surface morphology as a result of masking and adhesive effect of IL. Based on the study, it was believed that the uniformity of the surface that was observed in Figure 4.9 (c) and (d) were mainly caused by IL component. However, further investigation on the contribution of different number of IL substitution on β-CD/CPE surface was necessary.

4.2.1.2 Electrochemical characterization of the working electrodes by cyclic voltammetry using ferricyanide-ferrocyanide redox couple

The ferricyanide/ferrocyanide is one type of redox couple that has been extensively used for electrochemical characterization of new electrode materials (Scialdone *et al.*, 2012). In this study, the electrochemical behavior of the 40×10^{-6} mol L^{-1} of $[Fe(CN)_6]^{3-}$ /$[Fe(CN)_6]^{4-}$ was investigated in 0.1 mol L^{-1} of KCl solution at different electrodes i.e. CPE, β-CD-CPE, β-CD-1-BIMOTs/CPE and β-CD-2-BIMOTs/CPE with various scan rates (0.01 - 0.30 Vs^{-1}). The reduction and oxidation of redox couple preceded via one electron transfer process, as shown in Eq. 4.1 (Collyer *et al.*, 2003):

$$Fe^{(III)}(CN)_6^{3-} + e^- \leftrightharpoons Fe^{(II)}(CN)_6^{4-} \quad \textbf{(Eq. 4.1)}$$

Where the e^- is the exchanged electron.

The cyclic voltammogram for the redox reaction of $[Fe(CN)_6]^{3-}$/$[Fe(CN)_6]^{4-}$ at all electrode surfaces were shown in Figure 4.10 (a-d). From Figure 4.10, it was clear that a pair of well resolved redox can be observed in all voltammograms. In order to determine the number of electron transfer that was involved in the reaction and the reversibility of reaction, the anodic peak current to cathodic peak current ratio (i_{pa}/i_{pc}) and the peak to peak separation (ΔE) were calculated and tabulated in Table 4.2. From Table 4.2, the peak current ratio of the anodic and cathodic scan for the redox couple at all electrode surfaces were close to unity ($i_{pa}/i_{pc} = 1$, corresponding to one electron transfer) with the ΔE were in the range of 83 – 176 mV indicating that the electrode processes of $[Fe(CN)_6]^{3-}$ /$[Fe(CN)_6]^{4-}$ were reversible (Scialdone *et al.*, 2012).

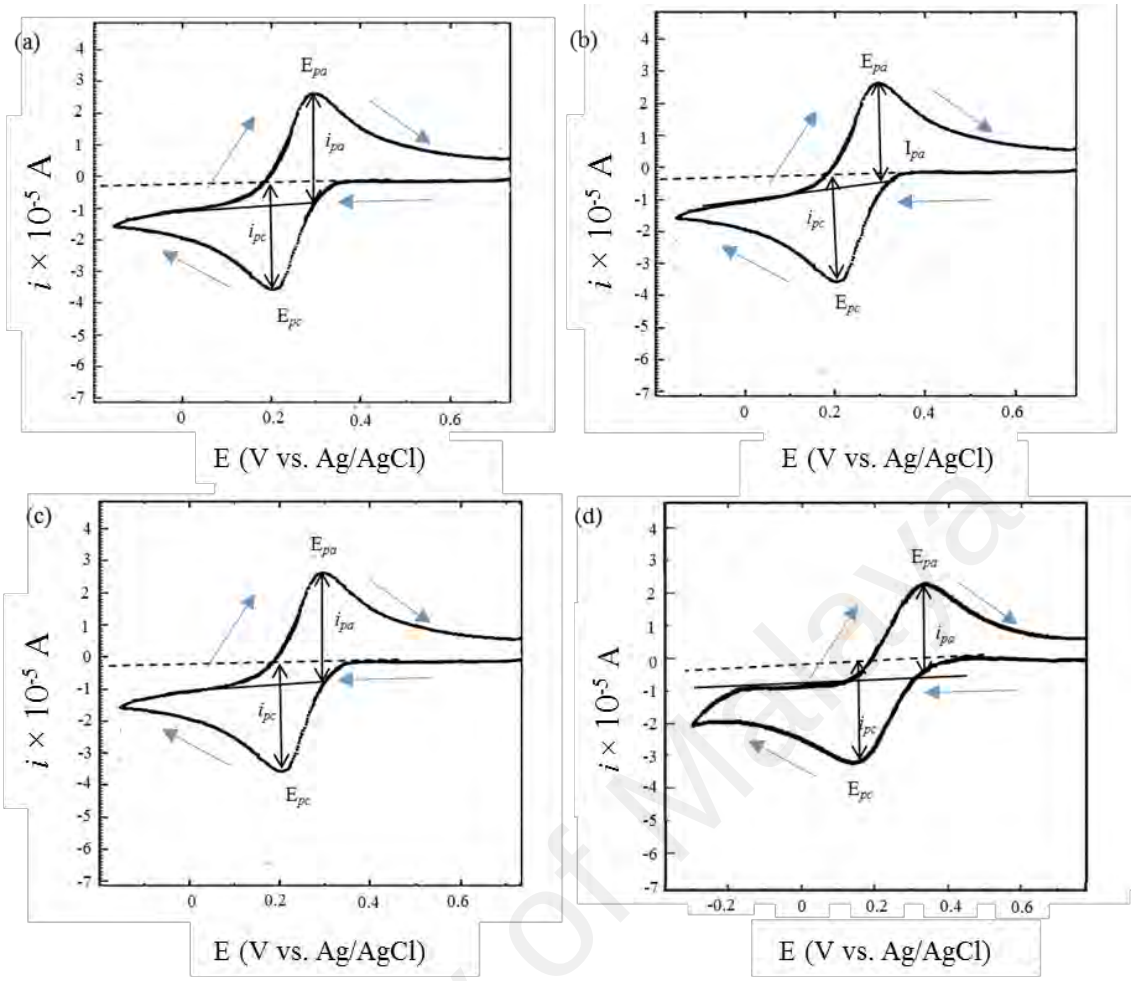

Figure 4.10: The cyclic voltammogram of solution containing of 40 × 10^{-6} mol L^{-1} $[Fe(CN)_6]^{3-}/[Fe(CN)_6]^{4-}$ couple at the surface of (a) CPE, (b) β-CD-CPE, (c) β-CD-1-BIMOTs/CPE and (d) β-CD-2-BIMOTs/CPE with scan rate of 0.1 Vs^{-1}

Table 4.2: The calculated i_{pa}/i_{pc} and ΔE for all studied electrodes

Type of electrode materials	i_{pa} , ×10^{-5} A	i_{pc}, ×10^{-5} A	E_{pa}, mV	E_{pc}, mV	i_{pa}/i_{pc}	ΔE= E_{pc}- E_{pa}
CPE	3.50	3.40	292.05	209.05	1.03	83.0
β-CD-CPE	3.25	3.45	318.91	174.87	0.94	144.0
β-CD-1-BIMOTs/CPE	3.55	3.45	316.47	172.42	1.03	114.1
β-CD-2-BIMOTs/CPE	2.95	3.10	326.20	150.45	0.95	175.8

The relationship between current response, i of $Fe(CN)_6]^{3-}$ and the scan rates was further investigated. Figure 4.11 showed the voltammogram of different scan rates (v) for $Fe(CN)_6]^{3-}$ and the plot of i versus square roots of scan rate ($v^{1/2}$) at all electrode surfaces. Based on the scan rate from 0.01 to 0.30 Vs^{-1} (Figure 4.11 (A(b), B(b), C(b) and D(b)), all i response values showed a good linear relationship with $v^{1/2}$ with a good regression ranging from 0.9728 to 0.9981%. These results proved that the electrode reactions were diffusion-controlled.

As a reversible system, the peak current for $[Fe(CN)_6]^{3-}/[Fe(CN)_6]^{4-}$ redox couple at 25°C was given by Randles-Sevcik equation (Eq. 4.2)(Wang & Zhang, 1994):

$$i_p = (2.69 \times 10^5) n^{3/2} A C D^{1/2} v^{1/2} \qquad \textbf{(Eq. 4.2)}$$

Where n is the number of electrons, A is the electrode area (in cm^2), C the concentration (in mol/cm^3), D the diffusion coefficient (in cm^2/s), and v the potential scan rate (V/s). From this equation, the diffusion coefficient (D) was calculated for all electrode surfaces based on the plot of i against $v^{1/2}$ (reduction process) as in Figure 4.11 A(b), B(b), C(b) and D(b) plots. The linear equations and the diffusion coefficient for all electrodes were tabulated in Table 4.3.

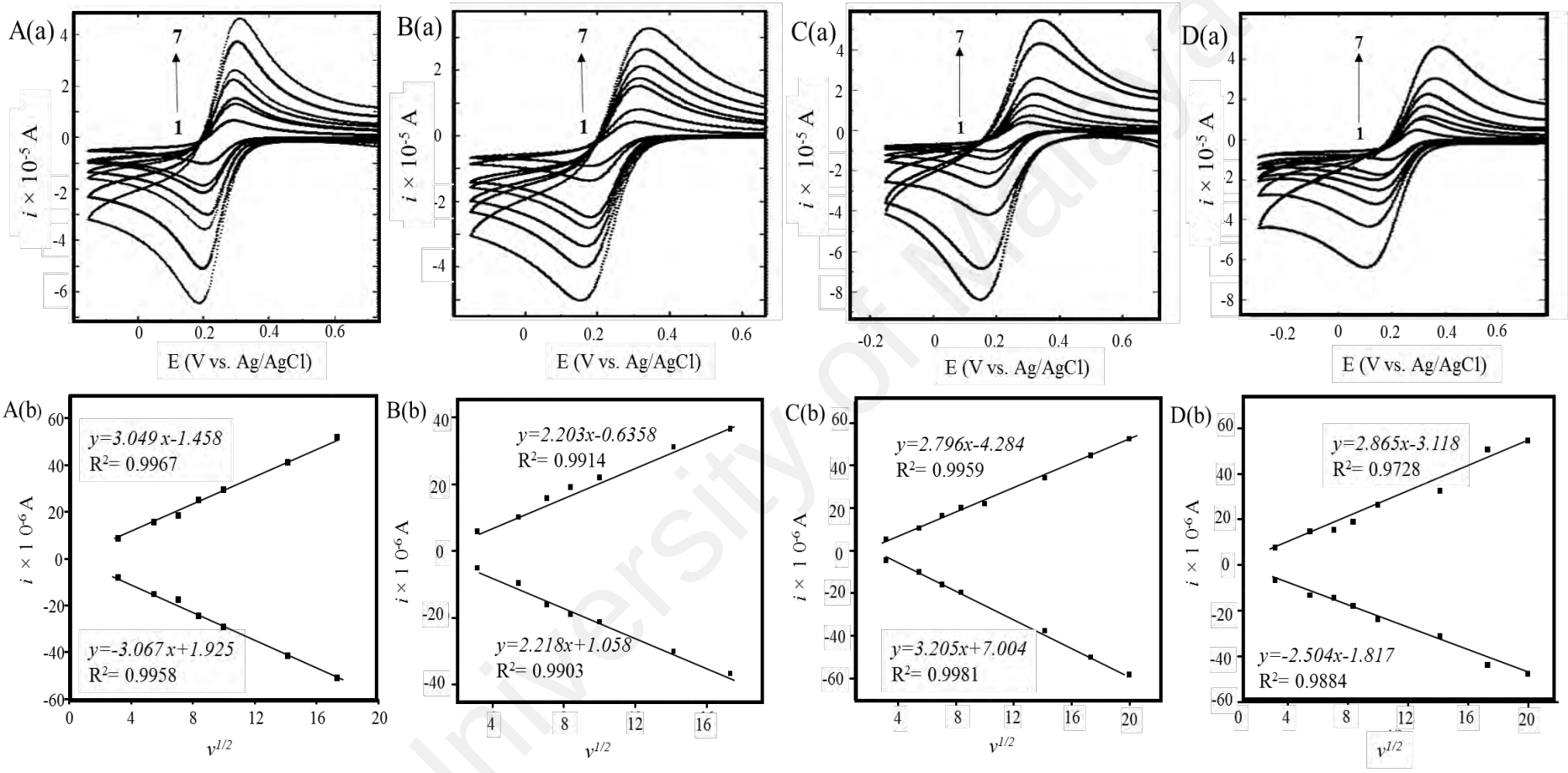

Figure 4.11: Cyclic voltammogram of 0.1 mol L^{-1} KCl solution containing of 40 × 10^{-6} mol L^{-1} $K_3[Fe(CN)_6]$ at the surface of A(a) CPE, B(a) β-CD/CPE, C(a) β-CD-1-BIMOTs/CPE and D(a) β-CD-2-BIMOTs/CPE at different *v*:1→7 correspond to 0.01, 0.03, 0.05, 0.07, 0.10, 0.20 and 0.30 Vs^{-1}, respectively. The plot of *i* against $v^{1/2}$ of $K_3[Fe(CN)_6]$ for A(b) CPE, B(b) β-CD/CPE, C(b) β-CD-1-BIMOTs/CPE and D(b) β-CD-2-BIMOTs/CPE electrodes

Table 4.3: Linear equations for i versus $v^{1/2}$ for $[Fe(CN)_6]^{3-}/[Fe(CN)_6]^{4-}$ redox couple at all electrodes and the calculated value of the diffusion coefficient (D) based on reduction process

Electrode surface	Linear equations	Diffusion coefficient (D), (cm^2/s)
CPE	$i = -3.067v^{1/2} + 1.925$	1.57×10^{-6}
β-CD/CPE	$i = -2.218v^{1/2} + 1.058$	0.82×10^{-6}
β-CD-1-BIMOTs/CPE	$i = -3.2501v^{1/2} + 7.004$	1.32×10^{-6}
β-CD-2-BIMOTs/CPE	$i = -2.504v^{1/2} + 1.817$	1.39×10^{-6}

From Table 4.3, the highest D value for ferricyanide/ferrocyanide redox couple was found using CPE which is 1.57×10^{-6} cm^2/s. The value of D is reduced upon the use of β-CD/CPE which is 0.82×10^{-6} cm^2/s. The introduction of ionic liquid monofunctionalized β-CD (β-CD-1-BIMOTs) on CPE has increased back the D value to 1.32×10^{-6} cm^2/s. Further increase of D value is observed using β-CD-2-BIMOTs/CPE (1.39×10^{-6} cm^2/s). The non-modified surface of CPE allow a non-selective accumulation of the ferricyanide. It is easier for the analyte to diffuse and being accumulated at the electrode surface without any barrier a with respective diffusion rate (in this case 1.57×10^{-6} cm^2/s). The β-CD was solely introduced for a selective guest accumulation on the β-CD/CPE. Since there is host-guest interaction complex occurred between ferricyanide and β-CD, there is no vacancy for the free molecule (ferricyanide) to be accumulated at the β-CD/CPE surface hence lowering the diffusion coefficient value from 1.57×10^{-6} cm^2/s to 0.82×10^{-6} cm^2/s.

From Table 4.2, the E_{pa} value for the oxidation of ferricyanide has been positively shifted indicates that the oxidation center of analyte was included in β-CD cavity. This lead to a more difficult oxidation process since the complex dissociation has been taken

place before the electron transfer process (Fritea *et al.*, 2015). The fabrication of β-CD-1-BIMOTs on CPE resulting an increase in diffusion coefficient value to 1.32×10^{-6} cm^2/s. The interaction between β-CD-1-BIMOTs and ferricyanide not only occurred inside the cavity, it is highly suspected that the IL has promoted the accumulation of ferricyanide at the β-CD-1-BIMOTs hydrophilic surface through a π-π and electrostatic interactions .The diffusion coefficient value was further increase with the use of ionic liquid difunctionalized β-CD (β-CD-2-BIMOTs) since the there is an increase of π-π and electrostatic interactions at β-CD-2-BIMOTs hydrophilic surface (1.39×10^{-6} cm^2/s). Further investigation on the effect of the number of IL and its substitution position (the geometry of the host) is very necessary to understand the host guest interaction between β-CD-ILs and the analyte of interest.

4.2.2 Recognition and response of the native and modified CPEs to 2,4-DCP

In this part of study, the electrochemical behavior of 50×10^{-6} mol L^{-1} of 2,4-DCP in 0.1 mol L^{-1} phosphate buffer solution (PBS, pH 7.2) were investigated at CPE, β-CD/CPE, β-CD-1-BIMOTs/CPE, β-CD-2-BIMOTs/CPE by cyclic voltammetry technique and the *v* applied was 0.10 Vs^{-1} (Figure 4.12). First, the electrochemical reaction of 2,4-DCP was investigated on the native CPE. Figure 4.12 (a) showed an irreversible oxidation peak of 2,4-DCP at 0.66 V with the *i* value of 4.43×10^{-7} A.

Then, the investigation was preceded with the native β-CD modified CPE (β-CD/CPE). Figure 4.12 (b) showed the same irreversible oxidation peak of 2,4-DCP at β-CD/CPE where the oxidation peak position shifted to a more positive value at 0.70 V with the *i* value of 4.50×10^{-7} A. The presence β-CD on the electrode surface had provided an artificial receptor to the CPE. Other than that, the fabrication of β-CD has increase the electrode surface active site at CPE for heterogeneous electron transfer hence enhancing the charge transfer at the electrode and electrolyte interface (Zhang *et al.*, 2014). This

explained the increment of the *i* response value for the oxidation of 2,4-DCP at β-CD/CPE compared to CPE.

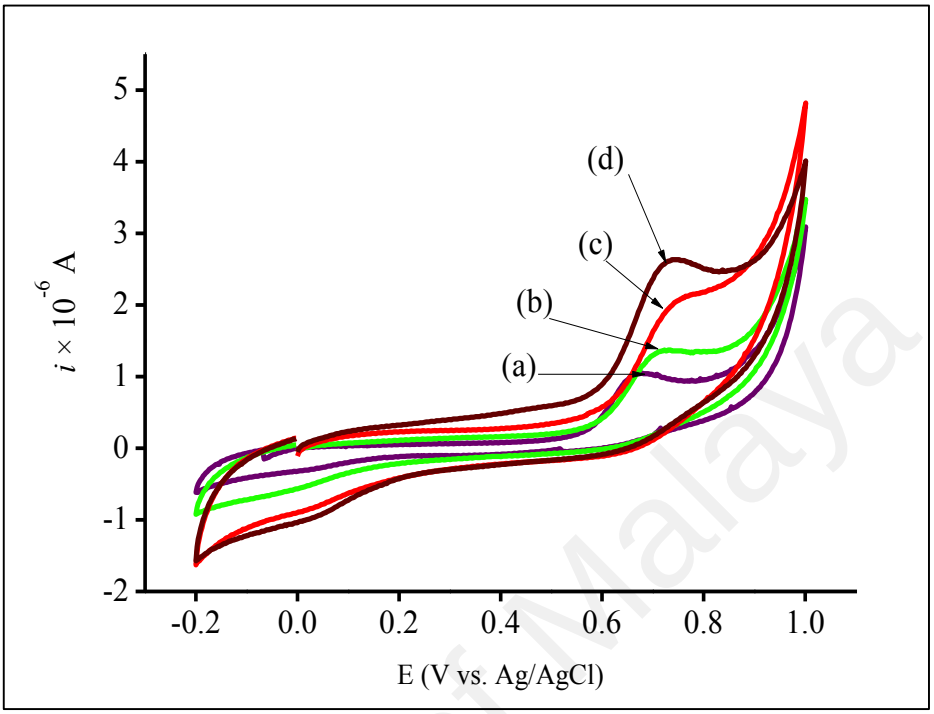

Figure 4.12: The cyclic voltammogram of solution (pH 7.2) containing of 50×10^{-6} mol L^{-1} of 2,4-DCP at the surface of (a) CPE, (b) β-CD/CPE, (c) β-CD-1-BIMOTs/CPE and (d) β-CD-2-BIMOTs/CPE with the scan rate (*v*) of 0.10 Vs^{-1}.

In the meantime, the oxidation of 2,4-DCP at β-CD-1-BIMOTs/CPE and β-CD-2-BIMOTs/CPE can be observed in Figure 4.12 (c) and (d); respectively. The oxidation of 2,4-DCP at β-CD-1-BIMOTs/CPE occurred at 0.73 V with the *i* value of 5.54×10^{-7} A, which was higher than the *i* response at CPE and β-CD /CPE. Finally, at the β-CD-2-BIMOTs/CPE, the 2,4-DCP underwent the oxidation at the peak potential of 0.72 V with the *i* value of 9.79×10^{-7} A. The highest *i* response was observed at β-CD-2-BIMOTs/CPE. This demonstrated that the presence of IL was responsible for the greater enhancement of the oxidation peak current of 2,4-DCP at β-CD-1-BIMOTs/CPE and β-CD-2-BIMOTs/CPE compared to the native CPE and β-CD/CPE.

Previous study had shown that the 2,4-DCP had a strong binding affinity towards β-CD-1-BIMOTs (Raoov *et al.*, 2013). Raoov *et al.* reported that the interaction between

the β-CD-1-BIMOTs host and 2,4-DCP (guest) had occurred not only via inclusion complex, but also governed by electrostatic and π-π interactions. The hydrophobic truncated cage of β-CD provides room for the formation of a stable inclusion complex with the guest analyte. Meanwhile, the imidazolium ring of the IL substituent interacted with 2,4-DCP through electrostatic and π-π interactions and triggered the compound to be more selective towards the targeted analyte. The imidazolium ring that bears a positive charge had promoted the access of 2,4-DCP towards the electrode surface, hence increasing the chance of the 2,4-DCP to undergo the electrochemical oxidation.

Besides, the modification of CPE with β-CD had shifted the peak potential value to a more positive value which was from 0.66 V (CPE) to 0.70 V (β-CD/CPE) and 0.72 V (β-CD-1-BIMOTs/CPE). The inclusion complex between β-CD and 2,4-DCP had increased the activation energy of the oxidation reaction in the β-CD cavity thus requiring an extra potential for anodic reaction to occur. From the voltammogram of Figure 4.12 (d), it was noticed that the disubstitution of IL on β-CD had shifted the peak potential value of 2,4-DCP from 0.73 V to 0.72 V. It is suspected that as the number of IL increased, the ionic conductivity of the β-CD-2-BIMOTs/CPE increased and the number of 2,4-DCP that was promoted to the electrode surface was also higher compared to β-CD-1-BIMOTs/CPE. Therefore, this explained why the value of *i* response at β-CD-2-BIMOTs/CPE was almost 1.8 times fold higher than β-CD-1-BIMOTs/CPE.

4.2.3 The investigation on the effect of modifier's percentage on CPE towards the current response of 2,4-DCP

The effect of electrode composition on the voltammetric current response, *i* has been evaluated using cyclic voltammetry analysis. The best and optimum ratio of graphite: paraffin oil: modifier (β-CD-1-BIMOTs and β-CD-2-BIMOTs) was the ratio that give the highest *i* value as the result of the oxidation of 2,4-DCP at modified CPEs. The amount

of β-CD-1-BIMOTs and β-CD-2-BIMOTs modifiers added to the carbon paste material gave a significant influence on the voltammetric response. Therefore, the percentage of the modifiers (β-CD-1-BIMOTs and β-CD-2-BIMOTs) and the graphite were varied in w/w % while the amount of paraffin oil used were fixed to a certain percentage throughout the experiment. Table 4.4 summarized the details for the electrode compositions of the modified CPE and their respective *i* response of the oxidation of 2,4-DCP. The plot of the *i* response against the percentage of the both modifiers and graphite were shown in Figure 4.13.

From Figure 4.13, it is shown that as the percentage of β-CD-1-BIMOTs and β-CD-2-BIMOTs changed from 11.3% to 18.9%, the value of *i* response was increased from $(0.20 \pm 0.01) \times 10^{-6}$ to $(0.40 \pm 0.01) \times 10^{-6}$ A and $(0.33 \pm 0.01) \times 10^{-6}$ to $(0.42 \pm 0.02) \times 10^{-6}$ A; respectively. The *i* values were decreased as the percentage of both β-CD-1-BIMOTs and β-CD-2-BIMOTs was increased from 18.9% to 24.9%. However, there was a slight increase in *i* value when 29.7 % of β-CD-1-BIMOTs was used. Further increased of the percentage of β-CD-1-BIMOTs at 33.7% and 36.9 % showed a reduced in *i* values to $(0.24 \pm 0.01) \times 10^{-6}$ A and $(0.26 \pm 0.02) \times 10^{-6}$ A; respectively.

Table 4.4: Optimization of the electrode compositions

Percentage, (w/w)%			**Current responses, *i***			
Graphite	**Paraffin oil**	**Modifier**	**β-CD-1-BIMOTS/CPE**		**β-CD-2-BIMOTS/CPE**	
			$\times 10^{-6}$ A	**Deviation**	**$\times 10^{-6}$ A**	**Deviation**
61.7	27	11.3	0.20	0.01	0.33	0.01
54.1	27	18.9	0.40	0.01	0.42	0.02
48.1	27	24.9	0.31	0.01	0.37	0.01
43.3	27	29.7	0.33	0.01	0.36	0.02
39.3	27	33.7	0.24	0.01	0.37	0.01
36.1	27	36.9	0.26	0.02	0.3311	0.0001

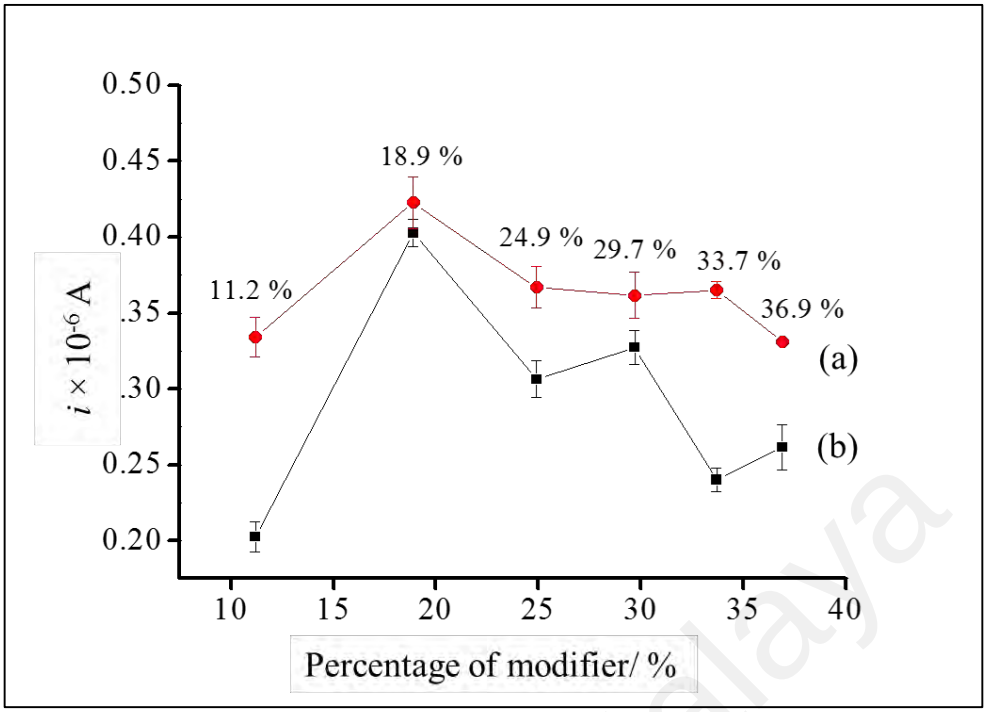

Figure 4.13: The *i* responses for the oxidation of 2,4-DCP (50×10^{-6} mol L^{-1}) in PBS pH 7.2 against the percentage of the modifier; (a) β-CD-1-BIMOTs and (b) β-CD-2-BIMOTs. The error bar length accounts for the relative standard deviations for 3 measurements

Similarly, as the amount of β-CD-2-BIMOTs increased from 18.9% to 24.9%, the values of *i* were also decreased. However, the value of *i* response became almost constant at the percentage of 24.9%, 29.7% and 33.7% of β-CD-2-BIMOTs added to the CPE. At the highest amount of β-CD-2-BIMOTs (36.9%), the *i* response value had dropped to a lower value which was at $(0.3311 \pm 0.001) \times 10^{-6}$ A. It was summarized that the optimum percentage of β-CD-1-BIMOTs and β-CD-2-BIMOTs that can be added to the graphite was 18.9% since it exhibited the highest *i* signal for the oxidation of 2,4-DCP. The percentage ratio of graphite powder: mineral oil: modifier of 54.1%:18.9%:27% was selected for further investigation. The use of β-CD-1-BIMOTs and β-CD-2-BIMOTs as CPE modifiers had definitely increased the IL moieties at the electrode surface and facilitated the increase of *i* responses. However, there were few limitations when an excess amount of modifier was used. There is high possibility that an excessive amount

of IL at the solution-electrode interface had made it difficult for 2,4-DCP to diffuse and undergo oxidation reaction at β-CD cavity.

4.2.4 The electrochemical behavior of 2,4-DCP

4.2.4.1 The pH dependence of the modified electrode current response to 2,4-DCP

The effect of pH on *i* response and the potential values for the oxidation of 2,4-DCP was investigated between pH 5.8-7.6 for β-CD-1-BIMOTs/CPE and β-CD-2-BIMOTs/CPE using cyclic voltammetry technique. Figure 4.14 showed that the direct electrochemistry of β-CD-1-BIMOTs/CPE and β-CD-2-BIMOTs was strongly dependent on the pH of the electrolyte of phosphate buffer solution (PBS). As can be seen in Figure 4.14 (a) and (b), the peak potential value of the oxidation of 2,4-DCP was shifted negatively with the increased of the electrolyte pH from 5.8 to 7.6. However, the *i* response value reached the maximum value at pH 7.2 for both β-CD-1-BIMOTs/CPE and β-CD-2-BIMOTs/CPE.

The pH of the solution also affect the existing form of 2,4-DCP. It is known that dissociation constant (pKa) value for the 2,4-DCP is 7.89. When the pH is less than 7.6, the 2,4-DCP was in its non-dissociated form but at a higher pH value, 2.4-DCP is mainly exist in the form of ions. When the pH > pKa, the ionized form of 2,4-DCP was dominant and consequently no proton participated in the reaction. Meanwhile, at a basic pH, a higher concentration of hydroxyl ions co-exists, which may replace the 2,4-DCP molecules in the adsorption sites at β-CD-1-BIMOTs/CPE and β-CD-2-BIMOTs/CPE surfaces. Therefore, based on the evaluation on the *i* response of β-CD-1-BIMOTs/CPE and β-CD-2-BIMOTs/CPE plotted in Figure 4.15, pH 7.2 was selected as the optimal pH in the following experiments.

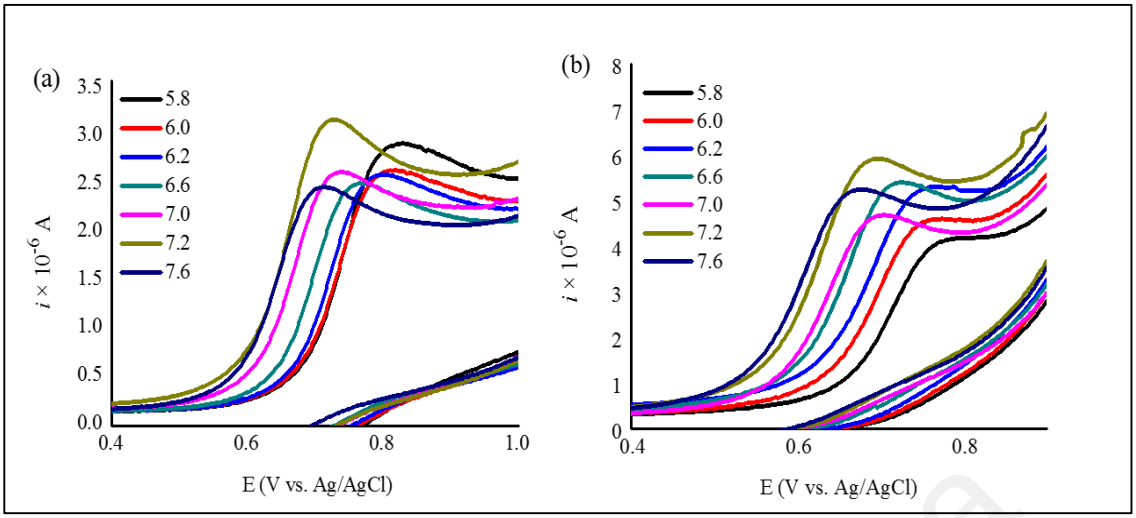

Figure 4.14: Cyclic voltammogram of *i* response of (a) β-CD-1-BIMOTs/CPE and (b) β-CD-2-BIMOTs/CPE on the oxidation of 50 × 10^{-6} mol L^{-1} 2,4-DCP in 0.1 mol L^{-1} PBS at different pH values with the scan rate applied of 0.10 Vs^{-1}

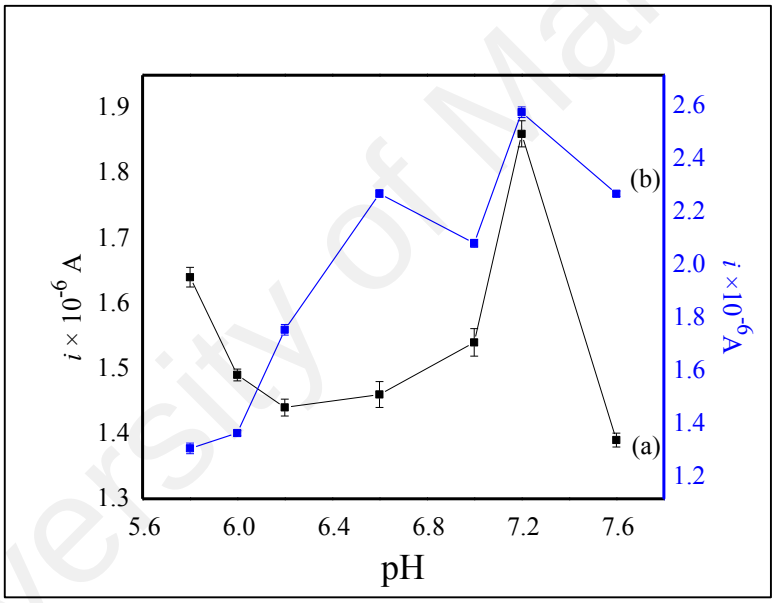

Figure 4.15: Plot of *i* response against pH for solution containing of 50 × 10^{-6} mol L^{-1} of 2,4-DCP at the surface of (a) β-CD-1-BIMOTs/CPE and (b) β-CD-2-BIMOTs/CPE. The error bar length accounts for the relative standard deviations for 3 measurements

A good linear relationship was obtained between the peak potential (E_p) and pH values for both modified electrodes (shown in Figure 4.16). The linear equation for both β-CD-1-BIMOTs/CPE and β-CD-2-BIMOTs/CPE are as follows;

$$E_{p(\beta-CD-1-BIMOTs/CPE)} = -0.0627pH + 1.1693 \quad \textbf{(Eq. 4.3)}$$

$$E_{p(\beta-CD-2-BIMOTs/CPE)} = -0.0586\ pH + 1.0974 \quad \textbf{(Eq. 4.4)}$$

From the linear plot shown in Figure 4.16 (a) and (b), the slope values were 62.7 mV and 58.6 mV per pH unit respectively, showing that equal numbers of electrons and protons were included in the oxidation of 2,4-DCP on both β-CD-1-BIMOTs/CPE and β-CD-2-BIMOTs/CPE. The number of electrons involved in the oxidation reaction of 2,4-DCP was discussed in Section 4.2.4.2.

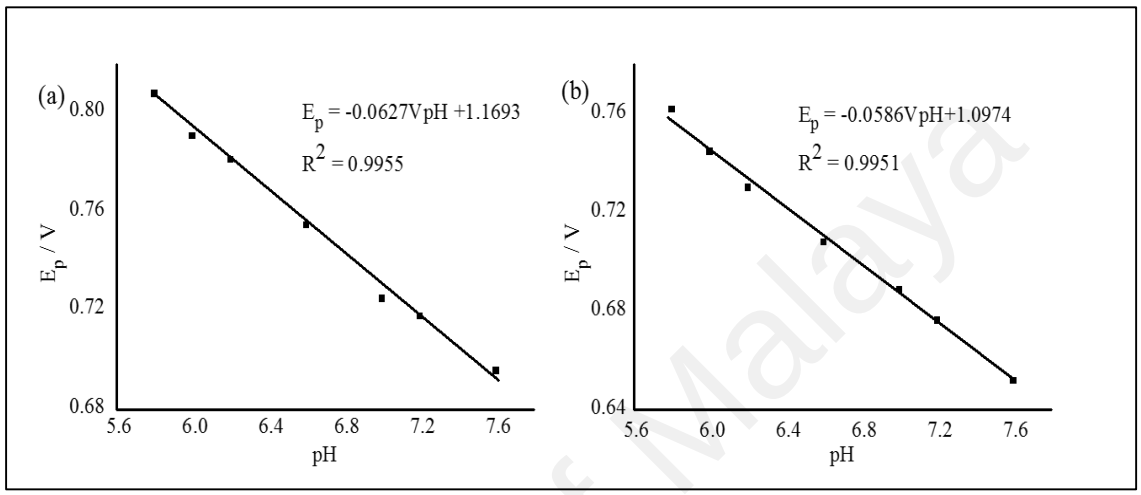

Figure 4.16: Plot of peak potential value against pH for the oxidation of 2,4-DCP at the surface of (a) β-CD-1-BIMOTs/CPE and (b) β-CD-2-BIMOTs/CPE

4.2.4.2 Effect of scan rates on the oxidation current value of 2,4-DCP

The reaction mechanism for the oxidation of 2,4-DCP at both modified CPEs can be evaluated through the scan rate study. The effect of scan rates on the oxidation current value at β-CD-1-BIMOTs/CPE and β-CD-2-BIMOTs/CPE were investigated and shown in Figure 4.17. As shown in Figure 4.17 (A) (i) and (ii), the *i* response value of the oxidation of 2,4-DCP was increased as the scan rate increased from 0.02 to 0.30 Vs^{-1}. The plot of *i* against $v^{1/2}$ was constructed for both β-CD-1-BIMOTs/CPE and β-CD-2-BIMOTs/CPE to determine the type of mass transport for 2,4-DCP at the electrode-electrolyte interface. From Figure 4.17 (B) (i) and (ii), both plots of *i* against $v^{1/2}$ were linear with both R^2 >0.990%. Based on Eq. 4.5 and Eq. 4.6, the oxidation of 2,4-DCP at both modified CPEs were governed by diffusion controlled.

$$i = 0.0924\ v^{1/2} + 0.130 \quad \text{(For β-CD-1-BIMOTs/CPE)} \qquad \ldots \textbf{(Eq. 4.5)}$$

$$i = 0.1835\ v^{1/2} - 0.051 \quad \text{(For β-CD-2-BIMOTs/CPE)} \qquad \ldots \textbf{(Eq. 4.6)}$$

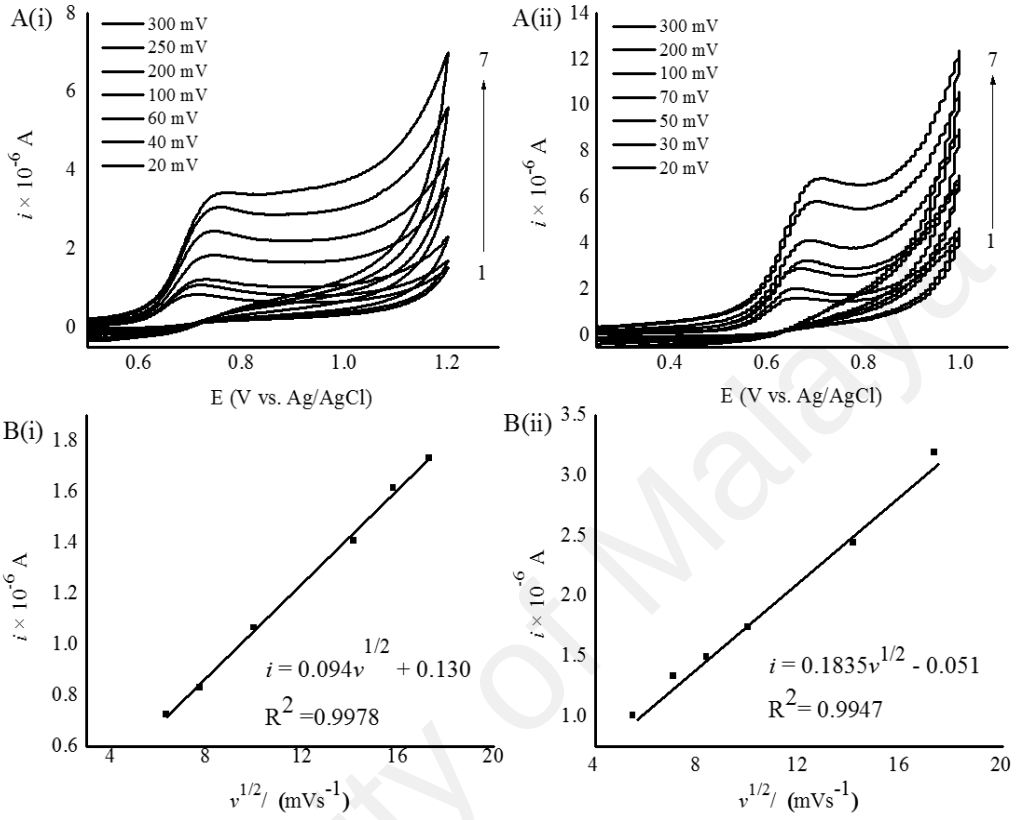

Figure 4.17: (A) The cyclic voltammogram of solution containing of 60 × 10^{-6} mol L^{-1} of 2,4-DCP at (i) β-CD-1- BIMOTs/CPE and (ii) β-CD-2-BIMOTs/CPE at different scan rate (v) and PBS pH 7.2. (B) Plot of i response against $v^{1/2}$ for oxidation of 2,4-DCP at (i) β-CD-1-BIMOTs/CPE and (ii) β-CD-2-BIMOTs/CPE

Meanwhile, a linear relationship between E_p and Napierian logarithm of v (ln v) can be used to calculate the number of electron transfer that involved in the oxidation of 2,4-DCP. The plot of E_p against ln v for both β-CD-1-BIMOTs and β-CD-2-BIMOTs modified CPE were shown in Figure 4.18. From Figure 4.18 (a) and (b), it was observed that the both E_p values for the oxidation of 2,4-DCP shifted positively as the scan rate increased. The linear equation for both plots were shown in Eq. 4.7 and Eq. 4.8; respectively.

At β-CD-1-BIMOTs/CPE surface;

$$E_p = 0.020 \ln v + 0.6579 \quad \textbf{(Eq. 4.7)}$$

At β-CD-2-BIMOTs/CPE surface,

$$E_p = 0.021 \ln v + 0.6029 \quad \textbf{(Eq. 4.8)}$$

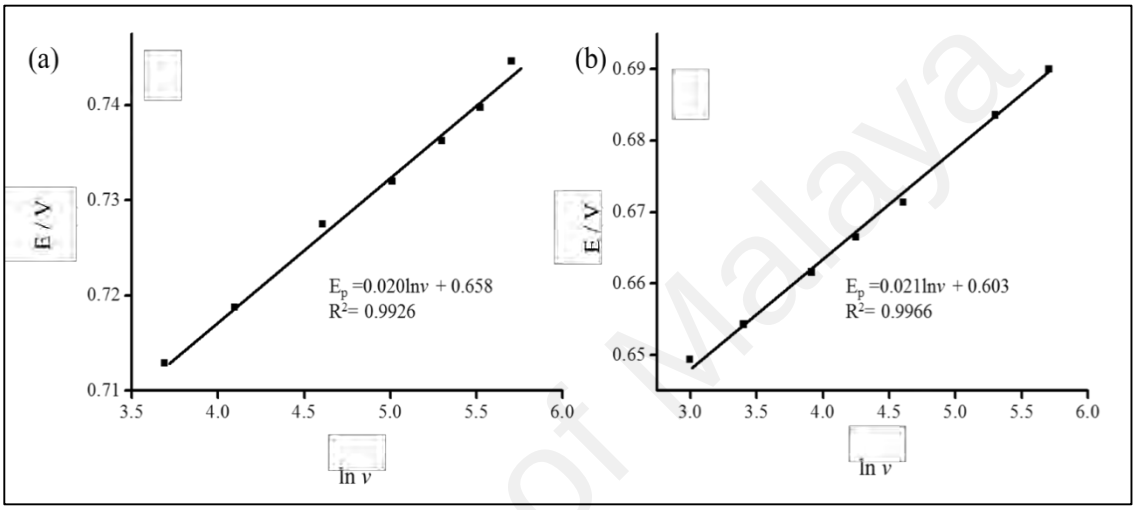

Figure 4.18: Plot of anodic peak potential E_p against Napierian logarithm of v (ln v) for oxidation of 2,4-DCP at (a) β-CD-1-BIMOTs/CPE and (b) β-CD-2-BIMOTs/CPE; respectively

The Laviron equation was used to determine the number of the electron transfer for the irreversible electrode process including for the oxidation of 2,4-DCP (Fotouhi *et al.*, 2012). The Laviron equation was expressed as in Eq. 4.9;

$$E_p = E^{\circ} - \frac{RT}{(1-\alpha)nF} \ln \frac{RTk_S}{(1-\alpha)nF} + \frac{RT}{(1-\alpha)nF} \ln v \quad \textbf{(Eq. 4. 9)}$$

Where R, T (in K) and F have their usual meaning, v is the scan rate, k_s is the standard rate constant, n is the number of the electron transfer and the α is the electron transfer coefficient which is the value for irreversible electrode process is presumed as 0.4 (Zhu *et al.*, 2016b). Based on Eq. 4.9, the calculated n value for the oxidation of 2,4-DCP at both β-CD-1-BIMOTs/CPE and β-CD-2-BIMOTs/CPE surfaces was approximately

equal to 2. As discussed in Section 4.2.4.1, the number of proton and electron involved in the oxidation process of 2,4-DCP is equal. Thus, the number of proton and electron involved in the oxidation process of 2,4-DCP on β-CD-1-BIMOTs/CPE and β-CD-2-BIMOTs/CPE was a two electron and two proton process which is similar to the previous reports (Dong *et al.*, 2016; Li *et al.*, 2014; Yu *et al.*, 2016; Zhan *et al.*, 2017).

4.2.5 The amperometric current response of modified CPEs on the oxidation of 2,4-DCP

The development of a reliable method for the electrochemical sensing of 2, 4-DCP using CPE modified ionic liquid functionalized β-cyclodextrin will be described below. The preliminary investigation on the oxidation of 2,4-DCP had been accomplished through the cyclic voltammetry technique. A more detail investigation was further conducted using the chrono-amperometry method. Chrono-amperometry technique was widely applicable due to the high sensitivity and reproducibility of the method (Karyakin *et al.*, 1995).

4.2.5.1 Effect of potential value on the current response for the oxidation of 2,4-DCP

The choroamperometric measurements were employed to evaluate the effect of potential E (V) on the current response (*i*) of β-CD-1-BIMOTs/CPE and β-CD-2-BIMOTs/CPE on the oxidation of 2,4-DCP. The dependency of the *i* response over the applied potentials was investigated and studied in the range of 0.60 V to 0.76 V and the sampling time was 35 s. From the amperometric measurement, the *i* against the potential was constructed at 50×10^{-6} mol L^{-1} 2,4-DCP in phosphate buffer solution (PBS, pH 7.2) and the PBS solution without the analyte as shown in Figure 4.19. From Figure 4.19 (a) and (b), it was shown that the increase of potential had increased the *i* response of the PBS solution with or without 2,4-DCP for both electrodes. Hence, the signal to

background (S/B) current ratio was plotted against the potential value to determine the optimal potential value as shown in Figure 4.20.

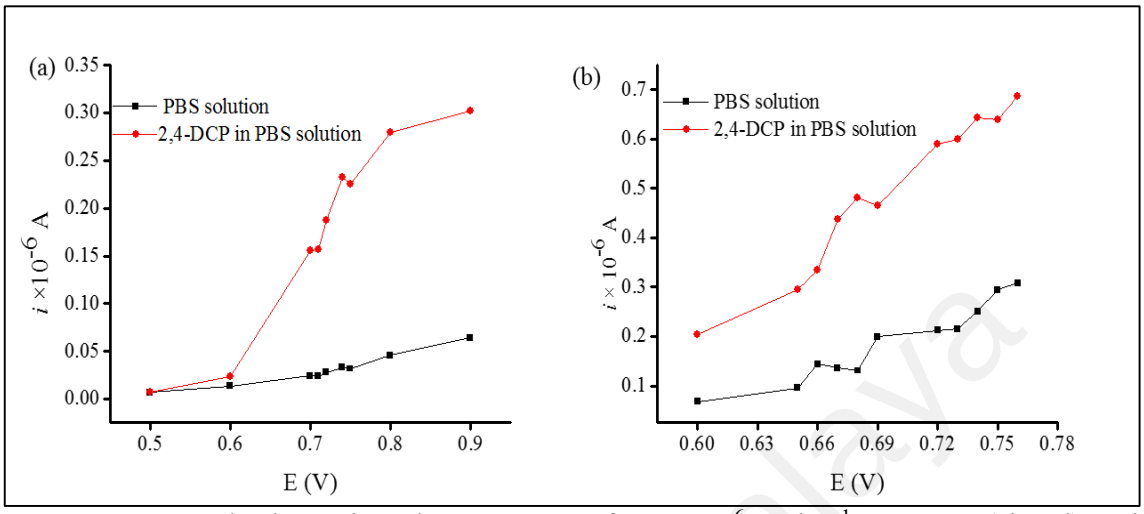

Figure 4.19: Hydrodynamic voltammogram of 50 × 10^{-6} mol L^{-1} 2,4-DCP (signal) and PBS without analyte (background) at pH 7.2 at a 35 s sampling time for (a) β-CD-1-BIMOTs/CPE and (b) β-CD-2-BIMOTs/CPE; respectively

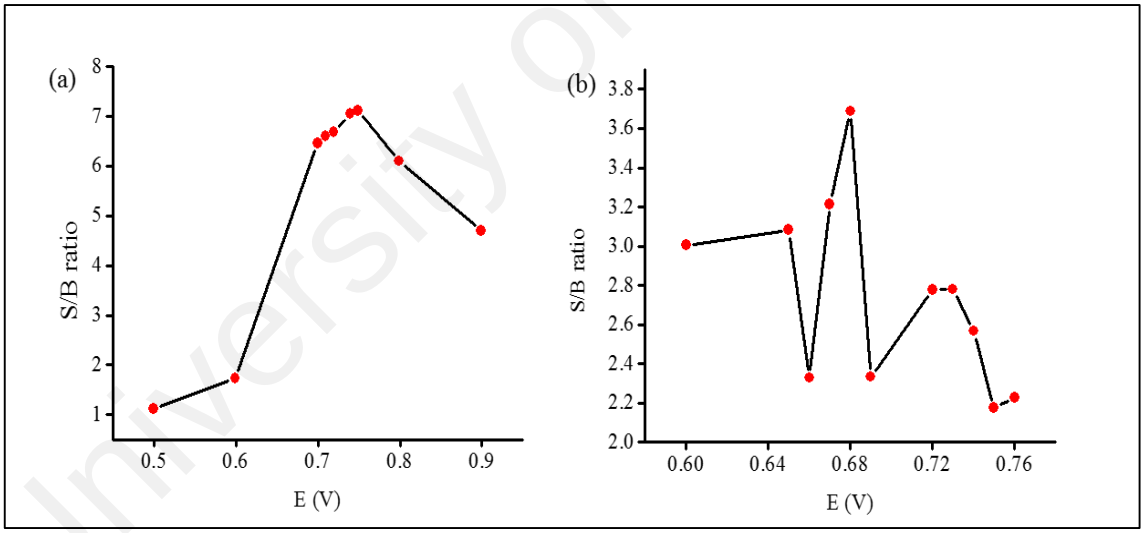

Figure 4.20: The hydrodynamic voltammogram of signal-to-background current ratio (S/B) for (a) β-CD-1-BIMOTs/CPE and (b) β-CD-2-BIMOTs/CPE; respectively

From Figure 4.20, we can observe that different number of IL substitution require a different E (V) value to be able to oxidize the 2,4-DCP at the modified CPE electrodes. The dependency of E (V) on number of IL substitution was clear where the one-position of IL substitution on β-CD required a higher E (V) value compared to that two positions of IL substitution. According to Sadeghi. *et al.*, the presence of IL did not only enhance

the *i* value by accelerating the electron transfer but also involved in decreasing the overpotential of the electrode (Sadeghi *et al.*, 2013). The result had supported the fact that IL did possess a crucial role as a component of the electrode. The enhancement of electron transfer kinetic with the increasing number of IL was closely related to the increase of electrostatic interaction between 2,4-DCP and the cationic imidazolium part of the electrode surface (Safavi *et al.*, 2006).

4.2.6 Method validation of chrono amperometric technique

4.2.6.1 Linear response, limit of detection (LOD), limit of quantification (LOQ) and sensitivity of the detection of 2,4-DCP at modified CPEs

Under the optimal condition, the chrono-amperometry measurement was recorded for different concentration of 2,4-DCP at β-CD-1-BIMOTs/CPE and β-CD-2-BIMOTs/CPE; respectively (shown in Figure 4.21). As can be seen in Figure 4.21 (a) and (b), in all cases, the *i* value increased with the increase of 2,4-DCP concentration. The calibration curves obtained for 2,4-DCP indicated a linear relationship ranging of (0 - 100) × 10^{-6} mol L^{-1} for both modified CPEs with a regression of *i* (10^{-6} A)= $0.0044C_{2,4\text{-DCP}}$ + 0.0435 (R^2 = 0.9963) and *i* (10^{-6} A) = $0.0039C_{2,4\text{-DCP}}$ + 0.1191 (R^2 = 0.9972); respectively for β-CD-1-BIMOTs/CPE and β-CD-2-BIMOTs/CPE (Figure 4.22).

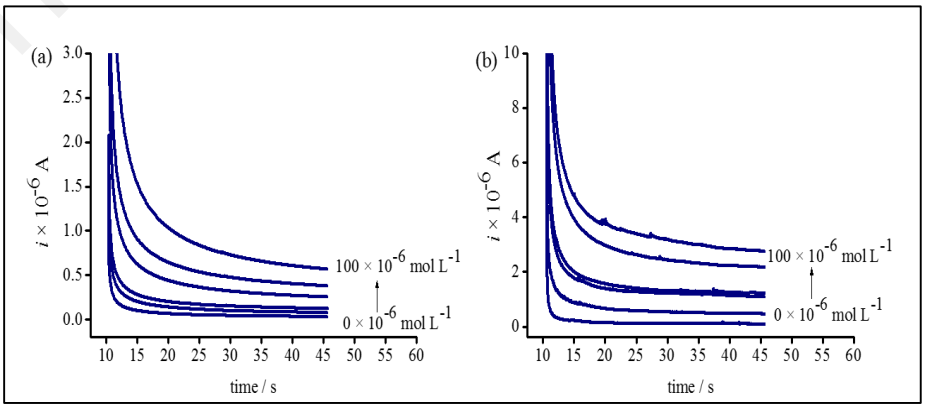

Figure 4.21: Amperomogram of (a) β-CD-1-BIMOTs/CPE and (b) β-CD-2-BIMOTs/CPE examined in 0.1 mol L^{-1} PBS (pH 7.2) containing different concentration of (0 – 100) × 10^{-6} mol L^{-1} 2,4-DCP at optimal potential

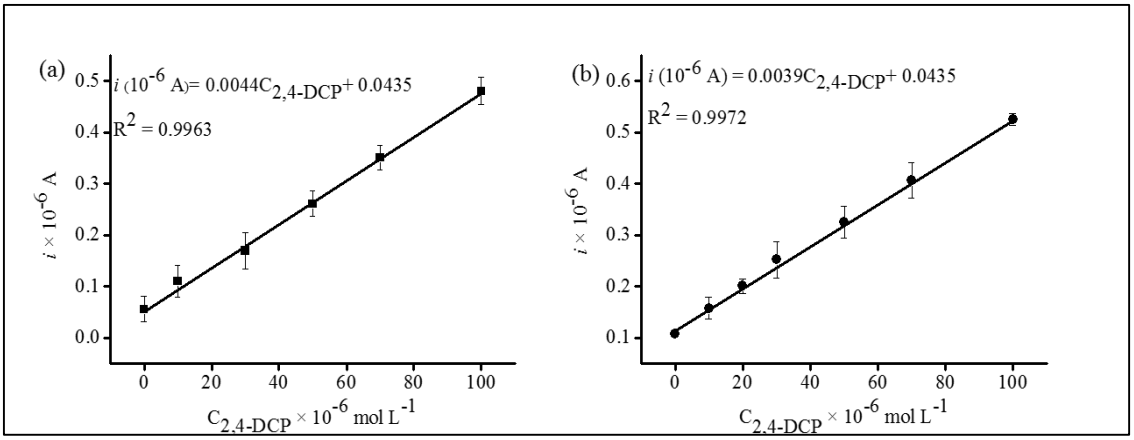

Figure 4.22: Linear calibration curve at a) β-CD-1-BIMOTs/CPE and (b) β-CD-2-BIMOTs/CPE examined in 0.1 mol L^{-1} PBS (pH 7.2) containing different concentration of (0 – 100) × 10^{-6} mol L^{-1} 2,4-DCP at optimal potential. The error bar length accounts for the relative standard deviations for 3 measurements

From the *i* against $C_{2,4\text{-DCP}}$ graph, the LOD and LOQ for β-CD-1-BIMOTs/CPE and β-CD-2-BIMOTs/CPE were calculated using the Eq. 3.3 and Eq. 3.4 as described in Section 3.4.5.3 while Eq. 3.5 and Eq. 3.6 were used to determine the selectivity of the modified CPEs. The LOD, LOQ, linear range and the sensitivity of both modified electrodes were tabulated in Table 4.5. From Table 4.5, it was shown that the LOD of the oxidation of 2,4-DCP at β-CD-1-BIMOTs/CPE was 1.3 × 10^{-6} mol L^{-1} which was lower than the value obtained at β-CD-2-BIMOTs/CPE (4.1 × 10^{-6} mol L^{-1}). As can been in the table, the sensitivity of β-CD-1-BIMOTs/CPE was 0.0060 μA/ μmol L^{-1} cm^{-2}, slightly higher than β-CD-2-BIMOTs/CPE, with 0.0055 μA/ μmol L^{-1} cm^{-2}. The linear range for β-CD-1-BIMOTs/CPE and β-CD-2-BIMOTs/CPE were in the range of (4.3 – 100) ×10^{-6} mol L^{-1} and (13.8 – 100) × 10^{-6} mol L^{-1}; respectively showing that β-CD-1-BIMOTs/CPE offered a better detection of the oxidation of 2,4-DCP.

Table 4.5: LOD, LOQ, linear range and sensitivity of the modified electrodes

Electrodes	**LOD**	**LOQ**	**Linear range**	**Sensitivity**
	× 10^{-6} *mol* L^{-1}			$\frac{\mu A}{\mu mol\ L^{-1}.\ cm^2}$
β-CD-1-BIMOTs/CPE	1.3	4.3	4.3 - 100	0.0060
β-CD-2-BIMOTs/CPE	4.1	13.8	13.8 - 100	0.0055

Table 4.6 listed the studies regarding the use of modified electrodes for the electrochemical determination of 2,4-DCP by amperometry and differential pulse voltammetry techniques. From the table, it had shown that the sensitivity of β-CD-1-BIMOTs/CPE and β-CD-2-BIMOTs/CPE were higher than tyrosine/MWCNTs/GCE (Kong *et al.*, 2009), PVA/F108/AuNPs/Lac/GCE (Liu *et al.*, 2011), MB-AG/GCE (Sun *et al.*, 2012). The LOD values obtained from this study were comparable to the detection of 2,4-DCP by tyrosine/MWCNTs/GCE (Kong *et al.*, 2009), HRP/MWCNT/GCE (Huang *et al.*, 2007), MIP/Chitosan/Nafion/GCE (Zhang *et al.*, 2013c), MIP/GCE (Zhang *et al.*, 2013b) and Cu/MOF/CPE (Cui *et al.*, 2018).

From Table 4.6, it was observed that the performance of CPE was comparable to the GCE electrodes in term of the electrochemical detection of 2,4-DCP. Other than that, it can be seen that the Cu/MOF that was regarded as highly conductive material gave a similar effect in comparison to β-CD-1-BIMOTs/CPE. However, it turned out that the β-CD-2-BIMOTs gave lower impact in comparison to β-CD-1-BIMOTs despite the higher number of IL substitution owned by β-CD-2-BIMOTs. Nevertheless, both β-CD-1-BIMOTs/CPE and β-CD-2-BIMOTs/CPE was a promising sensor for the determination of 2,4-DCP. Further investigation is necessary to investigate the interaction of both β-CD-1-BIMOTs and β-CD-2-BIMOTs towards 2,4-DCP.

Table 4.6: Comparison of recently published electrochemical methods in the determination of 2,4-DCP

Electrode	Techniques	Sensitivity / $\mu A/(\mu molL^{-1}.cm^2)$	Detection limit ($\mu molL^{-1}$)	Linear range ($\mu molL^{-1}$)	References
Tyrosine/MWCNTs/GCE	Amperometry	0.00425	0.66	2 - 100	(Kong *et al.*, 2009)
HRP/MWNT/GCE	Amperometry	0.00005	0.38	1.0 - 100	(Huang *et al.*, 2007)
MIP/chitosan/Nafion/GCE	Amperometry	0.0067	1.6	5 - 100	(Zhang *et al.*, 2013c)
MIP/GCE	DPV	-	1.6	5 - 100	(Zhang *et al.*, 2013b)
PVA/F108/AuNPs/Lac/GCE	Amperometry	0.0371	2.70	5 - 25	(Liu *et al.*, 2011)
MB-AG/GCE	Amperometry	0.00174	2.06	12.5 - 208	(Sun *et al.*, 2012)
CS/CDs-CTAB/GCE	DPV	-	0.01	0.04 - 8	(Yu *et al.*, 2016)
PEY/MWNTs-OH/GCE	DPV	-	0.0015	0.005 – 0.1 0.2 – 40	(Zhu *et al.*, 2016b)
GO/MIP/GCE	DPV	-	0.001	0.004 - 10	(Liang *et al.*, 2017)
DPG/GCE	SWV	-	0.25	5 - 80	(Peleyeju *et al.*, 2017)
Cu/MOF/CPE	Amperometry	-	1.1	4 - 100	(Cui *et al.*, 2018)
β-CD-1-BIMOTs/CPE	Amperometry	0.0060	1.3	4.3 - 100	This work
β-CD-2-BIMOTs/CPE	Amperometry	0.0055	4.1	13.8 - 100	This work

4.2.6.2 The reproducibility, repeatability and stability of the modified CPEs

The amperometric method was a reliable method to be used for the electrochemical determination of 2,4-DCP. However, the accuracy and the precision of the method needs to be accessed prior to the application of the method to the real samples. The main advantage of using the β-CD-1-BIMOTs/CPE and β-CD-2-BIMOTs/CPE is the easiness of surface renewability when it is necessary. The *i* value on of β-CD-1-BIMOTs/CPE and β-CD-2-BIMOTs/CPE after their seven-consecutive measurement of 50×10^{-6} mol L^{-1} 2,4-DCP were compared to evaluate the repeatability (intra-day precision) of the electrodes.

The RSD was calculated using Eq. 3.1 as described in Section 3.4.5.1. The average of the resulted values had relative standard deviation (RSD) of 1.40% and 0.92% respectively for β-CD-1-BIMOTs/CPE and β-CD-2-BIMOTs/CPE (shown in Figure 4.23). The inter-day precision (reproducibility) of β-CD-1-BIMOTs/CPE and β-CD-2-BIMOTs/CPE were evaluated using the seven independent surface electrodes. From Figure 4.23, the RSD values for both β-CD-1-BIMOTs/CPE and β-CD-2-BIMOTs/CPE were less than 5% which were 2.17% and 0.89%; respectively.

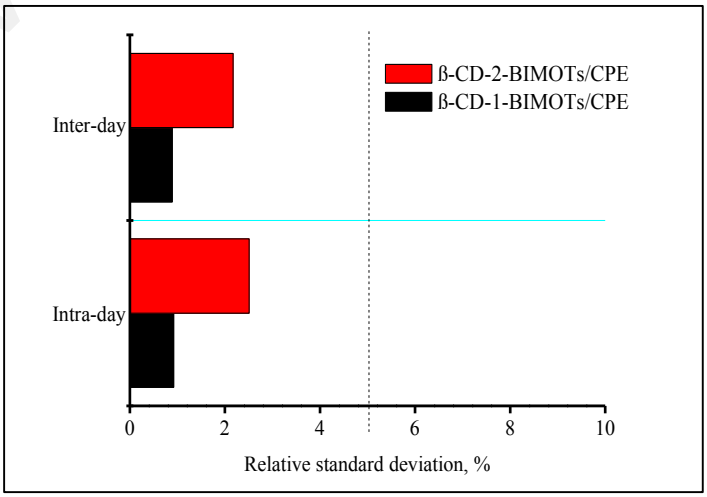

Figure 4.23: The RSD values for intra-day and inter-day precision of the amperometric measurement of 50×10^{-6} mol L^{-1} 2,4-DCP at β-CD-1-BIMOTs/CPE and β-CD-2-BIMOTs/CPE (n=7)

The stability of the modified electrodes was inspected by periodically repeating the measurement of 50 × 10^{-6} mol L^{-1} of 2,4-DCP for ten-consequence days. Figure 4.24 showed the plot of the amperometric current response, *i* of 2,4-DCP against the consecutive days of measurement at β-CD-1-BIMOTs/CPE and β-CD-2-BIMOTs/CPE; respectively. From Figure 4.24, it was observed that the current value retained higher than 97% from its original value. The reproducibility of each consecutive days were recorded, and the RSD value obtained from the current response of β-CD-1-BIMOTs/CPE and β-CD-2-BIMOTs/CPE were displayed in Figure 4.25. From Figure 4.25, it was shown that the RSD value for β-CD-1-BIMOTs/CPE measurements was less than 5%. However, for β-CD-2-BIMOTs/CPE, it was observed that RSD values were slightly higher than 5% which was about 7%. These results had indicated that the developed β-CD-1-BIMOTs/CPE and β-CD-2-BIMOTs/CPE sensor had good repeatability, reproducibility and stability.

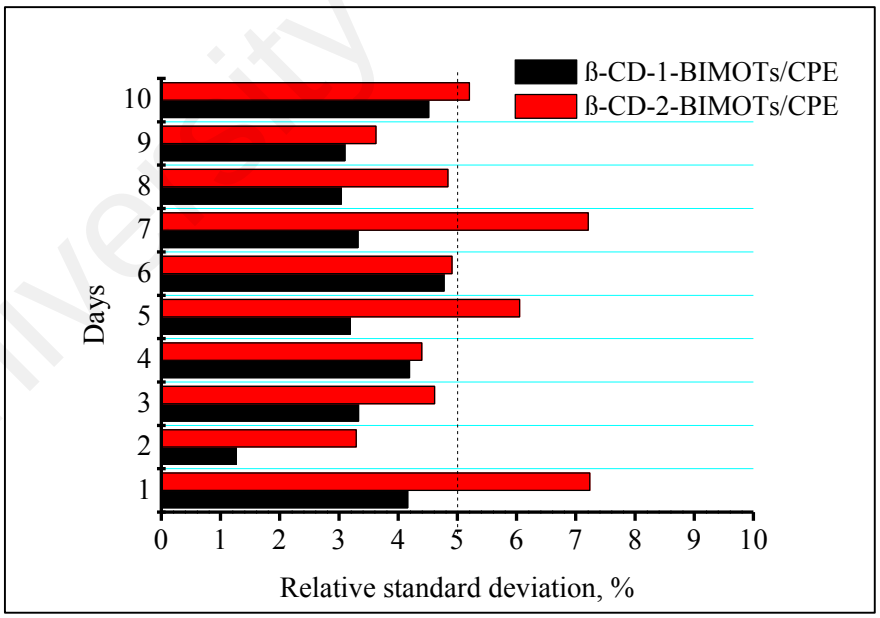

Figure 4.24: The RSD values of amperometric current response of 50 × 10^{-6} mol L^{-1} 2,4-DCP in PBS pH 7.2 for ten consequence days (n=7)

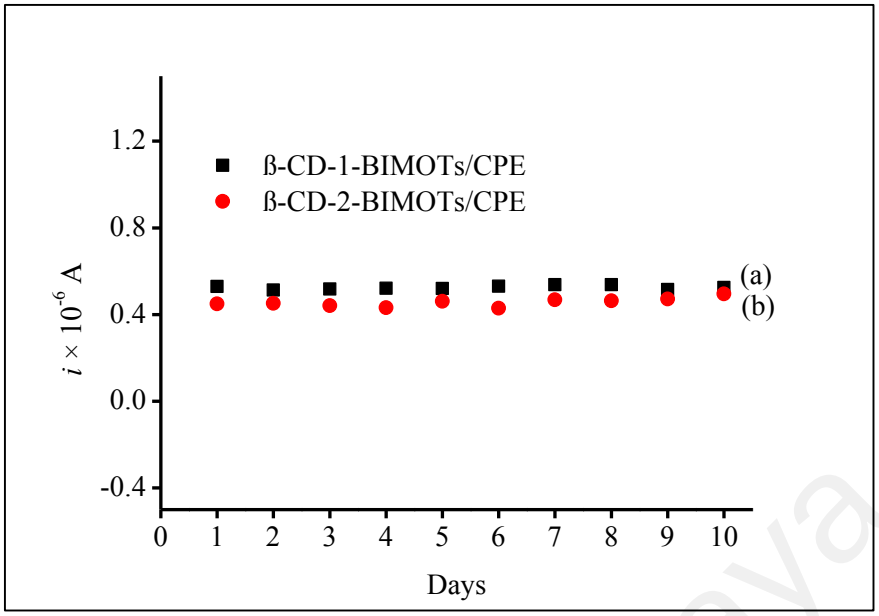

Figure 4.25: The relative standard deviation value calculated from the amperometric current response of 2,4-DCP for ten consequence days (n=7)

4.2.6.3 The impact of interference substances on the amperometric measurement of 2,4-DCP at modified CPEs

Considering that there were some concomitant substances presented especially in the real samples, the effect of possible interferences was investigated on the common ions and the analogues of 2,4-DCP which were phenol, 2-chlorophenol, 3-chlorophenol and 4-chlorophenol. The analogues of 2,4-DCP was prepared at the same concentration as 2,4-DCP which was 100×10^{-6} mol L^{-1} in PBS pH 7.2. Meanwhile, the concentration of common anions and cations to 2,4-DCP was prepared in 100:1 ratio. Under optimized conditions, the electrochemical response of 2,4-DCP was detected in the presence of each corresponding ions; K_2SO_4, Na_2SO_4, NH_4NO_3, KNO_3, NaOH, LiOH, $MgCl_2$, NH_4Cl, KCl, NaCl and LiCl. The detection of 2,4-DCP was also evaluated in the presence of each analogues (i.e. phenol, 2-chlorophenol, 3-chlorophenol and 4-chlorophenol). The tolerance limit of interfering was set to 5% and below.

From Figure 4.26, it was observed that the interfering percentage of all ions for both modified CPEs were lower than the acceptance tolerance limit value of 5%. The β-CD-1-BIMOTs/CPE response on 2,4-DCP was s not affected by the presence of each

analogues of 2,4-DCP (Figure 4.26 (a)). Meanwhile, as can be seen in Figure 4.26 (b), β-CD-2-BIMOTs/CPE responded to all analogues that had been added to the solution, which had affected the current value of 2,4-DCP detection. In the presence of its analogues, the β-CD-2-BIMOTs/CPE was found to be less selective towards 2,4-DCP in comparison to β-CD-1-BIMOTs/CPE. From the observation, it was suspected that the position of IL on β-CD controlled the host-guest inclusion complex between β-CD and 2,4-DCP. To have a better understanding on this phenomenon, the study on the inclusion complex of β-CD-1-BIMOTs/CPE and β-CD-2-BIMOTs/CPE towards 2,4-DCP was conducted by spectroscopy technique in the presence of all analogues where it will be discussed in Section 4.3.

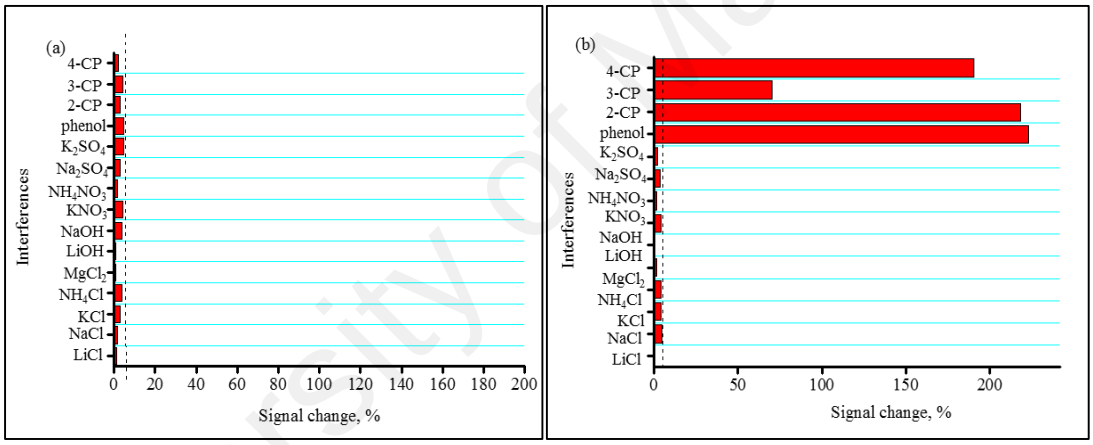

Figure 4.26: The influence of some possible interference substances on the determination of 100 × 10^{-6} mol L^{-1} of 2,4-DCP in PBS pH 7.2 at (a) β-CD-1-BIMOTs/CPE and (b) β-CD-2-BIMOTs/CPE; respectively

4.2.7 Analytical applications of the validated method on real samples

The applicability of the β-CD-1-BIMOTs/CPE and β-CD-2-BIMOTs/CPE were tested for the determination of the 2,4-DCP content in bottled mineral water, lake water and leachate from landfilled samples. The bottled mineral water was from Bleu mineral water meanwhile the collected lake water samples were obtained from Taman Jaya Lake, Petaling Jaya, in the state of Selangor. The leachate from landfill was obtained from Jeram Sanitary, Kapar, which was also in the state of Selangor. This was the first study to report on the application of the modified CPE sensor for the determination of 2,4-DCP. The pH

of the phosphate buffer solution (PBS) and all real samples was adjusted to 7.2. The linear calibration plot of 2,4-DCP was constructed as validated which was in the range of (4.3 – 100) × 10^{-6} mol L^{-1} and (13.8 – 100) × 10^{-6} mol L^{-1}; respectively for β-CD-1-BIMOTs/CPE and β-CD-2-BIMOTs/CPE. The optimum potential value of 0.75V for β-CD-1-BIMOTs/CPE and 0.68 V for β-CD-2-BIMOTs/CPE were applied for the amperometric measurement for the detection of 2,4-DCP.

None of the target analyte was detected by both electrodes. These samples were then spiked at a concentration of 25 × 10^{-6} mol L^{-1}, 50 × 10^{-6} mol L^{-1} and 80 × 10^{-6} mol L^{-1} of 2,4-DCP in order to investigate the effect of the sample's matrix. As shown in Table 4.7 (a) and (b), the recoveries of the spiked 2,4-DCP in the bottled mineral water, lake water and leachate from landfilled samples were satisfactory. The recovery (%) for mineral bottled water of β-CD-1-BIMOTs/CPE and β-CD-2-BIMOTs/CPE sensor were 89.3% - 107.5% and 102.5% - 115.9%; respectively. For the lake water, the obtained results lied within 98.7% - 107.9% and 104.9% - 113.4%; respectively for β -CD-1-BIMOTs/CPE and β-CD-2-BIMOTs/CPE sensor. The recoveries for leachate from landfilled were showing a good recovery range which was 85.5% - 117.7% (β-CD-1-BIMOTs/CPE) and 93.7%-105.7% (β-CD-2-BIMOTs/CPE). Overall, the RSD values for both working electrodes were less than 7%. This indicates that the sensors hold promise for practical applications especially for the detection of 2,4-DCP.

.

Table 4.7 (a): Determination of 2,4-DCP in environmental samples using β-CD-1-BIMOTs/CPE sensor

Sample	Added ($\times 10^{-6}$ mol L^{-1})	Found ($\times 10^{-6}$ mol L^{-1})	Recovery, %	RSD,%
Leachate	25	29.4	117.7	1.0
	50	51.0	102.0	3.1
	80	68.4	85.5	0.1
Lake water	25	24.7	98.7	3.7
	50	49.5	99.0	0.9
	80	86.3	107.9	0.7
Mineral water	25	26.8	107.3	3.2
	50	44.6	89.3	1.9
	80	86.0	107.5	0.3

Table 4.7 (b): Determination of 2,4-DCP in environmental samples using β-CD-2-BIMOTs/CPE sensor

Sample	Added ($\times 10^{-6}$ mol L^{-1})	Found ($\times 10^{-6}$ mol L^{-1})	Recovery, %	RSD,%
Leachate	25	25.5	102.0	7.3
	50	52.9	105.7	3.6
	80	74.8	93.7	3.0
Lake water	25	28.3	113.0	1.7
	50	56.7	113.4	2.7
	80	83.9	104.9	1.7
Mineral water	25	30.2	115.8	3.5
	50	53.3	102.5	5.8
	80	85.6	106.9	0.4

4.3 Spectrophotometric studies on the host-guest inclusion complex between β-CD-1-BIMOTs and β-CD-2-BIMOTs towards 2,4-DCP

In Section 4.2.6.3, it had been found that the selectivity of β-CD-1-BIMOTs/CPE and β-CD-2-BIMOTs/CPE towards the target analyte of 2,4-DCP differed greatly in the presence of phenol, 2-chlorophenol (2-CP), 3-chlorophenol (3-CP), 4-dichlorophenol (4-CP). In addition, there was a significant difference in the potential value that was required to oxidize the 2,4-DCP at β-CD-1-BIMOTs/CPE and β-CD-2-BIMOTs/CPE as shown Section 4.2.5.1. The differences exhibited by both sensors were probably related to the

geometry of β-CD-1-BIMOTs-2,4-DCP and β-CD-2-BIMOTs-2,4-DCP complexes. According to the study that was conducted by Chelli, *et al*., the geometrical structure of both host-guest complex and the driving forces had strongly affected the formation of the inclusion complex between the β-CD and the target analyte (Chelli *et al.*, 2007).

However, if we considered the complexation of a single analyte with different β-CD derivatives, the geometry of the different host itself will provide a different complexation property towards the desired analyte. For β-CD derivatives, both of β-CD and their reacting partners (the part of β-CD that has been modified) will be a decisive factor that determine how strong the host-guest complexation can be form (Szejtli, 1995). Herein, the host-guest inclusion complex mechanism between 2,4-DCP with two β-CD derivatives which was β-CD-1-BIMOTs and β-CD-2-BIMOTs in different techniques was studied. The spectroscopy techniques were employed in order to have a better understanding on the complexation of β-CD-1-BIMOTs-2,4-DCP and β-CD-2-BIMOTs-2,4-DCP.

Ionic liquid monofunctionalized β-cyclodextrin (β-CD-1-BIMOTs) had offered better complexation property towards 2,4-DCP in comparison to that of native β-CD (Raoov *et al.*, 2013). Rather than offering the cage for inclusion complex formation between β-CD and 2,4-DCP, β-CD-1-BIMOTs had provided an additional force through the IL where the electrostatic and π-π interaction towards 2,4-DCP. However, as discussed in previous section, the number of IL substitution and the IL positioning gave a great impact on the complexation between the β-CD cavity and 2,4-DCP. The interactions between 2,4-DCP with β-CD-1-BIMOTs and β-CD-2-BIMOTs had delivered further interesting example for structure/selectivity correlation.

4.3.1 The evaluation on the influence of the host structure on the selectivity by NMR techniques

In this section, the mechanism for the inclusion complex of β-CD-1-BIMOTs-2,4-DCP and β-CD-2-BIMOTs-2,4-DCP were evaluated by NMR techniques. The formation of inclusion complex can be observed by ^{1}H NMR and NOESY analysis. The ^{1}H NMR spectra with deduced structures of β-CD-1-BIMOTs, β-CD-2-BIMOTs, 2,4-DCP and the complexes were shown in Figure 4.27 (a) and (b). The values of the chemical shifts (δ) for different protons in β-CD-1-BIMOTs, β-CD-2-BIMOTs, 2,4-DCP and complexes were listed in Table 4.8 (a) and (b); respectively.

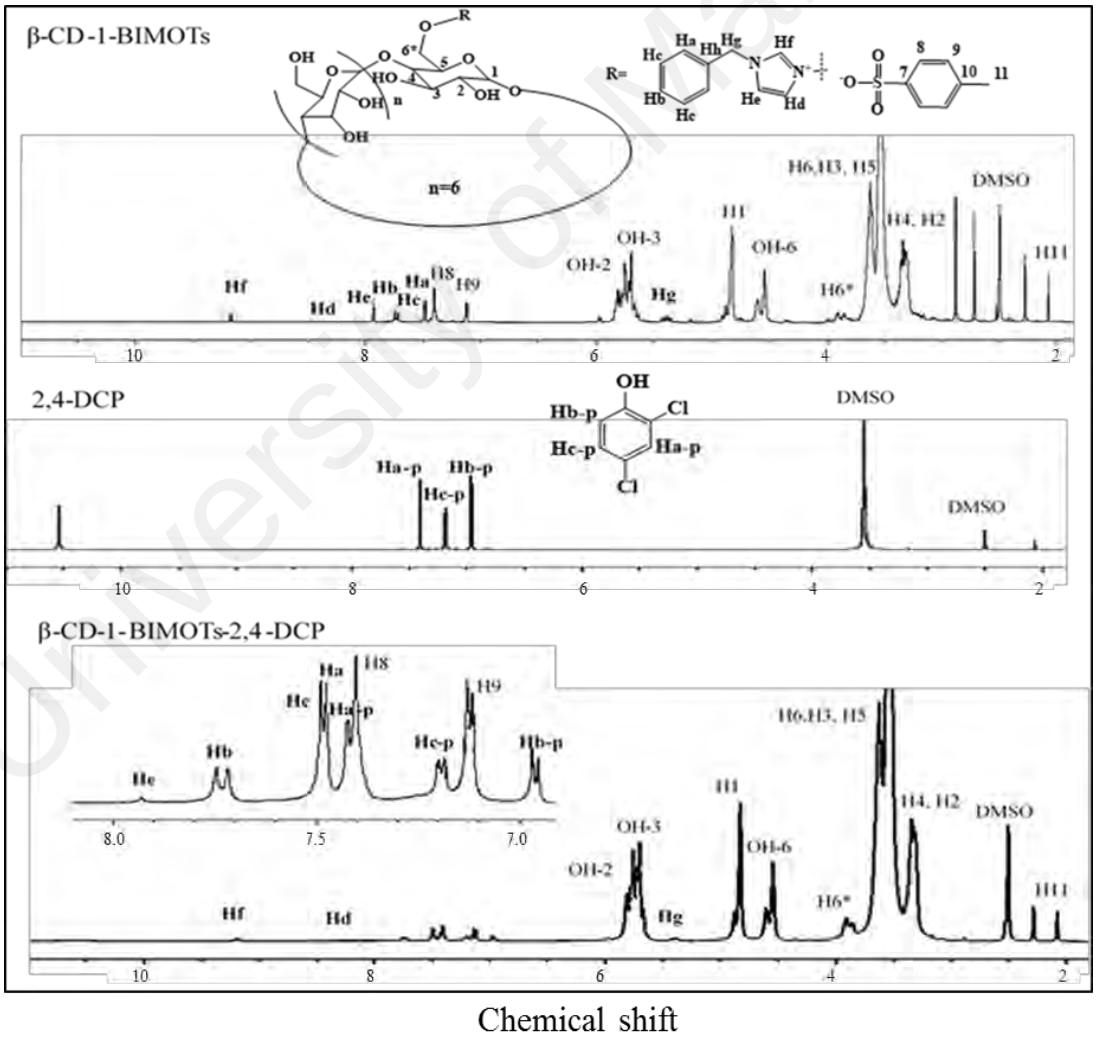

Figure 4.27 (a): ^{1}H-NMR spectrum of β-CD-1-BIMOTs, 2,4-DCP and β-CD-1-BIMOTs-2,4-DCP complex

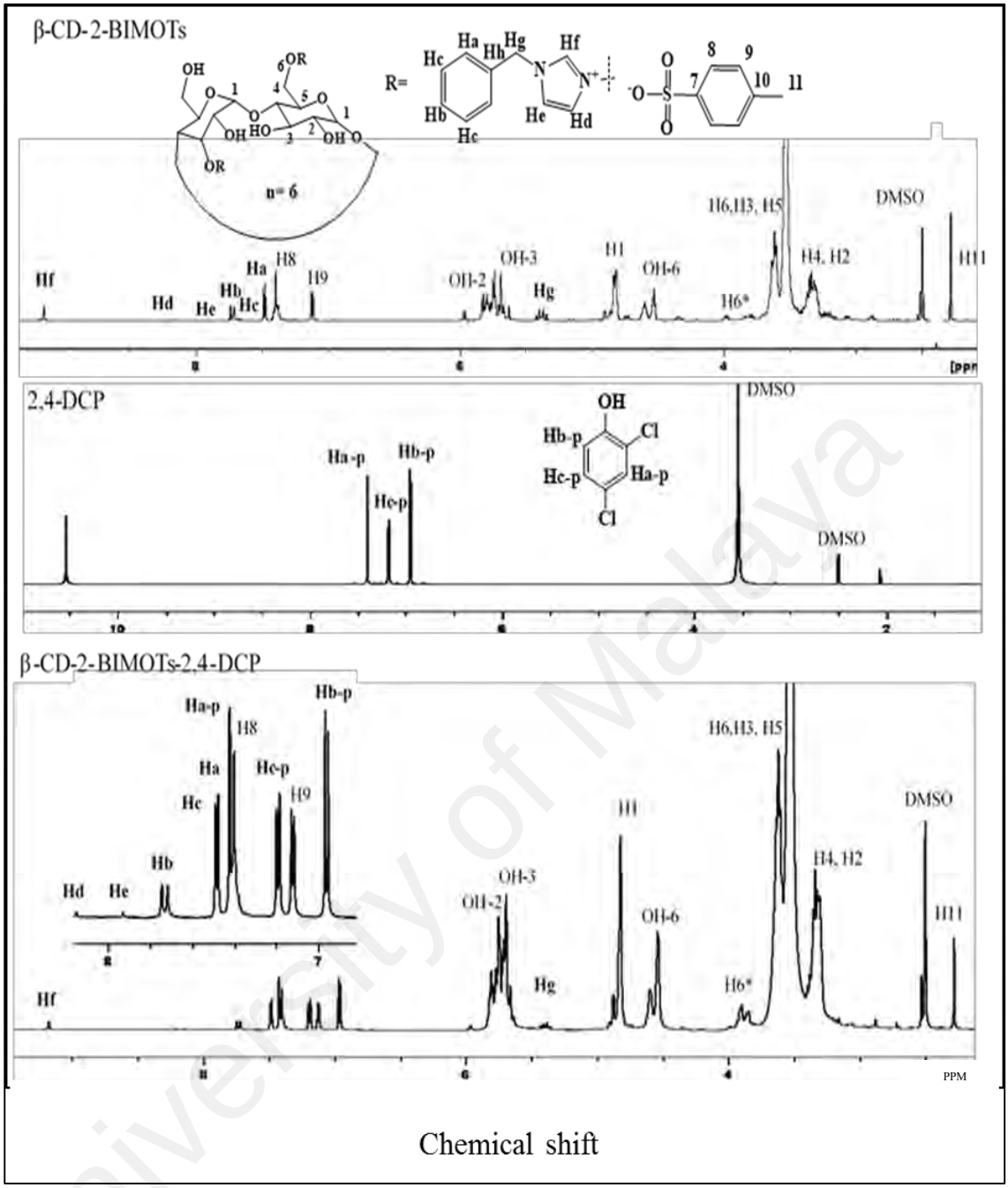

Figure 4.27 (b): ^{1}H-NMR spectrum of β-CD-2-BIMOTs, 2,4-DCP and β-CD-2-BIMOTs-2,4-DCP complex

Table 4.8 (a): Chemical shift (δ) of β-CD-1-BIMOTs, 2,4-DCP and β-CD-1-BIMOTs-2,4-DCP

Proton	β-CD-1-BIMOTs δ	2,4-DCP δ	β-CD-1-BIMOTs-2,4-DCP δ	Changes Δδ
H1	4.8204		4.8222	0.0018
H2	3.3100		3.3123	0.0020
H3	**3.6046**		**3.6186**	**0.0140**
H4	3.3453		3.3445	-0.0008
H5	**3.5864**		**3.5704**	**0.0160**
H6	3.6350		3.6324	-0.0026
H8	7.3990		7.4060	0.0070
H9	7.1200		7.1244	0.0045
H11	2.0726		2.0744	0.0018
Ha	7.4734		7.4732	0.0002
Hb	7.7280		7.7317	0.0037
Hc	7.4862		7.4942	0.0080
Hd	8.1920		8.2002	0.0405
He	7.9300		7.9272	0.0028
Hf	9.1636		9.1713	0.0077
Hg	5.3886		5.3910	0.0025
Hap		7.4011	7.4270	0.0260
Hbp		**6.9515**	**6.9478**	**0.0103**
Hcp		**7.1754**	**7.1895**	**0.0141**

Table 4.8 (b): Chemical shift (δ) of β-CD-2-BIMOTs, 2,4-DCP and β-CD-2-BIMOTs-2,4-DCP

Proton	β-CD-2-BIMOTs δ	2,4-DCP Δ	β-CD-2-BIMOTs-2,4-DCP δ	Changes Δδ
H1	4.8181		4.8223	0.0043
H2	**3.2950**		**3.3137**	**0.0187**
H3	3.6197		3.6212	-0.0015
H4	**3.3972**		**3.3815**	**0.0157**
H5	3.5939		3.5881	-0.0058
H6	3.6197		3.6212	0.0015
H8	7.3956		7.4211	0.0255
H9	7.1210		7.1223	0.0013
H11	2.0739		2.0740	0.0001
Ha	7.4776		7.4768	-0.0008
Hb	7.7259		7.7318	0.0059
Hc	7.4901		7.4902	0.0001
Hd	8.1663		8.1509	-0.0154
He	7.9274		7.9270	-0.0004
Hf	9.1551		9.1717	0.0166
Hg	5.3845		5.4042	0.0198
Hap		7.4011	7.4211	0.0201
Hbp		**6.9515**	**6.9609**	**0.0092**
Hcp		**7.1754**	**7.1913**	**0.0159**

According to Yuan *et al.*, the inclusion complex occurred when the chemical shift at H-3 and H-5 proton located inside the β-CD cavity was changed drastically (Yuan *et al.*, 2012). The spectra (Figure 4.28 (a)) and data (Table 4.8 (a)) showed higher Δδ at H3 and H5 interior proton of β-CD-1-BIMOTs-2,4-DCP. Meanwhile, there were small changes of the chemical shift at the exterior proton of H-1, H-2 and H-4 which was considered as negligible changes. There was also incorporation of the phenolic rings into β-CD-1-BIMOTs resulted from the strong intensity of Δδ at Hb-p and Hc-p protons of 2,4-DCP. The data obtained was in a good term with the previous study on β-CD-1-BIMOTs-2,4-DCP (Raoov *et al.*, 2013). From Raoov *et al.* and our NOESY spectrum on β-CD-1-BIMOTs-2,4-DCP complex as in Figure 4.28 (a), the strong changes on β-CD-1-BIMOTs protons (H-3, H-5) and 2,4-DCP phenolic protons (Hb-p and Hc-p) had proven that 2,4-DCP was successfully incorporated into the cavity of β-CD-1-BIMOTs. The phenomena can be explained as the formation of an inclusion complex occurred between β-CD-1-BIMOTs and 2,4-DCP.

Meanwhile, the analysis on ^{1}H NMR spectrum of β-CD-2-BIMOTs-2,4-DCP complex (Table 4.8 (b)) showed that the interaction of β-CD-2-BIMOTs and 2,4-DCP was slightly different compared to β-CD-1-BIMOTs-2,4-DCP. The Δδ of H3 and H5 interior proton of β-CD-2-BIMOTs-2,4-DCP complex (Figure 4.28 (b)) was not noticeable. However, the exterior proton of β-CD-2-BIMOTs-2,4-DCP complex; H-2 and H-4 showed a significantly stronger Δδ which were 0.0187 and 0.0157; respectively. This result had shown that 2,4-DCP might have an interaction at the outer cavity of the β-CD-2-BIMOTs. This was strengthened by the NOESY analysis (Figure 4.28 (b)) which shows that the strong intensity of the cross peaks for exterior proton of β-CD-2-BIMOTs (3.31-3.38 ppm, H-2, H-4) and 2,4-DCP (6.96-7.20 ppm, Hb-p, Hc-p) but no correlation peak for the interior proton of β-CD-2-BIMOTs (H-3, H-5). Hence, from the 2D NOESY NMR

analysis we can conclude that the phenolic ring of 2,4-DCP did not accommodate into β-CD-2-BIMOTs cavity but interact more with the exterior part of β-CD-2-BIMOTs.

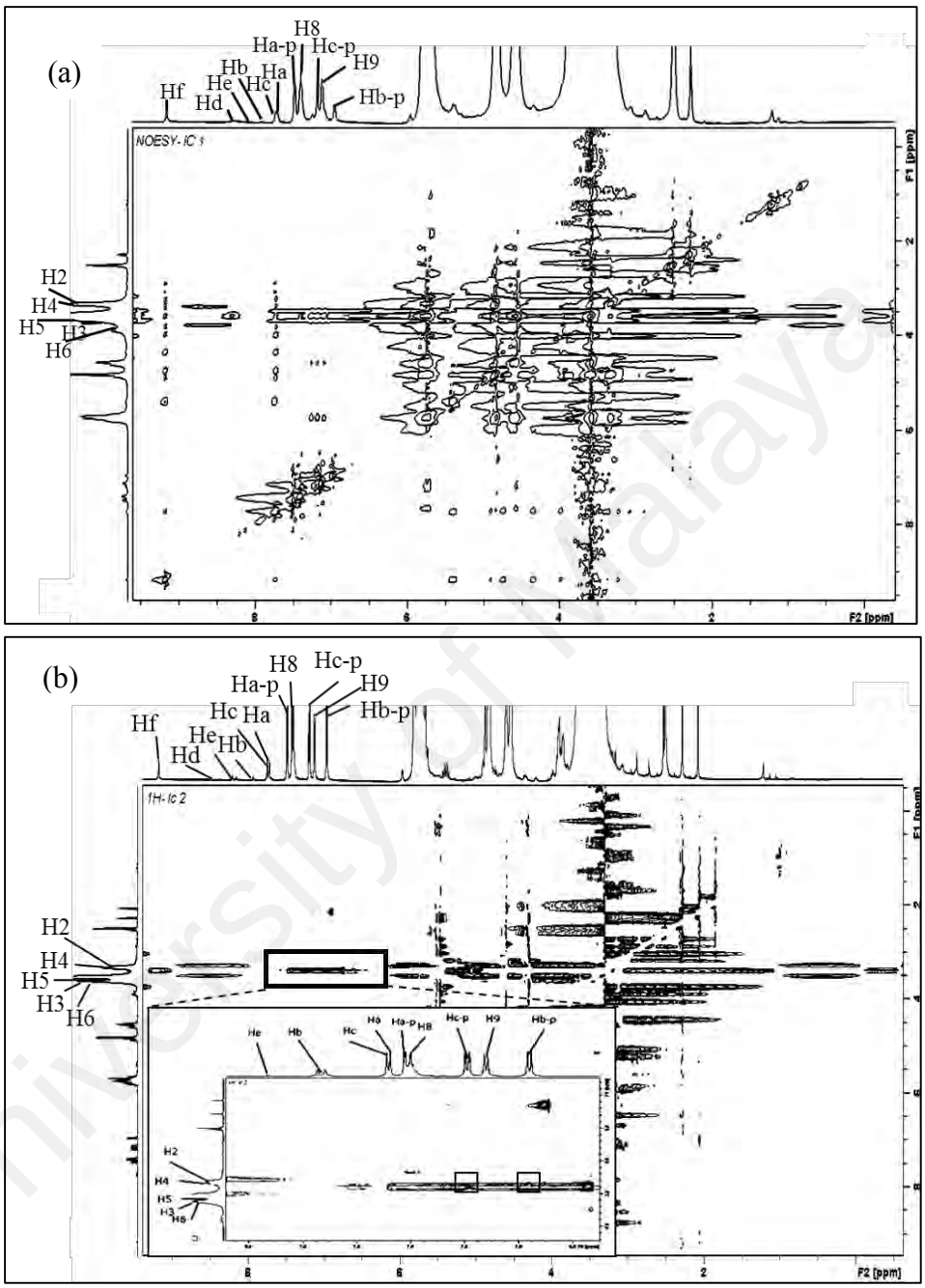

Figure 4.28: The two-dimensional NOESY spectrum of (a) β-CD-1-BIMOTs-2,4-DCP complex and (b) β-CD-1-BIMOTs-2,4-DCP in DMSO-D6

The penetration of a guest molecule into the hydrophobic cavity can occur either from primary or secondary face of β-CD depending on the size and the nature of the guest. A molecular modeling study that was reported by Huang *et al.* had shown that the phenol hydroxyl group preferred to face the secondary rim of the β-CD cavity (Huang *et al.*,

1997). From our investigation, we had found that the H-6 proton of the β-cyclodextrin of both β-CD-1-BIMOTs and β-CD-2-BIMOTs was not affected upon the formation of the complexes. This phenomenon strongly suggested that the incorporation of 2,4-DCP might have occurred at a wider side of the cavity.

4.3.2 The proposed schematic diagram for the inclusion complexes

The schematic diagram of the formation of β-CD-1-BIMOTs-2, 4-DCP and β-CD-2-BIMOTs-2,4-DCP were depicted in Figure 4.29. The analyte, which was 2, 4-DCP can be easily inserted into the cavity through the wider rim and formed β-CD-1-BIMOTs-2,4-DCP complex. The benzylimidazolium group that was located at C-6 position did not affect the formation of the complex since it was located at the narrow rim of the cavity. The second functionalization of benzylimidazolium was located at the C-3 position, which was at the wider rim of the cavity entrance. Both parts did interact with 2,4-DCP through π-π interactions. However, the presence of the ionic liquid at the secondary face might have hindered the insertion of the 2, 4-DCP resulting in the interaction between β-CD-2-BIMOTs and 2,4-DCP to occur more at the outside of the cavity than the inside.

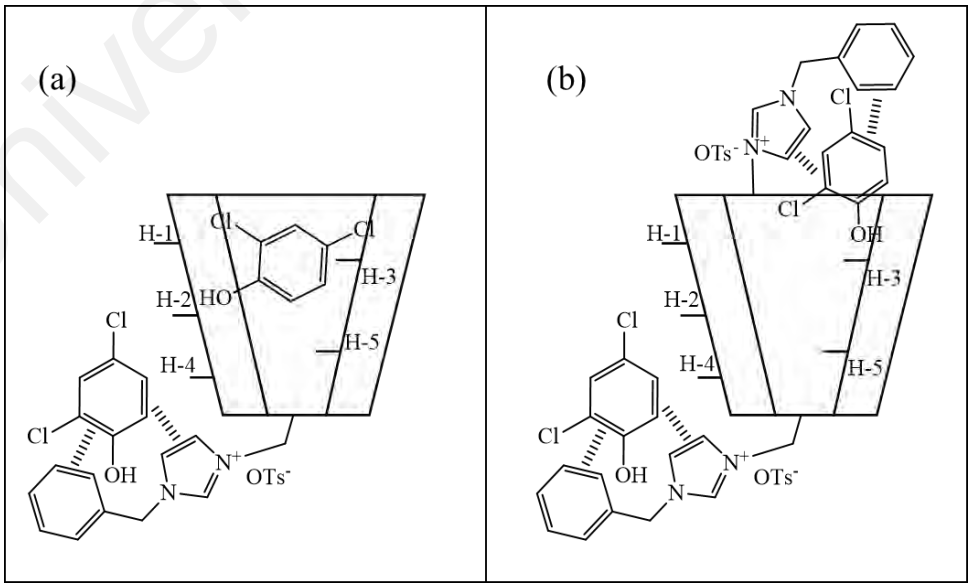

Figure 4.29: Schematic diagram on possible geometry for the formation of inclusion complex between (a) β-CD-1-BIMOTs and (b) β-CD-2-BIMOTs host with 2,4-DCP

4.3.3 UV-Vis spectral analysis of inclusion complexes between β-CD-ILs and 2,4-DCP

The inclusion complex of β-CDILs (β-CD-1-BIMOTs/ β-CD-2-BIMOTs) with 2,4-DCP in aqueous solution can be evaluated using ultra-violet and visible absorption spectroscopy (UV-Vis). The UV-Vis spectral analysis was applied not only to confirm the inclusion complex formation of β-CD-1-BIMOTs-2,4-DCP and β-CD-2-BIMOTs-2,4-DCP but also to acquire more information on the interactions between β-CD-IL and 2,4-DCP. The stock solution of β-CD-1-BIMOTs, β-CD-2-BIMOTs and 2,4-DCP were prepared in methanol meanwhile their standard solutions were prepared in a phosphate buffer solution (PBS, pH 7.2). In this context, the UV-Vis spectral of all standard solution were recorded in the phosphate buffer solution (PBS, pH 7.2).

Figure 4.30 showed the absorption spectra of (a) β-CD-1-BIMOTs and (b) β-CD-2-BIMOTs in the presence and the absence of 2,4-DCP. The λ_{max} of 2,4-DCP appeared at 287 nm. The obtained results showed that λ_{max} of β-CD-1-BIMOTs and β-CD-2-BIMOTs were obtained at 261 nm. The absorption spectra, before and after the formation of inclusion complexes were similar in term of its shape, with both complexes had shown higher absorption value than its host compounds. These results further supported the occurring of inclusion complex of β-CD-1-BIMOTs-2,4-DCP and β-CD-2-BIMOTs-2,4-DCP.

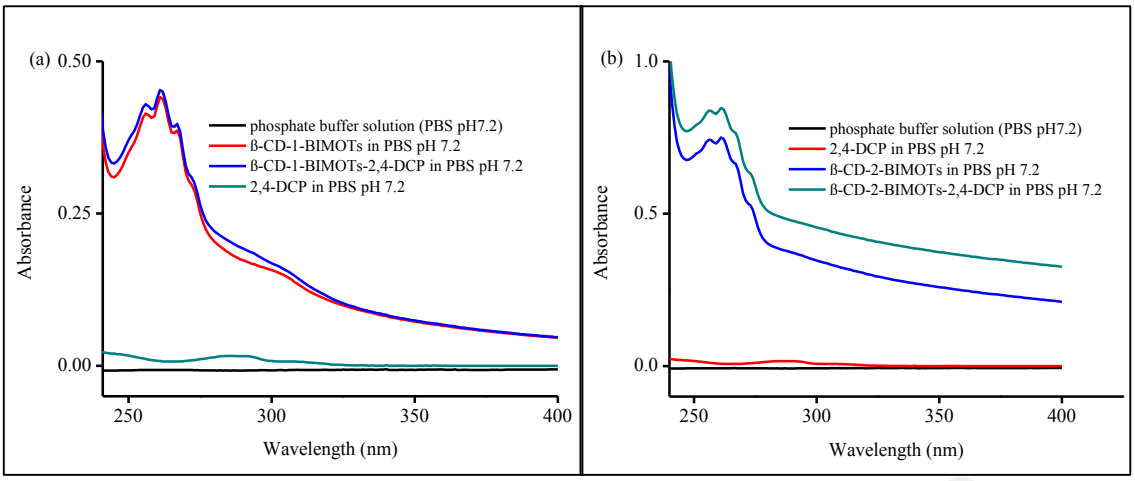

Figure 4.30: (a) Absorption spectra for 2,4-DCP, β-CD-1-BIMOTs and their complex. (b) Absorption spectra for 2,4-DCP, β-CD-2-BIMOTs and their complex. The [2,4-DCP]: 0.05 $\times 10^{-3}$ mol L^{-1}, [β-CD-1-BIMOTs]: 0.032 mol L^{-1} and [β-CD-2-BIMOTs]: 0.032 mol L^{-1}; at pH 7.2, T= 25 °C

The stoichiometry and the formation constant for both complexes were calculated and compared. The concentrations of β-CD-1-BIMOTs and β-CD-2-BIMOTs were varied (0, 0.001, 0.002, 0.003, 0.004 and 0.005 mol L^{-1}) while the concentration of 2,4-DCP was held constant at 0.05 mmol L^{-1}. Figure 4.31 showed the absorption spectra of 2,4-DCP with various concentration of (a) β-CD-1-BIMOTs and (b) β-CD-2-BIMOTs. The absorption spectra had shown that the addition of each β-CD-IL (at various concentration) to the 2,4-DCP solution will cause a noticeable increase in the absorption intensity. As a host, β-CD-1-BIMOTs and β-CD-2-BIMOTs will provide a hydrophobic microenvironment for 2,4-DCP and upon complexation, the molar absorption coefficient of the inclusion complex increased thus increasing the absorption intensity. The data obtained were used to illustrate the reciprocal plot for β-CD-1-BIMOTs-2,4-DCP and β-CD-2-BIMOTs-2,4-DCP inclusion complexes using Benisi-Hilderbrand equation (shown in Figure 4.32).

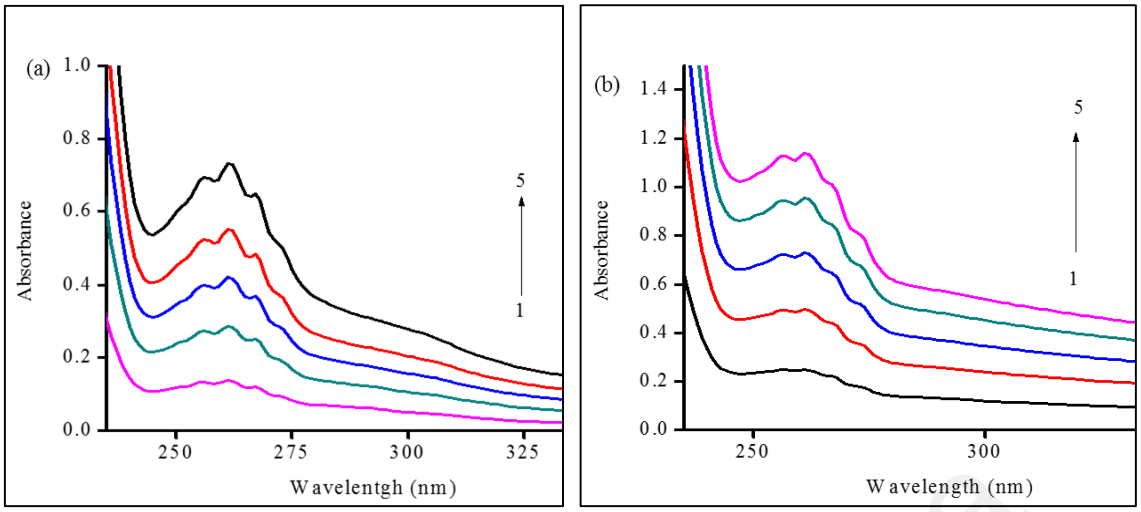

Figure 4.31: Absorption spectra of 2,4-DCP with various concentration of (a) β-CD-1-BIMOTs and (b) β-CD-2-BIMOTs; respectively at pH 7.2, T = 25 °C. From the lines 1 to 5: 0.001 mol L^{-1}, 0.002 mol L^{-1}, 0.003 mol L^{-1}, 0.004 mol L^{-1} and 0.005 mol L^{-1}

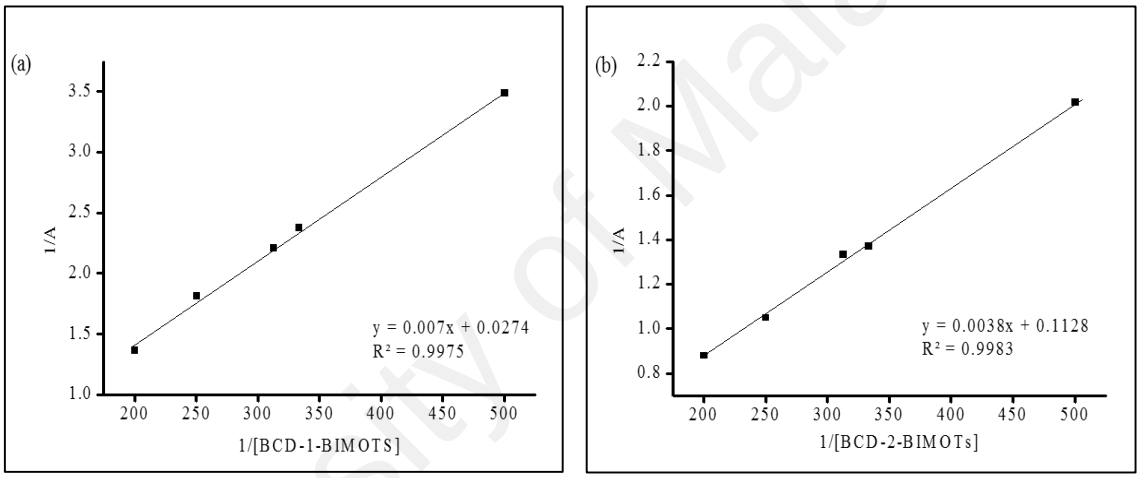

Figure 4.32: Reciprocal plot of (a) 1/A vs. 1/[β-CD-1-BIMOTs] and (b) 1/A vs. 1/[β-CD-2-BIMOTs]

The 2,4-DCP compound has only one benzene ring that can be included in the β-CD-1-BIMOTs or β-CD-2-BIMOTs; hence the theoretical value of stoichiometric ratio of the host-guest inclusion complex should be 1:1. The Benisi-Hilderbrand equation was shown as follows:

$$\frac{1}{A} = \frac{1}{\varepsilon[G]_0 k[\beta - \mathrm{CD} - \mathrm{n} - \mathrm{BIMOTs}]} + \frac{1}{\varepsilon[G]_0} \qquad \textbf{(Eq. 4. 3)}$$

where, A is the absorbance of the 2,4-DCP solution at each β-CD-ILs concentration; $[G]_0$ is the initial concentration of 2,4-DCP; K is the apparent formation constant; [β-CD-n-BIMOTs] is the concentration of β-CD-ILs, n is the number of IL substitution on β-CD,

and ε is the molar absorptivity. By using the Benisi-Hilderbrand equation, both β-CD-1-BIMOTs and β-CD-2-BIMOTs were observed to have a linear relationship from the reciprocal plot of 1/A against 1/[β-CD-n-BIMOTs] (Figure 4.32). This reciprocal plot clearly surmise that the stoichiometric ratio of both complexes was 1:1.

4.3.4 The effect of 2,4-DCP's analogues on β-CD-1-BIMOTs-2,4-DCP and β-CD-2-BIMOTs-2,4-DCP complexation

In Section 4.2.6.3, the interference study showed that the β-CD-1-BIMOTs and β-CD-2-BIMOTs had given different responses towards 2,4-DCP in the presence of phenol, 2-CP, 3-CP and 4-CP. In this context, the investigation on the interaction of β-CD-1-BIMOTs and β-CD-2-BIMOTs with phenol, 2-CP, 3-CP and 4-CP were constructed using the same method that was applied for 2,4-DCP as described in Section 4.3.3. All binding constants and stoichiometry ratio of β-CD-1-BIMOTs and β-CD-2-BIMOTs inclusion complexes with all analytes were measured at 25 °C and calculated using Benisi-Hilderbrand Equation (Eq. 4.3), tabulated in Table 4.9 (a) and (b).

Table 4.9 (a): The stoichiometry ratio and binding constant for all β-CD-1-BIMOTs complexes

β-CD-1-BIMOTs complexes	**Stoichiometry ratio**	**Binding constant, (M^{-1})**
β-CD-1-BIMOTs-2,4-DCP	1:1	3.9
β-CD-1-BIMOTs-4-CP	1:1	66.9
β-CD-1-BIMOTs-3-CP	1:1	54.5
β-CD-1-BIMOTs-2-CP	1:1	64.9
β-CD-1-BIMOTs-Phenol	1:1	84.4

Table 4.9 (b): The stoichiometry ratio and binding constant for all β-CD-2-BIMOTs complexes

β-CD-2-BIMOTs complexes	Stoichiometry ratio	Binding constant, (M^{-1})
β-CD-2-BIMOTs-2,4-DCP	1:1	29.7
β-CD-2-BIMOTs-4-CP	1:1	45.0
β-CD-2-BIMOTs-3-CP	1:1	59.5
β-CD-2-BIMOTs-2-CP	1:1	54.8
β-CD-2-BIMOTs-Phenol	1:1	58.5

Table 4.9 (a) and (b) shows the stoichiometry ratio and binding constant for all β-CD-1-BIMOTs and β-CD-2-BIMOTs complexes; respectively with phenol, 2-CP, 3-CP, 4-CP and 2,4-DCP. Based on the experimental results, phenol, 2-CP, 3-CP, 4-CP and 2,4-DCP formed a stable 1:1 complex with β-CD-1-BIMOTs (Table 4.9 (a)) and β-CD-2-BIMOTs (Table 4.9 (b)); respectively. These stoichiometric ratios were found to be similar to the literature where 2-CP, 3-CP, 4-CP and 2,4-DCP formed a stable 1:1 complexes with native β-CD (Leyva *et al.*, 2001; Sanyo, 1992). The stoichiometry ratio of all studied inclusion complexes was in accordance with the result that was generally obtained for the aromatic compounds (Kfoury *et al.*, 2014).

Based on Table 4.9 (a), the highest binding constant value was observed on β-CD-1-BIMOTs-phenol complex which was 84.4 M^{-1}. The other β-CD-1-BIMOTs-CPs complexes also showed a slightly lower binding constant value which were 64.9 M^{-1} (β-CD-1-BIMOTs-2-CP), 54.5 M^{-1} (β-CD-1-BIMOTs-3-CP) and 66.9 M^{-1} (β-CD-1-BIMOTs-4-CP) except for the β-CD-1-BIMOTs-2,4-DCP complex. β-CD-1-BIMOTs-2,4-DCP complex showed a very low binding constant value which was 3.9 M^{-1}. From the binding constant value (Table 4.9 (a)), it had demonstrated that phenol, 2-CP, 3-CP

and 4-CP had strong interaction with β-CD-1-BIMOTs. The weakest interaction was observed for β-CD-1-BIMOTs-2,4-DCP complex.

Meanwhile, the value of binding constant for all β-CD-2-BIMOTs-phenolic complexes (Table 4.9 (b)) were calculated to be lower than β-CD-1-BIMOTs complexes except for β-CD-2-BIMOTs-2,4-DCP. Formation of an inclusion complex of phenol with ionic liquid difunctionalized β-CD (β-CD-2-BIMOTs) had shown a reduced binding constant value which was from 84.4 M^{-1} to 58.5 M^{-1}. Similar observations were found on β-CD-2-BIMOTs-2-CP and β-CD-2-BIMOTs-4-CP complexes where the value dropped to 54.8 M^{-1} and 45.0 M^{-1}; respectively. For 3-CP, there was no significant changes on the binding constant upon the formation of inclusion complex with β-CD-1-BIMOTs and β-CD-2-BIMOTs. Surprisingly, the binding constant value for β-CD-2-BIMOTs-2,4-DCP complex had a significant increment which was from 3.9 M^{-1} to 29.7 M^{-1}. From the binding constant value, it was shown that β-CD-2-BIMOTs also had a strong interaction with phenol, 2-CP, 3-CP and 4-CP but had demonstrated a weaker interaction with 2,4-DCP.

The NMR and UV-Vis analysis (Section 4.3.1 and 4.3.3) had supported the formation of the inclusion complexes of β-CD-1-BIMOTs-2,4-DCP and β-CD-2-BIMOTs-2,4-DCP. Both β-CD-1-BIMOTs and β-CD-2-BIMOTs seems to have a different way to interact with 2,4-DCP. As can be seen in Figure 4.29 in Section 4.3.2, both complexes were predicted to have different inclusion complex orientation. Generally, phenol and chlorophenols accommodated β-CD through the wider rim site with the hydroxyl group of phenolic compound preferably facing the secondary 2- and 3- hydroxyl oxygen (tail first orientation) (Huang *et al.*, 1997).

Referring to the structure of β-CD-1-BIMOTs (Figure 4.28 (a)), the guest easily entered the cavity through the secondary surface and formed intermolecular hydrogen-bond interaction inside the cavity. According to Huang *et al.*, when the benzene ring was

deeper inside the cavity, the inclusion complex become more stable until their minimum conformer was reached (Huang *et al.*, 1997). The stability of the all β-CD-1-BIMOTs complexes depended on the size/shape-fit between host and the guest. This explained the difference in the binding constant value obtained for all analyte studied.

At the optimum conditions prepared for the electrochemical oxidation of 2,4-DCP, the possible interferences showed a negligible effect on the oxidation peak current signal for respective target analyte. Specifically, when the optimum potential was applied to the β-CD-1-BIMOTs/CPE (0.75 V), only 2,4-DCP was diffused from the bulky electrolyte solution to the electrolyte/electrode interface, hence successfully accommodated the β-CD-1-BIMOTs cavity. As the cavity was being occupied by the 2,4-DCP, this analyte will be selectively oxidized at the β-CD-1-BIMOTs/CPE surface.

In the presence of common ions and the 2,4-DCP's analogues, different outcomes were observed at β-CD-2-BIMOTs/CPE. It was discovered that the respective electrode surface was not selective towards 2,4-DCP. The NMR analysis demonstrated that all inclusion complexes will occur at the exterior part of β-CD-2-BIMOTs wider rim. As the optimum potential was applied to the electrode (0.68 V), the 2,4-DCP that was pre-concentrated at the electrode/electrolyte interface will undergo the oxidation process without being incorporated into the β-CD-2-BIMOTs's cavity.

The IL moiety that had been occupied with the C-3-OH position had hindered the insertion of the guest analyte. Consequently, the β-CD-2-BIMOTs/CPE surface was unable to identify the target analyte amongst all analogues hence giving a false current response that was contributed by both 2,4-DCP and its analogues. This explained why the binding constant value for certain β-CD-2-BIMOTs-analogues complexes were lowered compared to β-CD-2-BIMOTs–analogues complexes. Lower potential value was required for the electron transfer to occur since the oxidation processes occurred more outside β-CD-2-BIMOTs cavity.

This inclusion complex study had clearly described why β-CD-1-BIMOTs and β-CD-2-BIMOTs will have a different selectivity results towards 2,4-DCP selected analogues studied. The IL positioning (especially the second IL substitution at C-3-OH position) had strongly affected the complexation process yet controlling the selectiveness of these β-CD-ILs towards 2,4-DCP. Despite the selectivity factor, the sensitivity, reproducibility of the carbon paste electrode (CPE) that had been modified with β-CD-2-BIMOTs was still comparable to the β-CD-1-BIMOTs/CPE. Further molecular modelling studies are necessary to acquire a more details picture of all inclusion complexes studied. The molecular modeling studies had provided a better insight into geometry and inclusion mode of the 2,4-DCP and its analogues inside β -CD-1-BIMOTs and β-CD-2-BIMOTs cavities.

CHAPTER 5: CONCLUSION AND FUTURE DIRECTION

5.1 Conclusion

The new carbon paste electrode modifiers β-CD-1-BIMOTs and β-CD-2-BIMOTs were prepared, characterized and fabricated on the CPE. The β-CD-1-BIMOTs/CPE and β-CD-2-BIMOTs/CPE working electrode were successfully characterized, optimized, validated and applied for the enrichment of the detection of 2,4-DCP in environmental samples of mineral water, lake water and landfill leachate. Both β-CD-1-BIMOTs/CPE and β-CD-2-BIMOTs/CPE sensors had shown an improvement on the voltammetry peak current for anodic determination of 2,4-DCP compared to the native β-CD/CPE and CPE. Due to the synergic property boosted by IL functionalized β-CD, both modified CPE have shown a good linear detection range of 4.3-100.0$\times10^{-6}$ mol L^{-1} and 13.8-100.0 $\times10^{-6}$ mol L^{-1}; respectively for β-CD-1-BIMOTs/CPE and β-CD-2-BIMOTs/CPE which the value were comparable to the literature studies. The obtained LOD for both β-CD-1-BIMOTs/CPE and β-CD-2-BIMOTs/CPE were 1.3×10^{-6} mol L^{-1} and 4.3 $\times10^{-6}$ mol L^{-1}; respectively with LOQ of 4.3 $\times10^{-6}$ mol L^{-1} and 13.8 $\times10^{-6}$ mol L^{-1}; respectively. The application of β-CD-1-BIMOTs/CPE and β-CD-2-BIMOTs/CPE in the environmental samples recorded a good recovery of 2,4-DCP with satisfactory precision of 85.5-117.7 % (RSD <3.72) and 93.7-113.4 % (RSD <7.34); respectively. The electrochemical results provided that only β-CD-1-BIMOTs/CPE indicated a good performance for future development of 2,4-DCP sensor instead of β-CD-2-BIMOTs/CPE due to its poor selectivity properties. Based on the evaluation on the inclusion complexes of β-CD-1-BIMOTs-2,4-DCP and β-CD-2-BIMOTs-2,4-DCP through 2D NOESY NMR spectroscopy and UV-Vis spectrometry, the inclusion complexes for both complexes occurred with 1:1 stoichiometry ratio. The spectroscopic investigation has discovered that the formation of inclusion complex of β-CD-1-BIMOTs and β-CD-2-BIMOTs with 2,4-DCP and its selected analogues were difference in term of their interaction geometries.

Specifically, the whole 2,4-DCP structure was predicted to enter the β-CD-1-BIMOTs cavity upon the formation of inclusion complex. Meanwhile, the complex of β-CD-2-BIMOTs-2,4-DCP occurred mainly on the exterior part of the β-CD-2-BIMOTs cavity. From the results, it is disclosed that the interaction of 2,4-DCP with β-CD-ILs were strictly governed by the number of IL substitution and position on β-CD.

5.2 Future direction

A further investigation on the interaction of β-CD-1-BIMOTs and β-CD-2-BIMOTs with 2,4-DCP is in need. A proper computational methodology is necessary to simulate the inclusion process and optimize the complex structures. Besides, the functionalization of IL (of the same respective IL) on C-2 free hydroxyl at the secondary face of β-CD is very essential to understand more regarding the relationship between the positioning of IL on β-CD towards their formation of inclusion complex with 2,4-DCP. Other than that, the application of β-CD-1-BIMOTs/CPE and β-CD-2-BIMOTs/CPE should be prolonged with a different kind of electroactive compounds that can possibly form inclusion complexes with β-CD.

REFERENCES

Abbaspour, Abdolkarim, & Noori, Abolhassan. (2011). A cyclodextrin host–guest recognition approach to an electrochemical sensor for simultaneous quantification of serotonin and dopamine. *Biosensors and Bioelectronics, 26*(12), 4674-4680.

Abdolmaleki, Azizeh, Ghasemi, Fatemeh, & Ghasemi, Jahan B. (2017). Computer-aided drug design to explore cyclodextrin therapeutics and biomedical applications. *Chemical Biology & Drug Design, 89*(2), 257-268.

Abdul Aziz, Md, & Kawde, Abdel-Nasser. (2013). Gold nanoparticle-modified graphite pencil electrode for the high-sensitivity detection of hydrazine. *Talanta, 115*, 214-221.

Absalan, Ghodratollah, Akhond, Morteza, Karimi, Raziye, & Ramezani, Amir M. (2018). Simultaneous determination of captopril and hydrochlorothiazide by using a carbon ionic liquid electrode modified with copper hydroxide nanoparticles. *Microchimica Acta, 185*(2), Articles#97.

Afkhami, Abbas, Soltani-Felehgari, Farzaneh, Madrakian, Tayyebeh, & Ghaedi, Hamed. (2014). Surface decoration of multi-walled carbon nanotubes modified carbon paste electrode with gold nanoparticles for electro-oxidation and sensitive determination of nitrite. *Biosensors and Bioelectronics, 51*, 379-385.

Afsharmanesh, Elahe, Karimi-Maleh, Hassan, Pahlavan, Ali, & Vahedi, Javad. (2013). Electrochemical behavior of morphine at ZnO/CNT nanocomposite room temperature ionic liquid modified carbon paste electrode and its determination in real samples. *Journal of Molecular Liquids, 181*, 8-13.

Alahmadi, Sana M., Mohamad, Sharifah, & Maah, Mohd Jamil. (2012). Synthesis and Characterization of Mesoporous Silica Functionalized with Calix[4]arene Derivatives. *International Journal of Molecular Sciences, 13*(10), 13726-13736.

Alavi-Tabari, Seyed, Khalilzadeh, Mohammad A., & Karimi-Maleh, Hassan. (2018). Simultaneous determination of doxorubicin and dasatinib as two breast anticancer drugs uses an amplified sensor with ionic liquid and ZnO nanoparticle. *Journal of Electroanalytical Chemistry, 811*, 84-88.

Amani-Beni, Zahra, & Nezamzadeh-Ejhieh, Alireza. (2017). A novel non-enzymatic glucose sensor based on the modification of carbon paste electrode with CuO nanoflower: designing the experiments by response surface methodology (RSM). *Journal of Colloid and Interface Science, 504*, 186-196.

Antuña-Jiménez, Daniel, Díaz-Díaz, Goretti, Blanco-López, M. Carmen, Lobo-Castañón, M. Jesús, Miranda-Ordieres, Arturo J., & Tuñón-Blanco, Paulino. (2012). Chapter

1 - Molecularly Imprinted Electrochemical Sensors: Past, Present, and Future. In Songjun Li, Yi Ge, Sergey A. Piletsky & Joseph Lunec (Eds.), *Molecularly Imprinted Sensors* (pp. 1-34). Amsterdam: Elsevier.

Arabali, Vahid, Ebrahimi, Mahmoud, Abbasghorbani, Maryam, Gupta, Vinod Kumar, Farsi, Mohammad, Ganjali, MR, & Karimi, Fatemeh. (2016a). Electrochemical determination of vitamin C in the presence of NADH using a CdO nanoparticle/ionic liquid modified carbon paste electrode as a sensor. *Journal of Molecular Liquids, 213*, 312-316.

Arabali, Vahid, Ebrahimi, Mahmoud, Gheibi, Siamak, Khaleghi, Fatemeh, Bijad, Majede, Rudbaraki, Ali, Abbasghorbani, Maryam, & Ganjali, MR. (2016b). Bisphenol A analysis in food samples using modified nanostructure carbon paste electrode as a sensor. *Food Analytical Methods, 9*(6), 1763-1769.

Ariz, Idoia, Cruchaga, Saioa, Lasa, Berta, Moran, Jose F, Jauregui, Ivan, & Aparicio-Tejo, Pedro M. (2012). The physiological implications of urease inhibitors on N metabolism during germination of Pisum sativum and Spinacea oleracea seeds. *Journal of Plant Physiology, 169*(7), 673-681.

ATSDR. (2007). Comprehensive Environmental Response, Compensation, and Liability Act (CERCLA) Priority List of Hazardous Substances. Retrieved 10 April 2017, from https://www.epa.gov/enforcement/comprehensive-environmental-response-compensation-and-liability-act-cercla-and-federal.

Badruddoza, AZM, Hidajat, K, & Uddin, MS. (2010). Synthesis and characterization of β-cyclodextrin-conjugated magnetic nanoparticles and their uses as solid-phase artificial chaperones in refolding of carbonic anhydrase bovine. *Journal of Colloid and Interface Science, 346*(2), 337-346.

Baghayeri, Mehdi, Sedrpoushan, Alireza, Mohammadi, Alireza, & Heidari, Masoud. (2017). A non-enzymatic glucose sensor based on NiO nanoparticles/functionalized SBA 15/MWCNT-modified carbon paste electrode. *Ionics, 23*(6), 1553-1562.

Bagheri, Hasan, Shirzadmehr, Ali, & Rezaei, Mosayeb. (2015). Designing and fabrication of new molecularly imprinted polymer-based potentiometric nano-graphene/ionic liquid/carbon paste electrode for the determination of losartan. *Journal of Molecular Liquids, 212*, 96-102.

Bakker, Eric, & Qin, Yu. (2006). Electrochemical Sensors. *Analytical Chemistry, 78*(12), 3965-3984.

Bandodkar, Amay J, Jia, Wenzhao, & Wang, Joseph. (2015). Tattoo-based wearable electrochemical devices: a review. *Electroanalysis, 27*(3), 562-572.

Banjare, Manoj Kumar, Behera, Kamalakanta, Satnami, Manmohan L, Pandey, Siddharth, & Ghosh, Kallol K. (2017). Supra-molecular inclusion complexation of ionic liquid 1-butyl-3-methylimidazolium octylsulphate with α-and β-cyclodextrins. *Chemical Physics Letters, 689*, 30-40.

Beitollahi, Hadi, Ivari, Susan Ghofrani, & Torkzadeh-Mahani, Masoud. (2018). Application of antibody–nanogold–ionic liquid–carbon paste electrode for sensitive electrochemical immunoassay of thyroid-stimulating hormone. *Biosensors and Bioelectronics, 110*, 97-102.

Beitollahi, Hadi, Tajik, Somayeh, & Jahani, Shohreh. (2016). Electrocatalytic Determination of Hydrazine and Phenol Using a Carbon Paste Electrode Modified with Ionic Liquids and Magnetic Core shell Fe_3O_4@ SiO_2/MWCNT Nanocomposite. *Electroanalysis, 28*(5), 1093-1099.

Benvidi, Ali, Nafar, Mohammad Taghi, Jahanbani, Shahriar, Tezerjani, Marzieh Dehghan, Rezaeinasab, Masoud, & Dalirnasab, Sudabeh. (2017). Developing an electrochemical sensor based on a carbon paste electrode modified with nano-composite of reduced graphene oxide and $CuFe_2O_4$ nanoparticles for determination of hydrogen peroxide. *Materials Science and Engineering: C, 75*, 1435-1447.

Beytur, Murat, Kardaş, Faruk, Akyıldırım, Onur, Özkan, Abdullah, Bankoğlu, Bahar, Yüksek, Haydar, Yola, Mehmet Lütfi, & Atar, Necip. (2018). A highly selective and sensitive voltammetric sensor with molecularly imprinted polymer based silver@ gold nanoparticles/ionic liquid modified glassy carbon electrode for determination of ceftizoxime. *Journal of Molecular Liquids, 251*, 212-217.

Biglari, Hamed, Afsharnia, Mojtaba, Alipour, Vali, Khosravi, Rasoul, Sharafi, Kiomars, & Mahvi, Amir Hossein. (2017). A review and investigation of the effect of nanophotocatalytic ozonation process for phenolic compound removal from real effluent of pulp and paper industry. *Environmental Science and Pollution Research, 24*(4), 4105-4116.

Bors, Milena, Bukowska, Bożena, Pilarski, Radosław, Gulewicz, Krzysztof, Oszmiański, Jan, Michałowicz, Jaromir, & Koter-Michalak, Maria. (2011). Protective activity of the Uncaria tomentosa extracts on human erythrocytes in oxidative stress induced by 2,4-dichlorophenol (2,4-DCP) and catechol. *Food and Chemical Toxicology, 49*(9), 2202-2211.

Brady, Bernadette, Lynam, Nuala, O Sullivan, Thomas, Ahern, Cormac, & Darcy, R. (2000). 6^A-O-*p*-Toluenesulfonyl-beta-cyclodextrin. *Organic Syntheses, 77*, 220-224.

Brandariz, Isabel, & Iglesias, Emilia. (2013). Local Anesthetics: Acid-base Behaviour and Inclusion with Cyclodextrins. *Current Organic Chemistry, 17*(24), 3050-3063.

Bukowska, Bożena. (2003). Effects of 2,4-D and its metabolite 2,4-dichlorophenol on antioxidant enzymes and level of glutathione in human erythrocytes. *Comparative Biochemistry and Physiology Part C: Toxicology & Pharmacology, 135*(4), 435-441.

Butmee, Preeyanut, Tumcharern, Gamolwan, Saejueng, Pranorm, Stankovic, Dalibor, Ortner, Astrid, Jitcharoen, Juthamas, Kalcher, Kurt, & Samphao, Anchalee. (2019). A direct and sensitive electrochemical sensing platform based on ionic liquid functionalized graphene nanoplatelets for the detection of bisphenol A. *Journal of Electroanalytical Chemistry, 833*, 370-379.

Capodaglio, Andrea G, Callegari, Arianna, & Molognoni, Daniele. (2016). Online monitoring of priority and dangerous pollutants in natural and urban waters: a state-of-the-art review. *Management of Environmental Quality: An International Journal, 27*(5), 507-536.

Ceylan, Zeynep, Sisman, Turgay, Dane, Hatice, & Adil, Şeymanur. (2019). The Embryotoxicity of Some Phenol Derivatives on Zebrafish, Danio rerio. *Caspian Journal of Environmental Sciences, 17*(1), 11-22.

Chaiyo, Sudkate, Mehmeti, Eda, Žagar, Kristina, Siangproh, Weena, Chailapakul, Orawon, & Kalcher, Kurt. (2016). Electrochemical sensors for the simultaneous determination of zinc, cadmium and lead using a Nafion/ionic liquid/graphene composite modified screen-printed carbon electrode. *Analytica Chimica Acta, 918*, 26-34.

Chanysheva, Alina. (2016). *Electrochemical Sensing System for Detection of Organophosphate Neurotoxins.* Auburn University, Auburn, Alabama.

Cheek, G. T., & Nelson, R. F. (1978). Applications of Chemically Modified Electrodes to Analysis of Metal Ions. *Analytical Letters, 11*(5), 393-402.

Chelli, Saloua, Majdoub, Mustapha, Jouini, Mohamed, Aeiyach, Salah, Maurel, François, Chane-Ching, Kathleen I, & Lacaze, Pierre-Camille. (2007). Host–guest complexes of phenol derivatives with β-cyclodextrin: an experimental and theoretical investigation. *Journal of Physical Organic Chemistry, 20*(1), 30-43.

Chen, Xiaomei, Guo, Zhian, Wang, Yi, Liu, Yufeng, Xu, Yidong, Liu, Jie, Li, Zhiqiang, & Zhao, Jingchan. (2019). Temperature sensitive polymer-dispersive liquid–liquid microextraction with gas chromatography–mass spectrometry for the determination of phenols. *Journal of Chromatography A, 1592*, 183-187.

Chen, Yu, Ye, Yanchun, Wang, Liye, Guo, Yanwen, & Tan, Huimin. (2012). Synthesis of chitosan C6-substituted cyclodextrin derivatives with tosyl-chitin as the intermediate precursor. *Journal of Applied Polymer Science, 125*(S2), E378-E383.

Cheraghi, Somaye, Taher, Mohammad Ali, & Karimi-Maleh, Hassan. (2016). A novel strategy for determination of paracetamol in the presence of morphine using a carbon paste electrode modified with CdO nanoparticles and ionic liquids. *Electroanalysis, 28*(2), 366-371.

Chillawar, Rakesh R, Tadi, Kiran Kumar, & Motghare, Ramani V. (2015). Voltammetric techniques at chemically modified electrodes. *Journal of Analytical Chemistry, 70*(4), 399-418.

Coleman, Anthony W, Zhang, Ping, Ling, Chang-Chun, Miocque, Marcel, & Mascrier, Line. (1991). The first selective per-tosylation of the secondary OH-2 of β-cyclodextrin. *Tetrahedron Letters, 32*(32), 3997-3998.

Collyer, Stuart D, Davis, Frank, Lucke, Andrew, Stirling, Charles JM, & Higson, Séamus PJ. (2003). The electrochemistry of the ferri/ferrocyanide couple at a calix [4] resorcinarenetetrathiol-modified gold electrode as a study of novel electrode modifying coatings for use within electro-analytical sensors. *Journal of Electroanalytical Chemistry, 549*, 119-127.

Concheiro, Angel, & Alvarez-Lorenzo, Carmen. (2013). Chemically cross-linked and grafted cyclodextrin hydrogels: From nanostructures to drug-eluting medical devices. *Advanced Drug Delivery Reviews, 65*(9), 1188-1203.

Corb, Ioana, Manea, Florica, Radovan, Ciprian, Pop, Aniela, Burtica, Georgeta, Malchev, Plamen, Picken, Stephen, & Schoonman, Joop. (2007). Carbon-based Composite Electrodes: Preparation, Characterization and Application in Electroanalysis. *Sensors (Basel, Switzerland), 7*(11), 2626-2635.

Crini, Grégorio. (2014). Review: A History of Cyclodextrins. *Chemical Reviews, 114*(21), 10940-10975.

Crini, Grégorio, Fourmentin, Sophie, Fenyvesi, Éva, Torri, Giangiacomo, Fourmentin, Marc, & Morin-Crini, Nadia. (2018). Fundamentals and Applications of Cyclodextrins. *Cyclodextrin Fundamentals, Reactivity and Analysis*,*Volume 16*, (pp. 1-55). Cham: Springer International Publishing.

Cui, Meng, Li, Jingtong, Lu, Dayong, & Shao, Ziqiang. (2018). Development of a Metal-Organic Framework for the Sensitive Determination of 2,4-Dichlorophenol. *International Journal of Electrochemical Science, 13*(4), 3420-3428.

Cwiertnia, B., Hladon, T., & Stobiecki, M. (1999). Stability of diclofenac sodium in the inclusion complex with beta-cyclodextrin in the solid state. *Journal of Pharmacy and Pharmacology, 51*(11), 1213-1218.

Dai, Yun, Wang, Shuye, Wu, Jianhua, Tang, Jian, & Tang, Weihua. (2012). Dicationic AC regioisomer cyclodextrins: mono-6 A-ammonium-6 C-alkylimidazolium-β-cyclodextrin chlorides as chiral selectors for enantioseparation. *RSC Advances, 2*(33), 12652-12656.

de Boer, Frankjen Y, Imhof, Arnout, & Velikov, Krassimir P. (2019). Encapsulation of colorants by natural polymers for food applications. *Coloration Technology, 135*(3), 183-194.

Del Valle, E. M. Martin. (2004). Cyclodextrins and their uses: a review. *Process Biochemistry, 39*(9), 1033-1046.

Dhameja, Koushal, Chaudhary, Anjali, & Pahwa, Shilpa. (2018). Application of B-Cyclodextrin Drug Inclusion Complexes to Improve Solubility of Poorly Water Soluble Drug. *Journal of Basic Pharmacology and Toxicology, 2*(1), 18-21.

Dong, Sheying, Suo, Gaochao, Li, Nan, Chen, Zhen, Peng, Lei, Fu, Yile, Yang, Qin, & Huang, Tinglin. (2016). A simple strategy to fabricate high sensitive 2,4-dichlorophenol electrochemical sensor based on metal organic framework $Cu_3(BTC)_2$. *Sensors and Actuators B: Chemical, 222*, 972-979.

Duan, Xiuzhi, Cui, Yanhong, Zhang, Chao, Gao, Bao, & Deng, Dongshun. (2019). Solubilities and Thermodynamic Properties of NH_3 in Glycerin and its Derivatives. *Journal of Chemical & Engineering Data, 64*(3), 1131-1139.

El-Shal, Manal A, Attia, Ali K, & Abdulla, Shabaan A. (2013). β-Cyclodextrin modified carbon paste electrode for the determination of gemifloxacin and nadifloxacin. *Journal of Advanced Scientific Research, 4*(2), 25-30.

El Seoud, Omar A., Koschella, Andreas, Fidale, Ludmila C., Dorn, Susann, & Heinze, Thomas. (2007). Applications of Ionic Liquids in Carbohydrate Chemistry: A Window of Opportunities. *Biomacromolecules, 8*(9), 2629-2647.

Elyasi, Mojdeh, Khalilzadeh, Mohammad A., & Karimi-Maleh, Hassan. (2013). High sensitive voltammetric sensor based on Pt/CNTs nanocomposite modified ionic liquid carbon paste electrode for determination of Sudan I in food samples. *Food Chemistry, 141*(4), 4311-4317.

Endres, Frank, Abbott, Andrew, & MacFarlane, Douglas R. (2017). *Electrodeposition from ionic liquids* (2 ed.). United States: John Wiley & Sons.

Fang, Rou, Yi, Ling-Xiao, Shao, Yu-Xiu, Zhang, Li, & Chen, Guan-Hua. (2014). On-line preconcentration in capillary electrophoresis for analysis of agrochemical residues. *Journal of Liquid Chromatography & Related Technologies, 37*(10), 1465-1497.

Farjami, Fatemeh, Fasihi, Farshid, Alimohammadi, Forough, & Moradi, Seyed Esmaeil. (2019). Electrochemical Behavior and Highly Sensitive Voltammetric Determination of Doxepin in Pharmaceutical Preparations and Blood Serum Using Carbon Ionic Liquid Electrode. *Iranian Journal of Pharmaceutical Research, 18*(1), 91-101.

Feng, Qinzhong, Li, Haifang, Zhang, Zhiyong, & Lin, Jin-Ming. (2011). Gold nanoparticles for enhanced chemiluminescence and determination of 2, 4-dichlorophenol in environmental water samples. *Analyst, 136*(10), 2156-2160.

Fenyvesi, E, Vikmon, M, & Szente, L. (2016). Cyclodextrins in food technology and human nutrition: benefits and limitations. *Critical Reviews in Food Science and Nutrition, 56*(12), 1981-2004.

Floresta, Giuseppe, & Rescifina, Antonio. (2019). Metyrapone-β-cyclodextrin supramolecular interactions inferred by complementary spectroscopic/spectrometric and computational studies. *Journal of Molecular Structure, 1176*, 815-824.

Fotouhi, Lida, Fatollahzadeh, Maryam, & Heravi, Majid M. (2012). Electrochemical behavior and voltammetric determination of sulfaguanidine at a glassy carbon electrode modified with a multi-walled carbon nanotube. *International Journal of Electrochemical Science, 7*, 3919-3928.

Fouladgar, Masoud, Karimi-Maleh, Hassan, & Gupta, Vinod Kumar. (2015). Highly sensitive voltammetric sensor based on NiO nanoparticle room temperature ionic liquid modified carbon paste electrode for levodopa analysis. *Journal of Molecular Liquids, 208*, 78-83.

Freire, Mara G, Santos, Luis MNBF, Fernandes, Ana M, Coutinho, Joao AP, & Marrucho, Isabel M. (2007). An overview of the mutual solubilities of water–imidazolium-based ionic liquids systems. *Fluid Phase Equilibria, 261*(1-2), 449-454.

Fritea, Luminţa, Tertiş, Mihaela, Cristea, Cecilia, Cosnier, Serge, & Săndulescu, Robert. (2015). Simultaneous Determination of Ascorbic and Uric Acids in Urine Using an Innovative Electrochemical Sensor Based on β-Cyclodextrin. *Analytical Letters, 48*(1), 89-99.

Fu, Xiaohong, Pu, Lan, Wang, Jinyue, & Zhong, Zhaoyang. (2010). Ionic liquids-doped organic-inorganic hybrid film for electrochemical immunoassay for hepatitis B surface antigen. *Ionics, 16*(1), 51-56.

Fujita, Kyohhei, Fujiwara, Shoji, Yamada, Tatsuru, Tsuchido, Yuji, Hashimoto, Takeshi, & Hayashita, Takashi. (2017). Design and Function of Supramolecular Recognition Systems Based on Guest-Targeting Probe-Modified Cyclodextrin Receptors for ATP. *The Journal of Organic Chemistry, 82*(2), 976-981.

Fytianos, K., Voudrias, E., & Kokkalis, E. (2000). Sorption–desorption behaviour of 2,4-dichlorophenol by marine sediments. *Chemosphere, 40*(1), 3-6.

Gao, Yan-Sha, Wu, Li-Ping, Zhang, Kai-Xin, Xu, Jing-Kun, Lu, Li-Min, Zhu, Xiao-Fei, & Wu, Yao. (2015). Electroanalytical method for determination of shikonin based on the enhancement effect of cyclodextrin functionalized carbon nanotubes. *Chinese Chemical Letters, 26*(5), 613-618.

Gaofeng, W, Hong, X, & Mei, J. (2004). Biodegradation of chlorophenols. *China International Journal, 1*(6), 67-75.

Garba, Zaharaddeen N., Zhou, Weiming, Lawan, Ibrahim, Xiao, Wei, Zhang, Mingxi, Wang, Liwei, Chen, Lihui, & Yuan, Zhanhui. (2019). An overview of chlorophenols as contaminants and their removal from wastewater by adsorption: A review. *Journal of Environmental Management, 241*, 59-75.

Ge, Mengchen, Hussain, Ghulam, Hibbert, D. Brynn, Silvester, Debbie S., & Zhao, Chuan. (2019). Ionic Liquid-based Microchannels for Highly Sensitive and Fast Amperometric Detection of Toxic Gases. *Electroanalysis, 31*(1), 66-74.

Gidwani, Bina, & Vyas, Amber. (2015). A Comprehensive Review on Cyclodextrin-Based Carriers for Delivery of Chemotherapeutic Cytotoxic Anticancer Drugs. *BioMedical Research International, 2015*, 1-15.

Gonil, Pattarapond, Sajomsang, Warayuth, Ruktanonchai, Uracha Rungsardthong, Pimpha, Nuttaporn, Sramala, Issara, Nuchuchua, Onanong, Saesoo, Somsak, Chaleawlert-umpon, Saowaluk, & Puttipipatkhachorn, Satit. (2011). Novel quaternized chitosan containing β-cyclodextrin moiety: Synthesis, characterization and antimicrobial activity. *Carbohydrate Polymers, 83*(2), 905-913.

Guo, Lei, Pan, Xu, Zhang, Changneng, Liu, Weiqing, Wang, Meng, Fang, Xiaqin, & Dai, Songyuan. (2010). Ionic liquid electrolyte based on S-propyltetrahydrothiophenium iodide for dye-sensitized solar cells. *Solar Energy, 84*(3), 373-378.

Hanrahan, Grady, Patil, Deepa G, & Wang, Joseph. (2004). Electrochemical sensors for environmental monitoring: design, development and applications. *Journal of Environmental Monitoring, 6*(8), 657-664.

Hayyan, Maan, Mjalli, Farouq S., Hashim, Mohd Ali, AlNashef, Inas M., & Mei, Tan Xue. (2013). Investigating the electrochemical windows of ionic liquids. *Journal of Industrial and Engineering Chemistry, 19*(1), 106-112.

Honda, Masato, & Kannan, Kurunthachalam. (2018). Biomonitoring of chlorophenols in human urine from several Asian countries, Greece and the United States. *Environmental Pollution, 232*, 487-493.

House, W. A., Leach, D., Long, J. L. A., Cranwell, P., Smith, C., Bharwaj, L., Meharg, A., Ryland, G., Orr, D. O., & Wright, J. (1997). Micro-organic compounds in the Humber rivers. *Science of The Total Environment, 194-195*, 357-371.

Huang, Huayu, Wang, Mingxia, Wang, Yang, Li, Xinli, Niu, Zhiying, Wang, Xingyu, & Song, Jinxi. (2018). Electrochemical determination of 2,4-dichlorophenol by using a glassy carbon electrode modified with molybdenum disulfide, ionic liquid and gold/silver nanorods. *Microchimica Acta, 185*(6), Article#292.

Huang, MJ, Watts, John D, & Bodor, Nicholas. (1997). Theoretical studies of inclusion complexes of a-and b-cyclodextrin with benzoic acid and phenol. *International Journal of Quantum Chemistry, 65*(6), 1135–1152.

Huang, Shasheng, Qu, Yongxia, Li, Ruina, Shen, Jian, & Zhu, Liwei. (2007). Biosensor based on horseradish peroxidase modified carbon nanotubes for determination of 2,4-dichlorophenol. *Microchimica Acta, 162*(1), 261-268.

Humayun, Muhammad, Hu, Zhewen, Khan, Abbas, Cheng, Wei, Yuan, Yang, Zheng, Zhiping, Fu, Qiuyun, & Luo, Wei. (2019). Highly efficient degradation of 2,4-dichlorophenol over CeO_2/g-C_3N_4 composites under visible-light irradiation: Detailed reaction pathway and mechanism. *Journal of Hazardous Materials, 364*, 635-644.

Igbinosa, Etinosa O., Odjadjare, Emmanuel E., Chigor, Vincent N., Igbinosa, Isoken H., Emoghene, Alexander O., Ekhaise, Fredrick O., Igiehon, Nicholas O., & Idemudia, Omoruyi G. (2013). Toxicological Profile of Chlorophenols and Their Derivatives in the Environment: The Public Health Perspective. *The Scientific World Journal, 2013*, Articles#460215.

Jamali, Tahoora, Karimi-Maleh, Hassan, & Khalilzadeh, Mohammad A. (2014). A novel nanosensor based on Pt:Co nanoalloy ionic liquid carbon paste electrode for voltammetric determination of vitamin B9 in food samples. *LWT - Food Science and Technology, 57*(2), 679-685.

Jicsinszky, Laszlo, Caporaso, Marina, Tuza, Kata, Martina, Katia, Calcio Gaudino, Emanuela, & Cravotto, Giancarlo. (2016). Nucleophilic Substitutions of 6I-O-Monotosyl-β-cyclodextrin in a Planetary Ball Mill. *ACS Sustainable Chemistry & Engineering, 4*(3), 919-929.

Jouffroy, Matthieu, Armspach, Dominique, Matt, Dominique, & Toupet, Loïc. (2013). Regioselective di-and tetra-functionalisation of γ-cyclodextrin using capping methodology. *Organic & Biomolecular Chemistry, 11*(22), 3699-3705.

Kalcher, Kurt. (1990). Chemically modified carbon paste electrodes in voltammetric analysis. *Electroanalysis, 2*(6), 419-433.

Karci, Akın, Arslan-Alaton, Idil, Olmez-Hanci, Tugba, & Bekbölet, Miray. (2012). Transformation of 2,4-dichlorophenol by H_2O_2/UV-C, Fenton and photo-Fenton processes: Oxidation products and toxicity evolution. *Journal of Photochemistry and Photobiology A: Chemistry, 230*(1), 65-73.

Karimi-Maleh, Hassan, Sanati, Afsaneh L, Gupta, Vinod Kumar, Yoosefian, Mehdi, Asif, Mohammad, & Bahari, Ali. (2014). A voltammetric biosensor based on ionic liquid/NiO nanoparticle modified carbon paste electrode for the determination of nicotinamide adenine dinucleotide (NADH). *Sensors and Actuators B: Chemical, 204*, 647-654.

Karyakin, Arkady A, Gitelmacher, Olga V, & Karyakina, Elena E. (1995). Prussian blue-based first-generation biosensor. A sensitive amperometric electrode for glucose. *Analytical Chemistry, 67*(14), 2419-2423.

Kato, Dai, & Niwa, Osamu. (2013). Carbon-based electrode materials for DNA electroanalysis. *Analytical Sciences, 29*(4), 385-392.

Keskin, Seda, Kayrak-Talay, Defne, Akman, Uğur, & Hortaçsu, Öner. (2007). A review of ionic liquids towards supercritical fluid applications. *The Journal of Supercritical Fluids, 43*(1), 150-180.

Kfoury, Miriana, Landy, David, Auezova, Lizette, greige-gerges, Helene, & Fourmentin, Sophie. (2014). Effect of cyclodextrin complexation on phenylpropanoids' solubility and antioxidant activity. *Beilstein Journal of Organic Chemistry, 10*, 2322-2331.

Khaled, Elmorsy, Kamel, Manal S, Hassan, Hassan NA, Haroun, Ahmed A, Youssef, Ahmed M, & Aboul-Enein, Hassan Y. (2012). Novel multi walled carbon nanotubes/β-cyclodextrin based carbon paste electrode for flow injection potentiometric determination of piroxicam. *Talanta, 97*, 96-102.

Khan, Abdul Rauf, Forgo, Peter, Stine, Keith J., & D'Souza, Valerian T. (1998). Methods for Selective Modifications of Cyclodextrins. *Chemical Reviews, 98*(5), 1977-1996.

Khani, Hadi, Rofouei, Mohammad Kazem, Arab, Pezhman, Gupta, Vinod Kumar, & Vafaei, Zahra. (2010). Multi-walled carbon nanotubes-ionic liquid-carbon paste electrode as a super selectivity sensor: Application to potentiometric monitoring of mercury ion(II). *Journal of Hazardous Materials, 183*(1), 402-409.

Kong, Lingmi, Huang, Shasheng, Yue, Zenglian, Peng, Bin, Li, Mengyao, & Zhang, Jing. (2009). Sensitive mediator-free tyrosinase biosensor for the determination of 2,4-dichlorophenol. *Microchimica Acta, 165*(1), 203-209.

Krossing, I., Slattery, J. M., Daguenet, C., Dyson, P. J., Oleinikova, A., & Weingartner, H. (2006). Why are ionic liquids liquid? A simple explanation based on lattice and solvation energies. *Journal of the American Chemical Society, 128*(41), 13427-13434.

Kuwana, Theodore, & French, W. G. (1964). Electrooxidation or Reduction of Organic Compounds into Aqueous Solutions Using Carbon Paste Electrode. *Analytical Chemistry, 36*(1), 241-242.

Lenik, Joanna. (2017). Cyclodextrins based electrochemical sensors for biomedical and pharmaceutical analysis. *Current Medicinal Chemistry, 24*(22), 2359-2391.

Leyva, Elisa, Moctezuma, Edgar, Strouse, Jane, & García-Garibay, Miguel A. (2001). Spectrometric and 2D NMR Studies on the Complexation of Chlorophenols with Cyclodextrins. *Journal of Inclusion Phenomena and Macrocyclic Chemistry, 39*(1), 41-46.

Li, Jian, Ma, Mei, & Wang, Zijian. (2010a). In vitro profiling of endocrine disrupting effects of phenols. *Toxicology in Vitro, 24*(1), 201-207.

Li, Jianjun, Miao, Dandan, Yang, Ran, Qu, Lingbo, & Harrington, Peter de B. (2014). Synthesis of poly(sodium 4-styrenesulfonate) functionalized graphene/cetyltrimethylammonium bromide (CTAB) nanocomposite and its application in electrochemical oxidation of 2,4-dichlorophenol. *Electrochimica Acta, 125*, 1-8.

Li, Ning, Mei, Zheng, & Ding, Sheguang. (2010b). 2,4-Dichlorophenol sorption on cyclodextrin polymers. *Journal of Inclusion Phenomena and Macrocyclic Chemistry, 68*(1), 123-129.

Li, Yonghong, Zhai, Xiurong, Liu, Xinsheng, Wang, Ling, Liu, Herong, & Wang, Haibo. (2016). Electrochemical determination of bisphenol A at ordered mesoporous carbon modified nano-carbon ionic liquid paste electrode. *Talanta, 148*, 362-369.

Liang, Yiming, Yu, Lanlan, Yang, Ran, Li, Xiao, Qu, Lingbo, & Li, Jianjun. (2017). High sensitive and selective graphene oxide/molecularly imprinted polymer electrochemical sensor for 2, 4-dichlorophenol in water. *Sensors and Actuators B: Chemical, 240*, 1330-1335.

Lim, Jun Wei, Khoo, Kuan-Shiong, Lam, Houy-Yng, Lau, Zhen-Yin, Wuie, Alyna Ong Ching, Azlan, Anissa, & Beh, Hoe-Guan. (2019). PVA entrapped activated sludge beads coated with PAC for bioremediating 4-chlorophenol-bearing wastewater. *International Journal of Biomass and Renewables, 7*(2), 12-17.

Liu, Guiting, Yuan, Qijuan, Hollett, Geoffrey, Zhao, Wei, Kang, Yang, & Wu, Jun. (2018). Cyclodextrin-based host–guest supramolecular hydrogel and its application in biomedical fields. *Polymer Chemistry, 9*(25), 3436-3449.

Liu, Hongtao, He, Ping, Li, Zhiying, Sun, Chunyan, Shi, Lihong, Liu, Yang, Zhu, Guoyi, & Li, Jinghong. (2005). An ionic liquid-type carbon paste electrode and its polyoxometalate-modified properties. *Electrochemistry Communications, 7*(12), 1357-1363.

Liu, J., Niu, J., Yin, L., & Jiang, F. (2011). In situ encapsulation of laccase in nanofibers by electrospinning for development of enzyme biosensors for chlorophenol monitoring. *Analyst, 136*(22), 4802-4808.

Liu, Yangyang, Liang, Yiming, Yang, Ran, Li, Jianjun, & Qu, Lingbo. (2019). A highly sensitive and selective electrochemical sensor based on polydopamine functionalized graphene and molecularly imprinted polymer for the 2,4-dichlorophenol recognition and detection. *Talanta, 195*, 691-698.

Liu, Zhiguang, Zhang, Ai, Guo, Yujing, & Dong, Chuan. (2014). Electrochemical sensor for ultrasensitive determination of isoquercitrin and baicalin based on DM-β-cyclodextrin functionalized graphene nanosheets. *Biosensors and Bioelectronics, 58*, 242-248.

López-Nicolás, José Manuel, Rodríguez-Bonilla, Pilar, & García-Carmona, Francisco. (2014). Cyclodextrins and Antioxidants. *Critical Reviews in Food Science and Nutrition, 54*(2), 251-276.

López, Marta Sánchez-Paniagua, & López-Ruiz, Beatriz. (2018). Electrochemical biosensor based on ionic liquid polymeric microparticles. An analytical platform for catechol. *Microchemical Journal, 138*, 173-179.

Ma, Y., Han, J., Guo, Y., Lam, P. K., Wu, R. S., Giesy, J. P., Zhang, X., & Zhou, B. (2012). Disruption of endocrine function in in vitro H295R cell-based and in in vivo assay in zebrafish by 2,4-dichlorophenol. *Aquatic Toxicology, 106-107*, 173-181.

MacFarlane, DR, Meakin, P, Sun, J, Amini, N, & Forsyth, M. (1999). Pyrrolidinium imides: a new family of molten salts and conductive plastic crystal phases. *The Journal of Physical Chemistry B, 103*(20), 4164-4170.

Maduraiveeran, Govindhan, Sasidharan, Manickam, & Ganesan, Vellaichamy. (2018). Electrochemical sensor and biosensor platforms based on advanced nanomaterials for biological and biomedical applications. *Biosensors and Bioelectronics, 103*, 113-129.

Mahlambi, Mphilisi M, Malefetse, Tshepo J, Mamba, Bhekie B, & Krause, Rui WM. (2011). Polymerization of cyclodextrin-ionic liquid complexes for the removal of organic and inorganic contaminants from water *Ionic Liquids: Applications and Perspectives* (pp. 115-151). London: InTech.

Mahlambi, Mphilisi M., Malefetse, Tshepo J., Mamba, Bhekie B., & Krause, Rui W. (2010). β-Cyclodextrin-ionic liquid polyurethanes for the removal of organic pollutants and heavy metals from water: synthesis and characterization. *Journal of Polymer Research, 17*(4), 589-600.

Majidi, Leily, Yasaei, Poya, Warburton, Robert E, Fuladi, Shadi, Cavin, John, Hu, Xuan, Hemmat, Zahra, Cho, Sung Beom, Abbasi, Pedram, & Vörös, Márton. (2019). New Class of Electrocatalysts Based on 2D Transition Metal Dichalcogenides in Ionic Liquid. *Advanced Materials, 31*(4), Article#1804453.

Miao, Juan, Wang, Xin, Fan, Yunchang, Li, Jing, Zhang, Lina, Hu, Guitao, He, Can, & Jin, Can. (2018). Determination of total mercury in seafood by ion-selective electrodes based on a thiol functionalized ionic liquid. *Journal of Food and Drug Analysis, 26*(2), 670-677.

Michałowicz, J, & Duda, W. (2007). Phenols--Sources and Toxicity. *Polish Journal of Environmental Studies, 16*(3), 347-362.

Michałowicz, Jaromir, & Majsterek, Ireneusz. (2010). Chlorophenols, chlorocatechols and chloroguaiacols induce DNA base oxidation in human lymphocytes (in vitro). *Toxicology, 268*(3), 171-175.

Miraki, Mansoureh, Karimi-Maleh, Hassan, Taher, Mohammad A, Cheraghi, Somaye, Karimi, Fatemeh, Agarwal, Shilpi, & Gupta, Vinod Kumar. (2019). Voltammetric amplified platform based on ionic liquid/NiO nanocomposite for determination of benserazide and levodopa. *Journal of Molecular Liquids, 278*, 672-676.

Moriel, P, García-Suárez, Eduardo J, Martínez, M, García, Ana Beatriz, Montes-Morán, Miguel A, Calvino-Casilda, Vanesa, & Bañares, Miguel A. (2010). Synthesis, characterization, and catalytic activity of ionic liquids based on biosources. *Tetrahedron Letters, 51*(37), 4877-4881.

Mura, Paola. (2014). Analytical techniques for characterization of cyclodextrin complexes in aqueous solution: A review. *Journal of Pharmaceutical and Biomedical Analysis, 101*, 238-250.

Olaniran, Ademola O, & Igbinosa, Etinosa O. (2011). Chlorophenols and other related derivatives of environmental concern: properties, distribution and microbial degradation processes. *Chemosphere, 83*(10), 1297-1306.

Onozuka, Shigeharu, Kojima, Masayoshi, Hattori, Kenjiro, & Toda, Fujio. (1980). The regiospecific mono tosylation of cyclodextrins. *Bulletin of the Chemical Society of Japan, 53*(11), 3221-3224.

Osmani, Riyaz Ali M, Kulkarni, Parthasarathi K, Gowda, Vishakante, Hani, Umme, Gupta, Vishal K, Prerana, Madesh, & Saha, Chandani. (2018). Cyclodextrin-based nanosponges in drug delivery and cancer therapeutics: New perspectives for old problems *Applications of Nanocomposite Materials in Drug Delivery, Volume 2018* (pp. 97-147). Amsterdam: Elsevier.

Öter, Özlem, Aydin, Akif Cihan, Ongun, Merve Zeyrek, & Celik, Erdal. (2018). Development of a nanoscale-based optical chemical sensor for the detection of NO radical. *Turkish Journal of Chemistry, 42*(4), 1056-1071.

Pahlavan, Ali, Gupta, Vinod Kumar, Sanati, Afsaneh L, Karimi, Fatemeh, Yoosefian, Mehdi, & Ghadami, Mojtaba. (2014). ZnO/CNTs nanocomposite/ionic liquid carbon paste electrode for determination of noradrenaline in human samples. *Electrochimica Acta, 123*, 456-462.

Parmar, Vijaykumar, Patel, Gayatri, & Abu-Thabit, Nedal Y. (2018). 20 - Responsive cyclodextrins as polymeric carriers for drug delivery applications. In Abdel Salam Hamdy Makhlouf & Nedal Y. Abu-Thabit (Eds.), *Stimuli Responsive Polymeric Nanocarriers for Drug Delivery Applications, Volume 1* (pp. 555-580). Sawston: Woodhead Publishing.

Patel, M Siddik N, Ahmed, Mohd Hasib, Saqib, Mohammad, & Shaikh, Siraj N. (2019). Chemical Modification: A unique solutions to Solubility problem. *Journal of Drug Delivery and Therapeutics, 9*(2), 542-546.

Pedroza, Aura M, Mosqueda, Rodolfo, Alonso-Vante, Nicolas, & Rodriguez-Vazquez, Refugio. (2007). Sequential treatment via Trametes versicolor and UV/TiO_2/RuxSey to reduce contaminants in waste water resulting from the bleaching process during paper production. *Chemosphere, 67*(4), 793-801.

Peila, R., Migliavacca, G., Aimone, F., Ferri, A., & Sicardi, S. (2012). A comparison of analytical methods for the quantification of a reactive β-cyclodextrin fixed onto cotton yarns. *Cellulose, 19*(4), 1097-1105.

Pekec, Bruna, Oberreiter, Angelika, Hauser, Susanne, Kalcher, Kurt, & Ortner, Astrid. (2012). Electrochemical sensor based on a cyclodextrin modified carbon paste electrode for trans-resveratrol analysis. *International Journal of Electrochemical Science, 7*, 4089-4098.

Peleyeju, Moses G, Idris, Azeez O, Umukoro, Eseoghene H, Babalola, Jonathan O, & Arotiba, Omotayo A. (2017). Electrochemical Detection of 2, 4-Dichlorophenol on a Ternary Composite Electrode of Diamond, Graphene, and Polyaniline. *ChemElectroChem, 4*(5), 1074-1080.

Popr, Martin, Hybelbauerová, Simona, & Jindřich, Jindřich. (2014). A complete series of 6-deoxy-monosubstituted tetraalkylammonium derivatives of α-, β-, and γ-cyclodextrin with 1, 2, and 3 permanent positive charges. *Beilstein Journal of Organic Chemistry, 10*, Article#1390.

Puglisi, Antonino, & Yagci, Yusuf. (2019). Cyclodextrin-Based Macromolecular Systems as Cholesterol-Mopping Therapeutic Agents in Niemann–Pick Disease Type C. *Macromolecular Rapid Communications, 40*(1), Article#1800557.

Ramanathan, Subramanian, Elanthamilan, Elaiyappillai, Obadiah, Asir, Durairaj, Arulappan, Santhoshkumar, Palanisamy, Merlin, Johnson Princy, Ramasundaram, Subramanian, & Vasanthkumar, Samuel. (2019). Development of a electrochemical sensor for the detection of 2,4-dichlorophenol using a polymer nanocomposite of rGO. *Journal of Materials Science: Materials in Electronics, 30*(7), 7150-7162.

Rao, CN, Subbarayudu, K, & Venkateswarlu, P. (2010). Electrochemical reduction behaviour of donepezil at β-cyclodextrin modified carbon paste electrode. *Portugaliae Electrochimica Acta, 28*(5), 349-357.

Raoov, Muggundha, Mohamad, Sharifah, & Abas, Mhd. (2014). Synthesis and Characterization of β-Cyclodextrin Functionalized Ionic Liquid Polymer as a Macroporous Material for the Removal of Phenols and As(V). *International Journal of Molecular Sciences, 15*(1), 100-119.

Raoov, Muggundha, Mohamad, Sharifah, & Abas, Mohd Radzi. (2013). Removal of 2,4-dichlorophenol using cyclodextrin-ionic liquid polymer as a macroporous material: Characterization, adsorption isotherm, kinetic study, thermodynamics. *Journal of Hazardous Materials, 263, Part 2*, 501-516.

Reddaiah, Kasetty, Reddy, Tukiakula Madhusudana, Raghu, Pamula, & Swamy, Bahaddurghatta E Kumra. (2012). Electrochemical Determination of Quercetin at

β–Cyclodextrin Modified Chemical Sensor: A Voltammetric Study. *Analytical and Bioanalytical Electrochemistry, 4*, 122-134.

Renner, Rebecca. (2001). Ionic liquids: An industrial cleanup solution. *Environmental Science & Technology, 35*(19), 410A-413A.

Saad, Ahmed S, Al-Alamein, Amal M Abou, Galal, Maha M, & Zaazaa, Hala E. (2019). Voltammetric Determination of Lidocaine and Its Toxic Metabolite in Pharmaceutical Formulation and Milk Using Carbon Paste Electrode Modified with C18 Silica. *Journal of The Electrochemical Society, 166*(2), B103-B109.

Sadeghi, Roya, Karimi-Maleh, Hassan, Bahari, Ali, & Taghavi, Mehdi. (2013). A novel biosensor based on ZnO nanoparticle/1,3-dipropylimidazolium bromide ionic liquid-modified carbon paste electrode for square-wave voltammetric determination of epinephrine. *Physics and Chemistry of Liquids, 51*(6), 704-714.

Safaei, Mohadeseh, Beitollahi, Hadi, Shishehbore, Masoud Reza, & Tajik, Somayeh. (2019). Electrocatalytic determination of captopril using a carbon paste electrode modified with N-(ferrocenyl-methylidene) fluorene-2-amine and graphene/ZnO nanocomposite. *Journal of the Serbian Chemical Society, 84*(2), 175-185.

Safavi, Afsaneh, Maleki, Norouz, Moradlou, Omran, & Tajabadi, Fariba. (2006). Simultaneous determination of dopamine, ascorbic acid, and uric acid using carbon ionic liquid electrode. *Analytical Biochemistry, 359*(2), 224-229.

Sanati, Afsaneh L., Karimi-Maleh, Hassan, Badiei, Alireza, Biparva, Pourya, & Ensafi, Ali A. (2014). A voltammetric sensor based on NiO/CNTs ionic liquid carbon paste electrode for determination of morphine in the presence of diclofenac. *Materials Science and Engineering: C, 35*, 379-385.

Sánchez-Paniagua López, Marta, & López-Ruiz, Beatriz. (2018). Electrochemical biosensor based on ionic liquid polymeric microparticles. An analytical platform for catechol. *Microchemical Journal, 138*, 173-179.

Santillán-Mercado, Jaime A, Rodríguez-Avilés, Yaiel G, Bello, Samir A, González-Feliciano, José A, & Nicolau, Eduardo. (2017). Electrospun Cellulose and Nanocellulose Composites as a Biomaterial *Electrospun Biomaterials and Related Technologies, Volume 2017* (pp. 57-107). New York: Springer.

Santos, Mayara CG, Silva, Glaura Goulart, Santamaria, Ricardo, Ortega, Paulo FR, & Lavall, Rodrigo Lassarote. (2019). A Discussion on Operational Voltage and Efficiencies of Ionic-Liquid based Electrochemical Capacitors. *The Journal of Physical Chemistry C, 123*(14), 8541-8549.

Sanyo, Hamai. (1992). Hydrogen Bonding in Inclusion Complexes of Heptakis(2,3,6-tri-O-methyl)-β-cyclodextrin with Chlorophenols in Organic Solvents. *Bulletin of the Chemical Society of Japan, 65*(9), 2323-2327.

Scialdone, O., Guarisco, C., Grispo, S., Angelo, A. D', & Galia, A. (2012). Investigation of electrode material – Redox couple systems for reverse electrodialysis processes. Part I: Iron redox couples. *Journal of Electroanalytical Chemistry, 681*, 66-75.

Seymour, Bryan T, Fu, Wenxin, Wright, Roger AE, Luo, Huimin, Qu, Jun, Dai, Sheng, & Zhao, Bin. (2018). Improved Lubricating Performance by Combining Oil-Soluble Hairy Silica Nanoparticles and an Ionic Liquid as an Additive for a Synthetic Base Oil. *ACS Applied Materials & Interfaces, 10*(17), 15129-15139.

Shahmiri, Mandana Roodbari, Bahari, Ali, Karimi-Maleh, Hassan, Hosseinzadeh, Rahman, & Mirnia, Norodin. (2013). Ethynylferrocene–NiO/MWCNT nanocomposite modified carbon paste electrode as a novel voltammetric sensor for simultaneous determination of glutathione and acetaminophen. *Sensors and Actuators B: Chemical, 177*, 70-77.

Shamsadin-Azad, Zahra, Taher, Mohammad A, Cheraghi, Somaye, & Karimi-Maleh, Hassan. (2019). A nanostructure voltammetric platform amplified with ionic liquid for determination of tert-butylhydroxyanisole in the presence kojic acid. *Journal of Food Measurement and Characterization, 13*(1), 1-7.

Sidwaba, Unathi, Ntshongontshi, Nomaphelo, Feleni, Usisipho, Wilson, Lindsay, Waryo, Tesfaye, & Iwuoha, Emmanuel I. (2019). Manganese Peroxidase-Based Electro-Oxidation of Bisphenol A at Hydrogellic Polyaniline-Titania Nanocomposite-Modified Glassy Carbon Electrode. *Electrocatalysis, 10*(4), 1-9.

Sing, Kenneth SW. (1985). Reporting physisorption data for gas/solid systems with special reference to the determination of surface area and porosity (Recommendations 1984). *Pure and Applied Chemistry, 57*(4), 603-619.

Sinniah, Subathra, Mohamad, Sharifah, & Manan, Ninie S. A. (2015). Magnetite nanoparticles coated with β-cyclodextrin functionalized-ionic liquid: Synthesis and its preliminary investigation as a new sensing material. *Applied Surface Science, 357*, 543-550.

Srinivasan, K, Stalin, T, & Sivakumar, K. (2012). Spectral and electrochemical study of host–guest inclusion complex between 2, 4-dinitrophenol and β-cyclodextrin. *Spectrochimica Acta Part A: Molecular and Biomolecular Spectroscopy, 94*, 89-100.

Stoimenovski, Jelena, Izgorodina, Ekaterina I, & MacFarlane, Douglas R. (2010). Ionicity and proton transfer in protic ionic liquids. *Physical Chemistry Chemical Physics, 12*(35), 10341-10347.

Stradiotto, Nelson R., Yamanaka, Hideko, & Zanoni, Maria Valnice B. (2003). Electrochemical sensors: a powerful tool in analytical chemistry. *Journal of the Brazilian Chemical Society, 14*, 159-173.

Sulaiman, R., Hadj-Kali, M. K., Hasan, S. W., Mulyono, S., & AlNashef, I. M. (2019). Investigating the solubility of chlorophenols in hydrophobic ionic liquids. *The Journal of Chemical Thermodynamics, 135*, 97-106.

Sun, Ping, & Armstrong, Daniel W. (2010). Ionic liquids in analytical chemistry. *Analytica Chimica Acta, 661*(1), 1-16.

Sun, Wei, Hou, Fei, Gong, Shixing, Han, Lin, Wang, Wencheng, Shi, Fan, Xi, Jingwen, Wang, Xiuli, & Li, Guangjiu. (2015). Direct electrochemistry and electrocatalysis of hemoglobin on three-dimensional graphene modified carbon ionic liquid electrode. *Sensors and Actuators B: Chemical, 219*, 331-337.

Sun, Wei, Li, Xiaoqing, Wang, Yan, Zhao, Ruijun, & Jiao, Kui. (2009). Electrochemistry and electrocatalysis of hemoglobin on multi-walled carbon nanotubes modified carbon ionic liquid electrode with hydrophilic $EMIMBF_4$ as modifier. *Electrochimica Acta, 54*(17), 4141-4148.

Sun, Yongling, Wang, Liping, & Liu, Huihong. (2012). Myoglobin functioning as cytochrome P450 for biosensing of 2, 4-dichlorophenol. *Analytical Methods, 4*(10), 3358-3363.

Szejtli, J. (1995). Selectivity/structure correlation in cyclodextrin chemistry. *Supramolecular Chemistry, 6*(1-2), 217-223.

Szejtli, József. (2013). *Cyclodextrin Technology, Volume 1* (pp. 48-58). New York: Springer Science & Business Media.

Tan, Zhi-qiang, Liu, Jing-fu, & Pang, Long. (2012). Advances in analytical chemistry using the unique properties of ionic liquids. *TrAC Trends in Analytical Chemistry, 39*, 218-227.

Tiwari, Gaurav, Tiwari, Ruchi, & Rai, Awani K. (2010). Cyclodextrins in delivery systems: Applications. *Journal of Pharmacy and Bioallied Sciences, 2*(2), 72-79.

Tripodo, Giuseppe, Wischke, Christian, Neffe, Axel T, & Lendlein, Andreas. (2013). Efficient synthesis of pure monotosylated beta-cyclodextrin and its dimers. *Carbohydrate Research, 381*, 59-63.

Trojanowicz, M., Drzewicz, P., Pańta, P., Głuszewski, W., Nałęcz-Jawecki, G., Sawicki, J., Sampa, M. H. O., Oikawa, H., Borrely, S. I., Czaplicka, M., & Szewczyńska, M. (2002). Radiolytic degradation and toxicity changes in γ-irradiated solutions of 2,4-dichlorophenol. *Radiation Physics and Chemistry, 65*(4), 357-366.

Upadhyay, Sharad S., Kalambate, Pramod K., & Srivastava, Ashwini K. (2017). Enantioselective analysis of Moxifloxacin hydrochloride enantiomers with graphene-β-Cyclodextrin-nanocomposite modified carbon paste electrode using adsorptive stripping differential pulse Voltammetry. *Electrochimica Acta, 248*, 258-269.

Ureta-Zanartu, MS, Bustos, P, Berrıos, C, Diez, MC, Mora, ML, & Gutiérrez, C. (2002). Electrooxidation of 2, 4-dichlorophenol and other polychlorinated phenols at a glassy carbon electrode. *Electrochimica Acta, 47*(15), 2399-2406.

Van Aken, Pieter, Van den Broeck, Rob, Degrève, Jan, & Dewil, Raf. (2017). A pilot-scale coupling of ozonation and biodegradation of 2, 4-dichlorophenol-containing wastewater: The effect of biomass acclimation towards chlorophenol and intermediate ozonation products. *Journal of Cleaner Production, 161*, 1432-1441.

Vekariya, Rohit L. (2017). A review of ionic liquids: Applications towards catalytic organic transformations. *Journal of Molecular Liquids, 227*, 44-60.

Vinodh, Mickey, Alipour, Fatemeh H., Mohamod, Abdirahman A., & Al-Azemi, Talal F. (2012). Molecular Assemblies of Porphyrins and Macrocyclic Receptors: Recent Developments in Their Synthesis and Applications. *Molecules, 17*(10), 11763-11799.

Vytřas, Karel, Švancara, Ivan, & Metelka, Radovan. (2009). Carbon paste electrodes in electroanalytical chemistry. *Journal of the Serbian Chemical Society, 74*(10), 1021-1033.

Waldiya, Manmohansingh, Bhagat, Dharini, Narasimman, R, Singh, Shivam, Kumar, Arvind, Ray, Abhijit, & Mukhopadhyay, Indrajit. (2019). Development of Highly Sensitive H_2O_2 Redox Sensor from Electrodeposited Tellurium Nanoparticles using Ionic Liquid. *Biosensors and Bioelectronics, 132,* 319-325.

Wan, Hao, Yin, Heyu, Lin, Lu, Zeng, Xiangqun, & Mason, Andrew J. (2018). Miniaturized planar room temperature ionic liquid electrochemical gas sensor for rapid multiple gas pollutants monitoring. *Sensors and Actuators B: Chemical, 255*, 638-646.

Wang, Huai You, Han, Juan, & Feng, Xia Guang. (2007). Spectroscopic study of orange G–β-cyclodextrin complex and its analytical application. *Spectrochimica Acta Part A: Molecular and Biomolecular Spectroscopy, 66*(3), 578-585.

Wang, J, & Zhang, Z. (1994). *Analytical Chemistry*. New York: Trans Tech Publication.

Wang, Peng, Zakeeruddin, Shaik M, Moser, Jacques-E, & Grätzel, Michael. (2003). A new ionic liquid electrolyte enhances the conversion efficiency of dye-sensitized solar cells. *The Journal of Physical Chemistry B, 107*(48), 13280-13285.

Wang, Yang, Wu, Yichun, Xie, Jing, & Hu, Xiaoya. (2013). Metal–organic framework modified carbon paste electrode for lead sensor. *Sensors and Actuators B: Chemical, 177*, 1161-1166.

Wang, Yun-Kun, Pan, Xin-Rong, Sheng, Guo-Ping, Li, Wen-Wei, Shi, Bing-Jing, & Yu, Han-Qing. (2015). Development of an energy-saving anaerobic hybrid membrane bioreactors for 2-chlorophenol-contained wastewater treatment. *Chemosphere, 140*, 79-84.

Wardak, Cecylia, & Lenik, Joanna. (2013). Application of ionic liquid to the construction of Cu(II) ion-selective electrode with solid contact. *Sensors and Actuators B: Chemical, 189*, 52-59.

Wei, Maochao, Tian, Dong, Liu, Shan, Zheng, Xiangli, Duan, Shuo, & Zhou, Changli. (2014). β-Cyclodextrin functionalized graphene material: A novel electrochemical sensor for simultaneous determination of 2-chlorophenol and 3-chlorophenol. *Sensors and Actuators B: Chemical, 195*, 452-458.

Wu, Xiuming, Zhao, Bo, Wu, Ping, Zhang, Hui, & Cai, Chenxin. (2009). Effects of ionic liquids on enzymatic catalysis of the glucose oxidase toward the oxidation of glucose. *The Journal of Physical Chemistry B, 113*(40), 13365-13373.

Xiao, Su-long, Wang, Qi, Yu, Fei, Peng, Yi-yun, Yang, Ming, Sollogoub, Matthieu, Sinaÿ, Pierre, Zhang, Yong-min, Zhang, Li-he, & Zhou, De-min. (2012). Conjugation of cyclodextrin with fullerene as a new class of HCV entry inhibitors. *Bioorganic & Medicinal Chemistry, 20*(18), 5616-5622.

Xu, Xiaomeng, Liu, Zhen, Zhang, Xin, Duan, Shuo, Xu, Shuai, & Zhou, Changli. (2011). β-Cyclodextrin functionalized mesoporous silica for electrochemical selective sensor: Simultaneous determination of nitrophenol isomers. *Electrochimica Acta, 58*, 142-149.

Yahaya, Abdulrazaq, Okoh, Omobola O., Agunbiade, Foluso O., & Okoh, Anthony I. (2019). Occurrence of phenolic derivatives in Buffalo River of Eastern Cape

South Africa: Exposure risk evaluation. *Ecotoxicology and Environmental Safety, 171*, 887-893.

Yaman, Yesim Tugce, Bolat, Gülçin, Yardimci, Ceren, & Abaci, Serdar. (2018). An ionic liquid/bismuth film-modified sensor for the electrochemical detection of cefixime. *Turkish Journal of Chemistry, 42*(3), 826-838.

Yang, Li-Juan, Chang, Qing, Zhou, Shu-Ya, Yang, Yun-Han, Xia, Fu-Ting, Chen, Wen, Li, Minyan, & Yang, Xiao-Dong. (2018). Host–guest interaction between brazilin and hydroxypropyl-β-cyclodextrin: preparation, inclusion mode, molecular modelling and characterization. *Dyes and Pigments, 150*, 193-201.

Yang, Lizhu, Xu, Ying, Wang, Xiuhua, Zhu, Jing, Zhang, Renyi, He, Pingang, & Fang, Yuzhi. (2011). The application of β-cyclodextrin derivative functionalized aligned carbon nanotubes for electrochemically DNA sensing via host–guest recognition. *Analytica Chimica Acta, 689*(1), 39-46.

Yu, Lanlan, Yue, Xiu, Yang, Ran, Jing, Shasha, & Qu, Lingbo. (2016). A sensitive and low toxicity electrochemical sensor for 2,4-dichlorophenol based on the nanocomposite of carbon dots, hexadecyltrimethyl ammonium bromide and chitosan. *Sensors and Actuators B: Chemical, 224*, 241-247.

Yu, Qiong, Liu, Yong, Liu, Xiaoying, Zeng, Xiandong, Luo, Shenglian, & Wei, Wanzhi. (2010). Simultaneous Determination of Dihydroxybenzene Isomers at MWCNTs/β-Cyclodextrin Modified Carbon Ionic Liquid Electrode in the Presence of Cetylpyridinium Bromide. *Electroanalysis, 22*(9), 1012-1018.

Yu, Xiaowei, Chen, Yankai, Chang, Luping, Zhou, Ling, Tang, Fengxiang, & Wu, Xiaoping. (2013). β-cyclodextrin non-covalently modified ionic liquid-based carbon paste electrode as a novel voltammetric sensor for specific detection of bisphenol A. *Sensors and Actuators B: Chemical, 186*(0), 648-656.

Yuan, Chao, Jin, Zhengyu, & Xu, Xueming. (2012). Inclusion complex of astaxanthin with hydroxypropyl-β-cyclodextrin: UV, FTIR, ^{1}H NMR and molecular modeling studies. *Carbohydrates Research, 89*(2), 492-496.

Yuan, Su-fen, Liu, Ze-hua, Lian, Hai-xian, Yang, Chuang-tao, Lin, Qing, Yin, Hua, Lin, Zhang, & Dang, Zhi. (2018). Fast trace determination of nine odorant and estrogenic chloro-and bromo-phenolic compounds in real water samples through automated solid-phase extraction coupled with liquid chromatography tandem mass spectrometry. *Environmental Science and Pollution Research, 25*(4), 3813-3822.

Zada, Amir, Qu, Yang, Ali, Sharafat, Sun, Ning, Lu, Hongwei, Yan, Rui, Zhang, Xuliang, & Jing, Liqiang. (2018). Improved visible-light activities for degrading pollutants on TiO_2/g-C_3N_4 nanocomposites by decorating SPR Au nanoparticles and 2,4-

dichlorophenol decomposition path. *Journal of Hazardous Materials, 342*, 715-723.

Zarei, Zohre, & Shemirani, Farzaneh. (2011). Modified-cold induced aggregation microextraction based on ionic liquid and fibre optic-linear array detection spectrophotometric determination of palladium in saline solutions. *International Journal of Environmental Analytical Chemistry, 91*(15), 1436-1446.

Zhan, Tianrong, Tan, Zhengwei, Tian, Xia, & Hou, Wanguo. (2017). Ionic liquid functionalized graphene oxide-Au nanoparticles assembly for fabrication of electrochemical 2,4-dichlorophenol sensor. *Sensors and Actuators B: Chemical, 246*, 638-646.

Zhan, Tianrong, Tian, Xia, Ding, Guiyan, Liu, Xien, Wang, Lei, & Teng, Hongni. (2019). Quaternarization strategy to ultrathin lamellar graphitic C_3N_4 ionic liquid nanostructure for enhanced electrochemical 2,4-Dichlorophenol sensing. *Sensors and Actuators B: Chemical, 283*, 463-471.

Zhang, C., & Bennett, G. N. (2005). Biodegradation of xenobiotics by anaerobic bacteria. *Applied Microbiology & Biotechnology, 67*(5), 600-618.

Zhang, Fenfen, Gu, Shuqing, Ding, Yaping, Zhang, Zhen, & Li, Li. (2013a). A novel sensor based on electropolymerization of β-cyclodextrin and L-arginine on carbon paste electrode for determination of fluoroquinolones. *Analytica Chimica Acta, 770*, 53-61.

Zhang, Hong, Zhang, Qifu, Miao, Chunguang, & Huang, Qing. (2018). Degradation of 2, 4-dichlorophenol in aqueous solution by dielectric barrier discharge: Effects of plasma-working gases, degradation pathways and toxicity assessment. *Chemosphere, 204*, 351-358.

Zhang, J. J., Yuan, J. H., Zhang, J. P., & Cheng, Z. (2013b). Quantum entanglement and phase transition in a two-dimensional photon-photon pair model. *Physica B: Condensed Matter, 408*(1), 16-21.

Zhang, Jianxiang, & Ma, Peter X. (2013). Cyclodextrin-based supramolecular systems for drug delivery: recent progress and future perspective. *Advanced Drug Delivery Reviews, 65*(9), 1215-1233.

Zhang, Jin, Lei, Jianping, Ju, Huangxian, & Wang, Chaoying. (2013c). Electrochemical sensor based on chlorohemin modified molecularly imprinted microgel for determination of 2,4-dichlorophenol. *Analytica Chimica Acta, 786*, 16-21.

Zhang, Wenna, Zhang, Wenwen, Chen, Shuai, Guo, Bin, Gu, Hua, Xue, Yu, Xue, Zexu, & Xu, Jingkun. (2019). Electrosynthesized alkyl-modified poly (3,

4-propylenedioxyselenophene) with superior electrochromic performances in an ionic liquid. *Journal of Electroanalytical Chemistry, 833*, 17-25.

Zhang, X., Zha, J., Li, W., Yang, L., & Wang, Z. (2008). Effects of 2,4-dichlorophenol on the expression of vitellogenin and estrogen receptor genes and physiology impairments in Chinese rare minnow (Gobiocypris rarus). *Environmental Toxicology, 23*(6), 694-701.

Zhang, Yafen, Guo, Gaiping, Zhao, Faqiong, Mo, Zhirong, Xiao, Fei, & Zeng, Baizhao. (2010). A novel glucose biosensor based on glucose oxidase immobilized on AuPt nanoparticle–carbon nanotube–ionic liquid hybrid coated electrode. *Electroanalysis: An International Journal Devoted to Fundamental and Practical Aspects of Electroanalysis, 22*(2), 223-228.

Zhang, Zhen, Gu, Shuqing, Ding, Yaping, Shen, Mingju, & Jiang, Lin. (2014). Mild and novel electrochemical preparation of β-cyclodextrin/graphene nanocomposite film for super-sensitive sensing of quercetin. *Biosensors and Bioelectronics, 57*, 239-244.

Zhao, Chuan, Burrell, Geoff, Torriero, Angel AJ, Separovic, Frances, Dunlop, Noel F, MacFarlane, Douglas R, & Bond, Alan M. (2008). Electrochemistry of room temperature protic ionic liquids. *The Journal of Physical Chemistry B, 112*(23), 6923-6936.

Zhao, Dongbin, Wu, Min, Kou, Yuan, & Min, Enze. (2002). Ionic liquids: applications in catalysis. *Catalysis Today, 74*(1), 157-189.

Zheng, Cao, Zhao, Jing, Bao, Peng, Gao, Jin, & He, Jin. (2011). Dispersive liquid–liquid microextraction based on solidification of floating organic droplet followed by high-performance liquid chromatography with ultraviolet detection and liquid chromatography–tandem mass spectrometry for the determination of triclosan and 2, 4-dichlorophenol in water samples. *Journal of Chromatography A, 1218*(25), 3830-3836.

Zhong, Ning, Byun, Hoe-Sup, & Bittman, Robert. (1998). An improved synthesis of 6-O-monotosyl-6-deoxy-β-cyclodextrin. *Tetrahedron Letters, 39*(19), 2919-2920.

Zhou, Liqin, Xu, Zhijun, Yi, Kai, Huang, Qiuyuan, Chai, Kungang, Tong, Zhangfa, & Ji, Hongbing. (2019). Efficient remediation of 2,4-dichlorophenol from aqueous solution using β-cyclodextrin-based submicron polymeric particles. *Chemical Engineering Journal, 360*, 531-541.

Zhu, Gangbing, Yi, Yinhui, & Chen, Jinhua. (2016a). Recent advances for cyclodextrin-based materials in electrochemical sensing. *TrAC Trends in Analytical Chemistry, 80*, 232-241.

Zhu, Xiaolin, Wu, Guanlan, Lu, Nan, Yuan, Xing, & Li, Baikun. (2017). A miniaturized electrochemical toxicity biosensor based on graphene oxide quantum dots/carboxylated carbon nanotubes for assessment of priority pollutants. *Journal of Hazardous Materials, 324*, 272-280.

Zhu, Xiaolin, Zhang, Kexin, Wang, Chengzhi, Guan, Jiunian, Yuan, Xing, & Li, Baikun. (2016b). Quantitative determination and toxicity evaluation of 2,4-dichlorophenol using poly(eosinY)/hydroxylated multi-walled carbon nanotubes modified electrode. *Scientific Reports, 6*(2016), Article#38657.

LIST OF PUBLICATIONS AND PAPERS PRESENTED

PUBLICATIONS

1. **Rasdi, F. L. M.**, Rahim, N. Y., Hasim, F. W., Prabu, S., Jumbri, K., Manan, N. S. A., & Mohamad, S. (2019). Influence of degree of substitution on the host-guest inclusion complex between ionic liquid substituted β-cyclodextrins with 2, 4-dichlorophenol: An electrochemical, NMR and molecular docking studies. *Journal of Molecular Liquids*, 292, Article#111334.

2. **Rasdi, F. L. M**., Mohamad, S., Manan, N. S. A., & Nodeh, H. R. (2016). Electrochemical determination of 2, 4-dichlorophenol at β-cyclodextrin functionalized ionic liquid modified chemical sensor: voltammetric and amperometric studies. *RSC Advances*, *6*(102), 100186-100194.

3. Mohamad, S., Chandrasekaram, K., **Rasdi, F. L. M**., Manan, N. S. A., Raoov, M., Sidek, N., & Fathullah, S. F. (2015). Supramolecular interaction of 2, 4-dichlorophenol and β-cyclodextrin functionalized ionic liquid and its preliminary study in sensor application. *Journal of Molecular Liquids*, *212*, 850-856.